To the Graduate Council:

I am submitting herewith a dissertation written by Huijuan Li entitled “Adaptive Voltage Control Methods using Distributed Energy Resources.” I have examined the final electronic copy of this dissertation for form and content and recommend that it be accepted in partial fulfillment of the requirements for the degree of Doctor of Philosophy, with a major in Electrical Engineering.

Fangxing (Fran) Li , Major Professor

We have read this dissertation
and recommend its acceptance:

Kevin Tomsovic

Yilu Liu

Xueping Li

Accepted for the Council:

Carolyn R. Hodges
Vice Provost and Dean of the Graduate School

(Original signatures are on file with official student records.)

Adaptive Voltage Control Methods using Distributed Energy Resources

A Dissertation Presented for the
Doctor of Philosophy Degree
The University of Tennessee, Knoxville

Huijuan Li
December 2010

Acknowledgements

I would like to thank my advisor, Dr. Fangxing (Fran) Li, for his continuous guidance and support not only in my doctoral study, but also in student life. His dedication in teaching, tutoring, and assistance to me is greatly appreciated.

I am very thankful to Dr. Yan Xu at Oak Ridge National Laboratory (ORNL) for her inspirational instructions and work on the experiment. I also thank Mr. D. Tom Rizy and Mr. John D. Kueck at Oak Ridge National Laboratory for their advice and help. In particular, the field experiment at ORNL presented in subsection 4.5 (Pages 51-55) was mainly performed by ORNL researchers including Dr. Yan Xu and Mr. Tom Rizy. The field experiment results are included in this dissertation for completeness.

I am also thankful to all the professors and students in the UT EECS Power Lab, including those already graduated. Your friendship, encouragement, and help were indeed beneficial to my studies and research work. In addition, I am very thankful to Dr. Kevin Tomsovic, Dr. Yilu Liu and Dr. Xueping Li, for their time and effort in serving as my committee members.

Finally, I would like to express my appreciation and love to my husband, Yong Yin, and my parents, En Li and Zhilan Zhou. They have always loved me, supported me, and encouraged me unconditionally.

Abstract

Distributed energy resources (DE) with power electronics interfaces and logic control using local measurements are capable of providing reactive power related to ancillary system services. In particular, local voltage regulation has drawn much attention in regards to power system reliability and voltage stability, especially from past major cascading outages. This dissertation addresses the challenges of controlling the DEs to regulate the local voltage in distribution systems.

First, an adaptive voltage control method has been proposed to dynamically modify the control parameters of a single DE to respond to system changes such that the ideal response can be achieved. Theoretical analysis shows that a corresponding formulation of the dynamic control parameters exists; hence, the adaptive control method is theoretically solid. Also, the field experiment test results at the Distributed Energy Communications and Controls (DECC) Laboratory in single DE regulation case confirm the effectiveness of this method.

Then, control methods have been discussed in the case of multiple DEs regulating voltages considering the availability of communications among all the DEs. When communications are readily available, a method is proposed to directly calculate the needed adaptive change of the DE control parameters in order to achieve the ideal response. When there is no communication available, an approach to adaptively and incrementally adjust the control parameters based on the local voltage changes is proposed. Since the impact from other DEs is implicitly considered in this approach, multiple DEs can collectively regulate voltages closely following the ideal response curve. Simulation results show that each method, with or without communications, can satisfy the fast response requirement for operational use without causing

oscillation, inefficiency or system equipment interference, although the case with communication can perform even faster and more accurate.

Since the proposed adaptive voltage regulation method in the case of multiple DEs without communication, has a high tolerance to real-time data shortage and can still provide good enough performance, it is more suitable for broad utility applications. The approach of multiple DEs with communication can be considered as a high-end solution, which gives faster and more precise results at a higher cost.

Table of Contents

1 Introduction 1
1.1. Background 1
1.1.1. Development of Distributed Energy Resources 1
1.1.2. Types of Distributed Energy Resources 3
1.1.3. Interconnection to Grid 5
1.1.4. Voltage Regulation by DE with PE Interface 7
1.2. Motivation 11
1.3. Dissertation Outline 13
1.4. Summary of Contributions 14
2 Literature Review 16
2.1. Chapter Introduction 16
2.2. Voltage Control in Distribution Systems with DEs 16
2.3. PE interfaces Design to Implement Voltage Regulation 21
2.4. Scope of this Work 23
3 Challenges of the Control Parameters for Voltage-Regulating Distributed Energy Resources 24
3.1. Chapter Introduction 24
3.2. Factors Affecting Dynamic Performance of Controller for Voltage Control 24
3.3. Simulations on Voltage Control with PE Interfaced DE 26
3.3.1. Impact of KP and KI on Voltage Regulation 26
3.3.2. Impact of DE Location on Voltage Regulation 30
3.3.3. Impact of Loading Level on Voltage Regulation 32
3.4. Chapter Summary and Discussion 35
4 Adaptive Voltage Control with a Single DE 36
4.1. Chapter Introduction 36
4.2. Implementation of Adaptive Method for DE Controller 36
4.2.1. Determine the DC Source Voltage 36
4.2.2. Set the Initial PI Controller Gains 38
4.2.3. Adaptively Adjusting the PI Controller Gain Parameters 40
4.3. Analytical Formulation of the Adaptive Method 42
4.4. Simulation Results 50
4.5. Field Experiment Results at ORNL 55
4.6. Chapter Conclusion 60
5. Voltage Regulation with Multiple DEs 61
5.1. Chapter Introduction 61
5.2. Challenges in Voltage Control with Multiple DEs 61
5.3. Theoretical Formulation of the Parameters for Multiple Voltage-Regulating DEs with Adaptive Control Method 68
5.4. Voltage Regulation with Communication 78
5.5. Voltage Regulation without Communication 98
5.6. Chapter Conclusion 112
6. Conclusions and Future Work 114

6.1. Dissertation Conclusion 114
6.2. Future Work 116
List of References 118
Publications during Ph.D. Study 126
Award 128
Vita 129

List of Figures

Figure 1.1. Distributed energy resources reshaping the traditional grid [1]. 2
Figure 1.2. Interconnection Interfaces of DE with Power Systems. 7
Figure 1.3. Parallel connection of a DE with PE converter. 9
Figure 1.4. Control diagram for voltage regulation. 10
Figure 3.1. Simplified model of the distribution system with multiple controllable DEs interfaced to it. 25
Figure 3.2. Single line diagram of the distribution system with DEs. 27
Figure 3.3. Voltage regulation with different control parameters-single DE case. 27
Figure 3.4. Voltage regulation with different control parameters-two DEs case. 29
Figure 3.5. Voltage regulation with different location of DE-single DE case. 31
Figure 3.6. Voltage response when DE1 at bus 4 and DE2 at bus 5. 31
Figure 3.7. Voltage response when DE1 at bus 2 and DE2 at bus 5. 32
Figure 3.8. Voltage responses with different amount of load-single DE case. 33
Figure 3.9. Voltage responses when load at bus 3 is 13.6kW+2.1kVar. 34
Figure 3.10. Voltage responses when load at bus 3 is 27.2kW+2.1kVar. 34
Figure 4.1. PWM voltage control by varying modulation index m_a. 37
Figure 4.2. Adaptive Control of the Voltage Regulation. 41
Figure 4.3. The desired and actual response of the controller. 42
Figure 4.4. A schematic diagram of a network and sources. 43
Figure 4.5. A radial test system. 47
Figure 4.6. Comparison of the value of K_P generated by the two methods. 48
Figure 4.7. Comparison of the value of K_I generated by the two methods. 49
Figure 4.8. Tracking ideal response by adjusting K_P and K_I with the two methods. 49
Figure 4.9. Voltage regulation with adaptive adjustment of K_P and K_I. 53
Figure 4.10. Comparing the desired and actual voltage deviations. 53
Figure 4.11. Real power injection. 54
Figure 4.12. Reactive power injection. 54
Figure 4.13. Non-adaptive voltage regulation with K_P and K_I fixed at the initial values. 55
Figure 4.14. ORNL's DECC Laboratory. 57
Figure 4.15. PCC voltage at the inverter without voltage regulation. 58
Figure 4.16. PCC voltage (in RMS) with non-adaptive voltage regulation. 58
Figure 4.17. PCC voltage (in RMS) with adaptive voltage regulation. 59
Figure 4.18. Comparison of the desired and actual voltage deviations. 60
Figure 5.1. A radial test system installed with two DEs. 63
Figure 5.2. Voltage responses of DE2 in Scenarios 1, 2, and 3. 64
Figure 5.3. Voltage regulation of DE1 in Scenario 2. 64
Figure 5.4. Voltage regulation of DE1 in Scenario 3. 65
Figure 5.5. Voltage response of DE2 in scenario 4 and scenario 5. 67
Figure 5.6. A schematic diagram of a network and with multiple DE sources. 69
Figure 5.7. Terminal voltage of DE1 - Scenario 5. 74
Figure 5.8. Terminal voltage of DE2 – Scenario 5. 75

Figure 5.9. The calculated value of K_P of DE1 in adaptive control - Scenario 5. 75
Figure 5.10. The calculated value of K_I of DE1 in adaptive control - Scenario 5. 76
Figure 5.11. The calculated value of K_P of DE2 in adaptive control - Scenario 5. 76
Figure 5.12. The calculated value of K_I of DE2 in adaptive control - Scenario 5. 77
Figure 5.13. Adaptive voltage adjusting algorithm with communication. 85
Figure 5.14 Voltage response of DE1 using the with-communication method when the reference voltages of DE1 and DE2 are 275.85 V and 275.70 V, respectively. 90
Figure 5.15. Voltage response of DE2 using the with-communication method when the reference voltages of DE1 and DE2 are 275.85 V and 275.70 V, respectively. 90
Figure 5.16. K_P of DE1 using the with-communication method when the reference voltages of DE1 and DE2 are 275.85 V and 275.70 V, respectively. 91
Figure 5.17. K_I of DE1 using the with-communication method when the reference voltages of DE1 and DE2 are 275.85 V and 275.70 V, respectively. 91
Figure 5.18. K_P of DE2 using the with-communication method when the reference voltages of DE1 and DE2 are 275.85 V and 275.70 V, respectively. 92
Figure 5.19. K_I of DE2 using the with-communication method when the reference voltages of DE1 and DE2 are 275.85 V and 275.70 V, respectively. 92
Figure 5.20. Ratio of the two consecutive voltage changes using the with-communication method when the reference voltages of DE1 and DE2 are 275.85 V and 275.70 V, respectively. ... 93
Figure 5.21. Voltage response of DE1 - only DE1 regulating voltage. 93
Figure 5.22. Voltage response of DE2 - only DE1 regulating voltage. 94
Figure 5.23. Voltage response of DE1 using the with-communication method when the reference voltages of DE1 and DE2 are 275.85 V and 275.10 V, respectively. 94
Figure 5.24. Voltage response of DE2 using the with-communication method when the reference voltages of DE1 and DE2 are 275.85 V and 275.10 V, respectively. 95
Figure 5.25. K_P of DE1 using the with-communication method when the reference voltages of DE1 and DE2 are 275.85 V and 275.10 V, respectively. 95
Figure 5.26. K_I of DE1 using the with-communication method when the reference voltages of DE1 and DE2 are 275.85 V and 275.10 V, respectively. 96
Figure 5.27. K_P of DE2 using the with-communication method when the reference voltages of DE1 and DE2 are 275.85 V and 275.10 V, respectively. 96
Figure 5.28. K_I of DE2 using the with-communication method when the reference voltages of DE1 and DE2 are 275.85 V and 275.10 V, respectively. 97
Figure 5.29. Ratio of the two consecutive voltage changes using the with-communication method when the reference voltages of DE1 and DE2 are 275.85 V and 275.10 V, respectively 97
Figure 5.30. Ideal voltage deviation from the reference in the regulation process. 101
Figure 5.31. Adaptive voltage adjusting algorithm without communication. 102
Figure 5.32. Voltage response of DE1 using the without-communication method when the reference voltages of DE1 and DE2 are 275.85 V and 275.70 V, respectively. 106
Figure 5.33. Voltage response of DE2 using the without-communication method when the reference voltages of DE1 and DE2 are 275.85 V and 275.70 V, respectively. 106
Figure 5.34. K_P of DE1 using the without-communication method when the reference voltages of DE1 and DE2 are 275.85 V and 275.70 V, respectively. 107

Figure 5.35. K_I of DE1 using the without-communication method when the reference voltages of DE1 and DE2 are 275.85 V and 275.70 V, respectively. 107
Figure 5.36. K_P of DE2 using the without-communication method when the reference voltages of DE1 and DE2 are 275.85 V and 275.70 V, respectively. 108
Figuure 5.37. K_I of DE2 using the without-communication method when the reference voltages of DE1 and DE2 are 275.85 V and 275.70 V, respectively. 108
Figure 5.38. Voltage response of DE1 using the without-communication method when the reference voltages of DE1 and DE2 are 275.85 V and 275.10 V, respectively. 109
Figure 5.39. Voltage response of DE2 using the without-communication method when the reference voltages of DE1 and DE2 are 275.85 V and 275.10 V, respectively. 109
Figure 5.40. K_P of DE1 using the without-communication method when the reference voltages of DE1 and DE2 are 275.85 V and 275.10 V, respectively. 110
Figure 5.41. K_I of DE1 using the without-communication method when the reference voltages of DE1 and DE2 are 275.85 V and 275.10 V, respectively. 110
Figure 5.42. K_P of DE2 using the without-communication method when the reference voltages of DE1 and DE2 are 275.85 V and 275.10 V, respectively. 111
Figure 5.43. K_I of DE2 using the without-communication method when the reference voltages of DE1 and DE2 are 275.85 V and 275.10 V, respectively. 111

1 Introduction

1.1. Background

1.1.1. Development of Distributed Energy Resources

The electrical power system grid is composed of the generation system, the transmission system, and the distribution system. Economies of scale in electricity generation lead to a large power output from generators. Conventionally, electrical power is generated centrally and transported over a long distance to the end users. However, since the last decade, there has been increasing interest in distributed energy resources (DE). Contrary to the conventional power plants, DE systems are small-scale electric power sources, typically ranging from 1kW to 10MW, located at or near the end users, usually in distribution systems as shown in Figure 1.1[1]. Typically, DE includes distributed generation (DG), distributed energy storage, and demand response efforts. These are reforming power systems.

Renewable energy technologies contribute to the development of DE. Some distributed generations are powered by renewable fuel, such as wind energy, solar energy, and biomass. Besides the technological innovations, the environment of power systems deregulation, energy security, and environmental concerns all boost the development of DE [1][4][5].

DE provides participants in the electricity market more flexibility in the changing market conditions. First, because many distributed generation technologies are flexible in operation, size, and expandability, they can provide standby capacity and peak shaving; and thus help reduce the price volatility in market. Secondly, DE can enhance the system's reliability by picking up part or all of the lost outputs from the failed generators. Third, because DEs supply electrical power locally, they could reduce transmission and distribution

congestions, thus saving the investment on expanding transmission and distribution capacity. Fourth, DE can also provide ancillary services for the grid support both in real power related services, such as load following, and reactive power related services, such as voltage regulation [4]-[8].

Energy security and environmental concerns also drive the development of DE. DE technologies generally use local renewable energy. Also, certain technologies, such as energy storage, combined heat and power systems (CHP), and demand-control devices, help improve energy conversion efficiency. Renewable energy and high efficiency technologies save the consumption of nonrenewable natural resources and reduce greenhouse gas emissions.

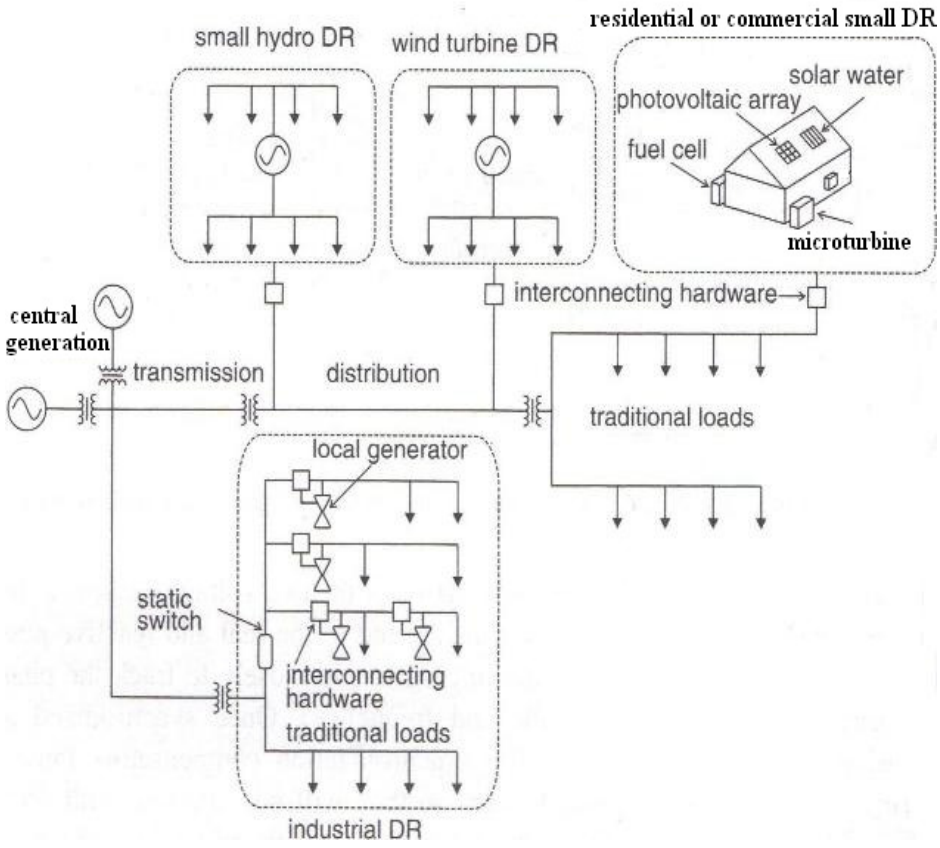


Figure 1.1. Distributed energy resources reshaping the traditional grid [1].

1.1.2. Types of Distributed Energy Resources

The most common types of distributed energy systems are summarized in this section [1][4][5].

A. Reciprocating Internal Combustion (IC) Engines

Reciprocating IC engines convert chemical (or heat) energy to mechanical energy from moving pistons. The pistons then spin a shaft and convert the mechanical energy into electrical energy through an electric generator. These engines can burn natural gas, propane, gasoline, etc. The electric generator is usually synchronous or induction type, and is typically connected directly to the electric power system.

B. Gas Turbine

A gas turbine is a rotary engine that extracts energy from a flow of combustion gas. High temperature, high pressure air is the heat transfer medium. Air is allowed to expand in the turbine thus converting the heat energy into mechanical energy that spins a shaft. The shaft is connected to a series of reduction gears that spin a synchronous generator directly connected to the electric power system.

C. Small Hydro-electrical Systems

Hydro-electric power systems can be driven from a water stream or accumulation reservoir and convert the potential energy into electricity. They are also directly connected to the grid without additional interfaces.

D. Microturbines

Microturbines work in a similar way to gas turbines. The majority of commercial devices use natural gas as the primary fuel. They can also burn gasoline, diesel, and alcohol. The generator is typically a high-speed permanent magnet generator (PMG) and produces high frequency electricity. Hence, the generator cannot be connected directly to the grid. The

power electronic (PE) interface is used to rectify the high frequency AC to the DC first and then convert the DC to AC which is compatible with the connecting electric power system.

E. Fuel cells

Fuel cells are electrochemical devices producing electricity continuously through the chemical reaction between the fuel (on the anode side), such as liquid hydrogen, and an oxidant (on the cathode side), in the presence of an electrolyte. There are several different types of fuel cells are currently available including phosphoric acid, molten carbonate, solid oxide, and proton exchange membrane (PEM). Fuel cells produce DC power, which requires a PE interface to convert DC to AC that is compatible with the electric power system.

F. Photovoltaic Systems

Photovoltaic (PV) systems directly convert solar light into electricity. PV modules consist of many photovoltaic cells, which are semiconductor devices capable of converting incident solar energy into DC current. Like fuel cells, PV modules also need a PE interface to convert DC power into AC power which is compatible with the electric power system.

G. Wind Systems

Wind power energy is derived from solar energy, due to the uneven distribution of temperatures in different areas of the Earth. Wind turbines convert wind energy (kinetic or mechanical) into electrical energy. Three basic types of wind turbine technologies are currently used for interconnecting with electric power systems: standard induction machine, doubly-fed induction generator (DFIG), and a conventional or permanent magnet synchronous generator. The last two designs require a PE interface to convert the electricity into AC power that is compatible with the electricity grid.

H. Energy Storage Systems

Energy storage can enhance the overall performance of DE systems. It permits DE to generate a constant output, despite load fluctuations or dynamic variations of primary energy (such as sun, wind, and hydropower sources). It enables DE to operate as a dispatchable unit and therefore benefits power systems by shaving the peak load, reducing power disturbances, and providing backup in the event of an outage. Energy storage systems include batteries, ultra-capacitors, flywheels, and superconducting magnetic storage system (SMES). Energy storage systems also require a PE interface.

1.1.3. Interconnection to Grid

The energy sources or prime movers in DE systems can be electrically connected to the power grid via three basic interconnection interfaces [5].

Synchronous Generator – Synchronous generators are rotating electric machines that convert mechanical power to electrical power. When connected to an electric power system, the rotational speed of the synchronous generator is constant, which is called the synchronous speed. The generator output is exactly in step with the power grid frequency. Synchronous generators are used when power production from the prime mover is relatively constant, e.g., most reciprocating engines and high power turbines (gas, steam, and hydro).

Induction Generator – Induction generators are asynchronous machines that require an external source to provide the reactive current necessary to establish the magnetic field. They are suited for rotating systems in which prime mover power is not stable, such as wind turbines and some small hydro applications. Induction generators require a supply of VARs from capacitors, the electric power system, or PE-based VAR generators.

Power Electronics – PE systems convert power statically, which provides an interface between a non-synchronous DE and a power system so that the two may be properly interconnected. PE technologies are based on power semiconductor devices, digital signal

processing technologies, and control algorithms. Certain DE systems produce DC voltage, e.g. fuel cells, PV devices, and storage batteries. In order to connect them with the AC power systems, DC-to-AC inverters are required to convert the DC voltage into AC with the frequency and voltage magnitude specified by the local utility. For a DE system producing non-synchronous AC electricity, like a microturbine, an AC-to-DC rectifier is used to transform AC into DC first and then convert DC to AC by using a DC-to-AC inverter.

Due to the flexible controllability both on the active power and reactive outputs plus a fast response speed, PE interfaces have great potential to benefit interconnected power systems. A variety of ancillary services exist in distribution systems than can be supplied by PE-interfaced DE systems. The ancillary services include: voltage control, harmonic compensation, load following, spinning reserve, supplemental reserve (non-spinning), backup supply, network stability, and peak shaving [7][8]. The capability for providing additional ancillary services makes DE systems very cost effective.

The three types of interface technologies are summarized in Figure 1.2. Although PE interfaces add additional costs to the DE systems, they enable additional controllability and flexibility in integrating the DE with the power systems and provide beneficial ancillary services for the grid support. As the price of PE and associated control systems decrease, this type of interconnection interface will become more prevalent in all types of DE systems.

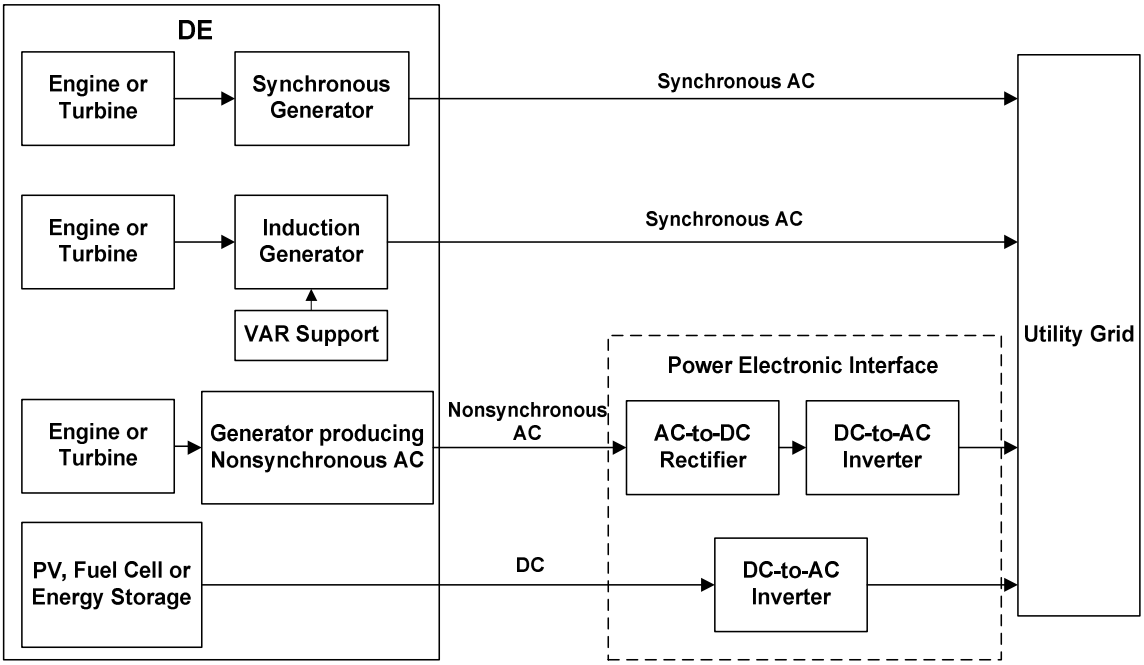


Figure 1.2. Interconnection Interfaces of DE with Power Systems.

1.1.4. Voltage Regulation by DE with PE Interface

A DE with a PE interface can provide a wide range of ancillary services, including voltage regulation which has drawn much interest because of the reactive power shortage and transportation problems in power systems. In this section, the implementation of a PE interface and control design for voltage regulation is introduced.

Figure 1.3 shows a parallel connection of the DE with a distribution system through a PE interface. The PE interface includes the inverter, a DC side capacitance or v_{dc}, and a DE such as a fuel cell, solar panel, or energy storage supplying a DC current. Coupling inductors L_c are also inserted between the inverter and the rest of the system. The PE interface is referred to as the compensator because voltage regulation using the DE is our primary concern. The compensator is connected, in parallel, with the load to the distribution system, which is simplified as an infinite voltage source (utility) with a system impedance of R_s+jωL_s.

The parallel compensator is connected through the coupling inductors L_c at the point of common coupling (PCC). The PCC voltage is denoted as v_t. By generating or consuming a certain amount of reactive power, the compensator regulates the PCC voltage v_t.

An instantaneous nonactive power theory [9][10] is adopted for the real-time calculation and control of DE voltage regulation. Here, nonactive power can be referred to as reactive power in the fundamental frequency plus non-fundamental frequency harmonics. In all the following equations, all the definitions are functions of time t. For instantaneous voltage $v(t)$ and instantaneous current $i(t)$:

$$\boldsymbol{v}(t) = [v_a(t), v_b(t), v_c(t)]^T \tag{1.1}$$

$$\boldsymbol{i}(t) = [i_a(t), i_b(t), i_c(t)]^T \tag{1.2}$$

Instantaneous real power p(t) and average real power P(t) are defined as:

$$p(t) = \boldsymbol{v}^T(t)\boldsymbol{i}(t) = \sum_{k=1}^{3} v_k(t) i_k(t) \tag{1.3}$$

$$P(t) = \frac{1}{T_c} \int_{t-T_c}^{t} p(\tau) d\tau \tag{1.4}$$

In a periodic system with period T, T_c is normally chosen as integral multiples of $T/2$ to eliminate current harmonics.

$V(t)$ and $I(t)$ are defined as:

$$V(t) = \sqrt{\frac{1}{T_c} \int_{t-T_c}^{t} \boldsymbol{v}^T(\tau)\boldsymbol{v}(\tau) d\tau} \tag{1.5}$$

$$I(t) = \sqrt{\frac{1}{T_c} \int_{t-T_c}^{t} \boldsymbol{i}^T(\tau)\boldsymbol{i}(\tau) d\tau} \tag{1.6}$$

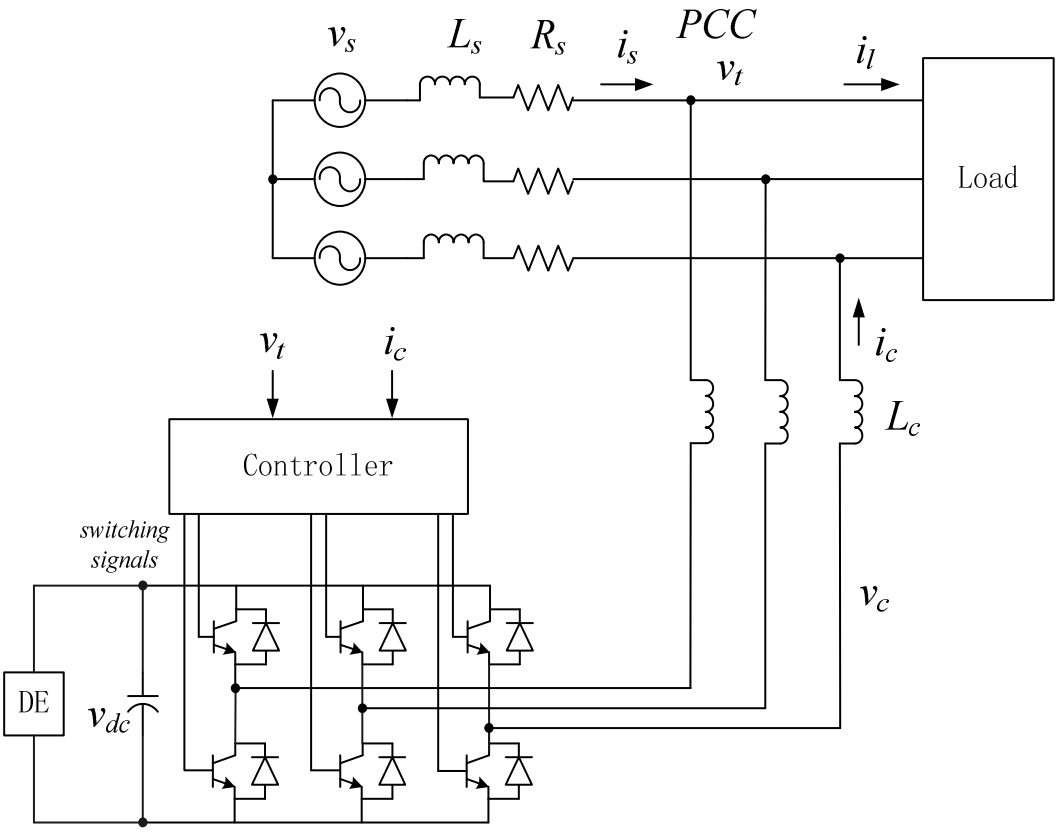


Figure 1.3. Parallel connection of a DE with PE converter.

As pointed out in [9][10], the generalized definition of nonactive power extends the traditional definition of instantaneous nonactive power from three-phase, balanced, and sinusoidal systems to more general cases. This unique feature makes it easy to apply in practical distribution systems in which there are challenges like single-phase, non-sinusoidal, unbalanced, and non-periodic waveforms. Therefore, it is suitable for real-time control in a real-world system and provides advantages for the design of control schemes.

A voltage regulation method is developed, based on the system configuration in Figure 1.3, with a PI feedback controller. The control diagram is shown in Figure 1.4. The PCC voltage, v_t is measured and its RMS value, V_t, is calculated. The RMS value is then compared to a voltage reference, V_t^* (which could be a utility specified voltage schedule and

possibly subject to adjustment based on load patterns like daily, seasonally, and on-and-off peak).

The error between the actual and reference is fed back to adjust the reference compensator output voltage v_c*, which is the reference for generating the pulse-width modulation (PWM) signals to drive the inverter. A sinusoidal PWM is applied here because of its simplicity for implementation. The compensator output voltage, v_c is controlled to regulate v_t to the reference V_t^*. The control scheme can be specifically expressed as:

$$v_c^* = v_t(t)[1 + K_p(V_t^*(t) - V_t(t)) + K_I \int_0^t (V_t^*(t) - V_t(t))dt] \quad (1.7)$$

where K_P and K_I are the proportional and integral gain parameters of the PI controller.

Equation (1.7) leads to reactive injection only when v^*_c is in phase with v_t. However, if a real power injection is also needed, it can be simply implemented using a desired phase angle shift applied to v^*_c in Eq. (1.7) because of the tight coupling between real power and phase angle.

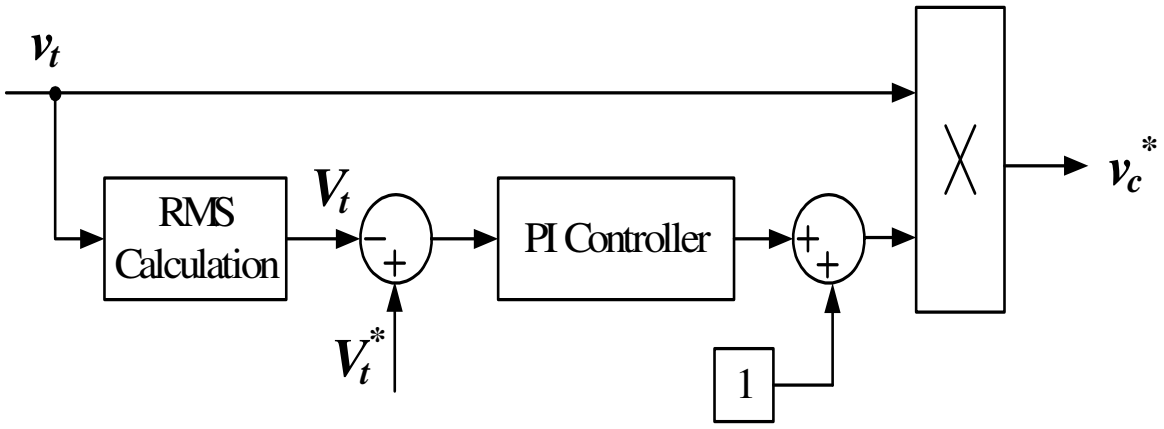


Figure 1.4. Control diagram for voltage regulation.

1.2. Motivation

Reactive power supply is the key controller of voltage in alternating current power systems. The supply of reactive power, as with capacitive loads, will cause voltage to rise; conversely, the absorption of reactive power, as with inductive loads, will cause voltage to drop. Dynamic sources of reactive power can rapidly change the amount of reactive power supplied or absorbed. Currently, generators and solid state devices such as static Var compensators are the most common dynamic sources of reactive power. A shortage of reactive power may contribute to cascading outages. For example, during the blackout of August 14, 2003, all the reactive reserves in northern Ohio were exhausted, and the voltage continued to fall and became unstable. Reactive reserves must be available to support voltage during contingencies. Moreover, reactive power supplied locally has much more impact than reactive power supplied from distant generators since reactive power supplied from distant generators must flow on transmission lines, where it is absorbed. Reactive power supplied locally could be a major component in improving system reliability, as well as improving system efficiency by reducing congestion. From the system reliability and safety point of view, exploitation of the reactive power capability of DE is imperative.

Using DE for Var support/voltage regulation is also cost effective. DE have been undergoing great developments. The total installed U.S. DE capacity, for those smaller than 5MW, is estimated to be 195GW, among which the reactive-power-capable DE are presently estimated at approximately 10% of the total installations [6]. If DE systems were designed to provide reactive power at the time of purchase, this amount could easily be 90% of the total installations. The generators are typically capable of operating at a 0.8 to 0.9 power factor. Thus, 200,000 MW of DE thus equipped could provide nearly 100,000 to 150,000 MVar of reactive power. The power and current ratings of the power electronics interface are required

to be larger to provide both active and reactive power instead of only active power, while the DE ratings should remain the same. If the power factor is 0.9, 0.48 MVar reactive power is provided from a 1 MW DE, i.e., the reactive power is 48% of the active power. The power and current ratings (i.e., capital costs) of the power electronics interface need to be only 11.1% larger than the no reactive power service case. If the DE can run at a 0.8 power factor, 0.75 MVar reactive power can be supplied from a 1 MW DE, and the power and current ratings are only increased by 25%. The reactive power capability is significant when compared to the additional costs incurred, which can create savings on the investment of additional Var compensation equipment.

Voltage control with DE at local buses also helps increase the DE penetration level in the grid. The injection of real power from DE into the grid causes voltage to rise at the PCC bus. If the connection bus's voltage is not controlled, the voltage will exceed the acceptable upper limit as the injection keeps increasing. A reasonable way to accommodate more DE capacity in the grid is to control the voltage at PCC by DE itself.

The advantages of using DE for Var support/voltage regulation have drawn much research interest. Much research work has been done in designing PE interface topologies and control schemes from a power electronic study point of view, which usually simplifies the power systems as an AC source and a load. However, power systems are quite dynamic and complicated. The different operation situations may affect the performance of the PE based DE with embedded voltage regulation function. How to integrate them into the power grid and make them perform properly still needs to be investigated. Therefore, in summary, the motivation of this dissertation is to investigate how to effectively perform voltage control with DEs from a "system" viewpoint.

1.3. Dissertation Outline

Literature relevant to this work is briefly reviewed in Chapter 2.

Chapter 3 addresses the challenge in the gain parameters of the PE controller introduced in section 1.1.4 and investigates, by means of simulations, what factors may affect the appropriate range of the gain parameters. The simulation results clearly show that the gain parameters determine the voltage regulation process, which stimulates the need for a solution to identify control parameters in real time for easy utility application.

In Chapter 4, an adaptive voltage control method is proposed to dynamically adjust control parameters to respond to system changes in the case of single DE regulating voltage. Theoretical analysis shows that a corresponding formulation of the dynamic control parameters exists; hence, it justifies the proposed adaptive control method. Both simulation and field experiments at the Distributed Energy Communications and Controls (DECC) Laboratory at the Oak Ridge National Laboratory were completed to test this method.

Chapter 5 addresses the application of the adaptive control methods in the case of multiple DEs participating in voltages regulation. The challenges raised by multiple DEs regulating voltages are identified. Theoretical analysis proves the formulation of the dynamic control parameters also exists in the case of multiple DEs participate in voltage regulation. Based on the availability of communications among voltage-regulating DEs, two control methods with or without communication, respectively, are proposed. Simulation results show that each method, with or without communications, can satisfy the fast response requirement for operational use without causing oscillation, inefficiency or system equipment interference, although the case with communication can perform even faster and more accurate.

Chapter 6 concludes the approach and methodology and points out the possible future work.

1.4. Summary of Contributions

The contribution of the work can be summarized as follows:

- It validates that the proportional-integral (PI) control parameters are critical to the stability of the voltage regulation with the DEs.
- It proposes an adaptive voltage control approach using PI feedback control for the case of single voltage-regulating DE as well as multiple DEs without communication. This adaptive voltage control based on local information only has a wide adaptability and is easy to implement by practicing engineers since it does not require detailed system data.
- It presents a theoretical analysis that proves the existence of a corresponding analytical formulation of the dynamic control parameters, KP and KI for the adaptive approach in the case of single voltage-regulating DE as well as the case of multiple voltage-regulating DEs. Since the theoretical formulation requires detailed system parameters, it is not preferred for practicing utility engineers. However, the analytical formulation shows that the adaptive approach has a solid theoretical foundation.
- The simulation and field experiment results in the case of single DE regulating voltage show that the proposed adaptive approach satisfies the rapid response and performance requirements needed for integration with existing system equipments.
- In the case of multiple voltage-regulating DEs, a high-end solution with extensive communication is also proposed. This can be viewed as a benchmark for the low-cost approach without communication. Though both approaches meet the

performance requirement very well as evidenced by the voltage response close enough to the ideal curve, this high-end solution with communication performs even faster and more accurate. Hence, it may be also useful for some special cases requiring superior performance.

2 Literature Review

2.1. Chapter Introduction

This chapter briefly reviews the existing works that are relevant to this work. Discussions include voltage control in distribution systems with DEs and PE interfaces design to implement voltage regulation. Also, the scope of the work is clarified.

2.2. Voltage Control in Distribution Systems with DEs

It is critical to maintain an acceptable voltage range at several key buses in a power system, such as a distribution substation, where the voltage will be stepped down from the sub-transmission level to the distribution level. The present voltage regulation is achieved mainly by regulating transformers with under load tap changing (ULTC) equipment at the substation and reactive-power-source devices, such as shunt capacitors, shunt reactors, synchronous condensers, static var compensators (SVC), and static synchronous compensators (STATCOM) [2].

ULTC transformers can regulate the voltage at the sending end and hence the voltage along the feeder. However, ULTC does not actually supply any reactive power when the transformer ratio adjusts, but merely re-distributes the power from the bus at the primary end of the transformer to the bus at the secondary end. Hence, it may cause the voltage at its primary end to drop significantly below the limit [2] [11]. Moreover, occasionally conflict in the voltage regulation directions may occur, such as the sending end is above the upper limit while the receiving end is below the lower limit.

Reactive power compensation devices are technically more effective if connected near the loads rather than at the substation. The large centralized reactive power support is easy to operate and maintain; however, it may yield unsatisfactory results, e.g. the voltage at the far bus is still low while the voltage at the near bus already exceeds the upper limit. Therefore, multiple small sized var resources spread across the distribution system versus a few large ones is more favorable [11]. Using dispersed DEs in the distribution systems for var support may take full advantage of these characteristics regarding the var/voltage support [12].

DE systems invoke challenges on conventional operations as well as providing benefits. With the increasing injection of active power from the DE, the voltage at the PCC will swell and exceed the upper limit of the acceptable range. In addition, for some DE systems with intermittent energy resources such as PV and wind, the voltage fluctuation at the PCC, caused by the changing active power injection, needs to be addressed as well [13][14]. How to accommodate more DE capacities in the grid and at the same time keep the voltage stable in an acceptable range has drawn much interest [15]-[36].

Conventional voltage regulation measures are applied to integrate the DE [15]-[18]. Voltage regulation performed by ULTC calls for two parameters: the equivalent impedance and the load center voltage. Therefore, in distribution networks with DG interconnections, these parameters should be designed with attention not only to load variations, but also to DE outputs. Reference [18] proposes a method for designing ULTC parameters with reference to variations of the DG outputs. The tests on the IEEE 13-bus system and a real network validate that the modified parameter design method is capable of maintaining the voltage at the sending end, in the acceptable range, with respect to the varying DG outputs.

The automatic voltage reference setting techniques are proposed in [15][17]. These methods provide a voltage reference setting for existing automatic voltage control (AVC)

relays and OLTC transformers to increase the DG that may be connected to the feeders. The technique measures essential voltages along multiple feeders or a statistical state-estimation algorithm which could be used to estimate the voltage magnitude at each network node based on limited measurement points [17]. The maximum and minimum voltages from the voltage measurements are selected and compared to the feeder voltage limits. The results are then used to determine a new voltage reference for the AVC relay.

As discussed previously, conventional voltage control methods may fail to satisfy the voltage requirements along the feeders. A controllable DE should be included in the voltage regulation practice. The unity power factor working mode cannot handle the voltage problem. Therefore, a voltage control mode should be permitted for countering steady-state overvoltage for distribution systems with DE to maximize their utilization [19].

The dispatch of reactive power outputs of the DE along with real power outputs is a way to control voltage across the distribution system. This type of method typically uses a constrained optimal power flow (OPF) as the tool to find the set points of the DE outputs and the voltage schedule for the system [20]-[23].

Reference [20] presents a coordinated voltage control method integrating conventional voltage regulation mechanisms with DE reactive power production, assuming the availability of a distribution management system. The constrained OPF algorithm with the objective of network loss reduction is used for voltage control at the distribution network considering transformer taps, condenser switching, and DE reactive power injections as control variables while operating limits are ensured to keep bus voltages in the statutory range and line loading below the maximum limit for the effective integration of DE into the power system operations. Additionally, a virtual power plant (VPP) concept is introduced, which is the representation of the aggregated capacity of DE under one single profile

operated as one unique entity from the viewpoint of any other power system factor. A VPP hides the inherent complexity and make the analysis or control of the entire system easier.

A combined real power and reactive power dispatch strategy is developed in [22][23]. The proposed approach is composed of two stages: a day-ahead economic scheduler that calculates the active power set points during the following day in order to minimize the overall costs; and an intra-day scheduler that, on the basis of measurements and short-term load and renewable production forecasts, updates the DE set points for both real and reactive power every 15 minutes for optimizing the voltage profile. The implementation of this procedure requires a centralized management as well.

Different from the conventional centralized optimization algorithm, a multi-agent based optimization approach is proposed in [24] that solves the dispatching problem in a distributed manner without the need for the exact system model. It models the problem as a reactive power dispatch problem with node voltage constraints, DE var capacity constraints, and power flow constraints. Each agent has the ability to sense its local variables to reformulate the optimization problem. Modest communication is needed among the multiple agents and thus the investment could be saved on the distribution management system that is necessary for the centralized optimization methods.

Market signals could also be utilized to aggregate the DE for the voltage support. An incentive based control for influencing active power flow with bidirectional energy management interfaces is proposed and tested in [21], along with tests on the direct reactive power control via the VPP approach and a parallel application of the two. The experimental results confirm that the voltage can be influenced effectively with both approaches, but the combination of both approaches is technically feasible and more effective.

In the presence of a distribution control center and communication infrastructure, optimization based methods can yield optimal solutions for the voltage regulation. However, for systems with no communication infrastructure, decentralized methods are more favorable.

Reference [26] proposed a local, intelligent, and auto-adaptive voltage regulation scheme for setting the voltage reference of the DE due to the lack of distribution system communication. A desired voltage window, encompassed by the admissible voltage window, is adaptively defined by the fuzzy logic based method. This window moves according to the quantity of reactive power provided or absorbed compared with the physical limits of the DE considered. The active power generation of the DG is also regulated in case the voltage exceeds the admissible range.

A local reactive power droop control is a decentralized reactive power sharing method. Droop functions are defined between the reactive power generation and the voltage deviation with the relation that the reactive power generation of the DE is increased with the decrease of actual voltage. A droop function can be linear or nonlinear [27]. Each DE operates in correspondence with local information and does not require communications, though it may not result in optimal solutions when compared to optimization based methods. The droop control method is usually embedded in the PE interface design [29]-[33].

A comparison of centralized control and decentralized control is performed in [28]. Optimal power flow is used to compare the centralized voltage control or active management and intelligent distributed voltage control of the DE. This shows that the latter one provides similar results to those obtained by centralized management in terms of the potential for connecting increased capacities of DE within existing networks.

The studies discussed so far are in steady state area. They address the voltage regulation with DE from a perspective of voltage reference setting. The following researches

[34]-[43] focus on the local PE interface designed to implement the voltage regulation function with the DE.

2.3. PE interfaces Design to Implement Voltage Regulation

PE interface devices are used to convert DC or AC power at an asynchronous frequency to AC power synchronized with the grid. Voltage source inverters (VSI) have been widely used in the interface design [36]-[42]. According to their control mechanism, VSIs can be classified as voltage controlled VSIs (VCVSIs) and current controlled VSIs (CCVSIs) [39]. VCVSIs use the amplitude and phase of an inverter output voltage to control the power flow, which can be viewed as a voltage source from the grid side. Coupling impedance is used to connect VCVSIs to the grid. A CCVSI uses switching instants to generate the desired current flow, which can be viewed as a current source. Therefore, only VCVSI can provide voltage support. Since the coupling of real power with voltage phase angle and reactive power with voltage magnitude, real power control can be realized through changing the phase shift between the inverter and the grid voltage; while voltage control can be realized by changing the amplitudes of the inverter output voltages in individual phases [36][42].

In the PE interface design from a power electronic point of view, the grid is usually simplified as an infinite system with equivalent impedance [37]-[40]. Most work focused on the control method structure design [31]-[44]. However, how to ensure that control parameters for voltage-regulating DE work efficiently and effectively using a systematic approach needs study.

Reference [45] analyzes the robust stability of a voltage and current control solution for a stand-alone DG unit using the structured singular value based method. A linear quadratic optimal control cost function is defined with scalar weighting which can be tuned to

achieve the desired transient performance while maintaining the stability robustness of the system under perturbations. Best tuning parameters are found by comparing the simulation results of the transient performance of the controller under different tuning parameters.

In control design, usually some root-mean-square value and average value are involved, such as the average real power in Eq. (2.1). Considering time shifting characteristic of Laplace transform, it can be transformed into Laplace *S* domain as Exp. (2.2). Since the existing of e^{-sT_c}, it is difficult to analyze the model. First order Padé approximation, presented in Exp. (2.3), is used in [30] to construct an approximate characteristic equation based on small signal stability analysis. The model could be used to find a range for controller parameters.

$$P = \frac{1}{T_c}\int_{t}^{t-T_c} p(t)dt \tag{2.1}$$

$$P(s) = \frac{1-e^{-sT_c}}{T_c s}p(s) \tag{2.2}$$

$$e^{-sT_c} \approx \frac{2-T_c s}{2+sT_c s} \tag{2.3}$$

The approximation method provides a way to analytically study the models involving time shifting characteristic, though the accuracy may not meet the requirement in some applications.

Optimal control methods could be used in the controller parameter tuning. A dynamic model of a wind turbine with DFIG, including its converters and controllers, is presented in [46], based on which the model for small signal stability analysis has been established. A parameter tuning method based on partial swarm optimization (PSO) is proposed to optimize the parameters of the controllers.

2.4. Scope of this Work

The problem of setting controller parameters of the PE interfaced DE for voltage regulation introduced in Section 1.1.4 is considered in this work. Several general assumptions are taken exclusively in the work.

- The power system under study is assumed to be a three phase synchronous power system with balanced loads and system components. Therefore, a one-line diagram will be used for better illustration.
- An aggregated network model is adopted. For example, a distribution line will be modeled as a resistance and reactance connected in series.
- The load is modeled as constant impedance. Future work will investigate the dynamic impact of the load.
- The DE is modeled as a constant voltage source neglecting the additional components on the DC voltage control since the local AC voltage control function of DE is the main concern of this work.

An adaptive voltage control method has been proposed to dynamically modify control parameters to respond to system changes. Theoretical analysis shows that a corresponding formulation of the dynamic control parameters exists; hence, the adaptive control method is theoretically solid. Simulation and field experiment test results in the case of single DE regulating voltage at the Distributed Energy Communications and Controls (DECC) Laboratory confirm that this method is capable of satisfying the fast response requirement for operational use without causing oscillation, inefficiency, or system equipment interference. Since this method has a high tolerance to real-time data shortage and is widely adaptive to variable power system operational situations, it is quite suitable for broad utility applications.

3 Challenges of the Control Parameters for Voltage-Regulating Distributed Energy Resources

3.1. Chapter Introduction

The implementation of the voltage control with the PE interfaced DE introduced in Chapter 1 is tested by simulation in a radial system. The factors affecting the dynamic performance of the controller are explored.

3.2. Factors Affecting Dynamic Performance of Controller for Voltage Control

The control method introduced in Chapter 1 is based on feedback control and the error between the PCC and reference voltage is the feedback signal. A simplified model representing the control of multiple DEs interfaced to the utility network is shown in Figure 3.1.

The control signal of the PI controller is applied to the inverter to generate a voltage at the PCC with the distribution system. Ideally the inverters generate the same voltage as their inputs. Thus, only the distribution network characteristics affect the response of the voltage regulation, and therefore affect the appropriate range of K_P, K_I. In the following study of the impact of a distribution network on the PI controller parameters, loads are modeled as constant impedance. The DEs including their PE interface are modeled as voltage sources. All the buses in the system are grouped into two types: voltage source buses where there is current injection (or absorption); and load buses where the current injection is zero. The analysis is in the Laplace S domain and the nodal voltage equation is shown in (3.1):

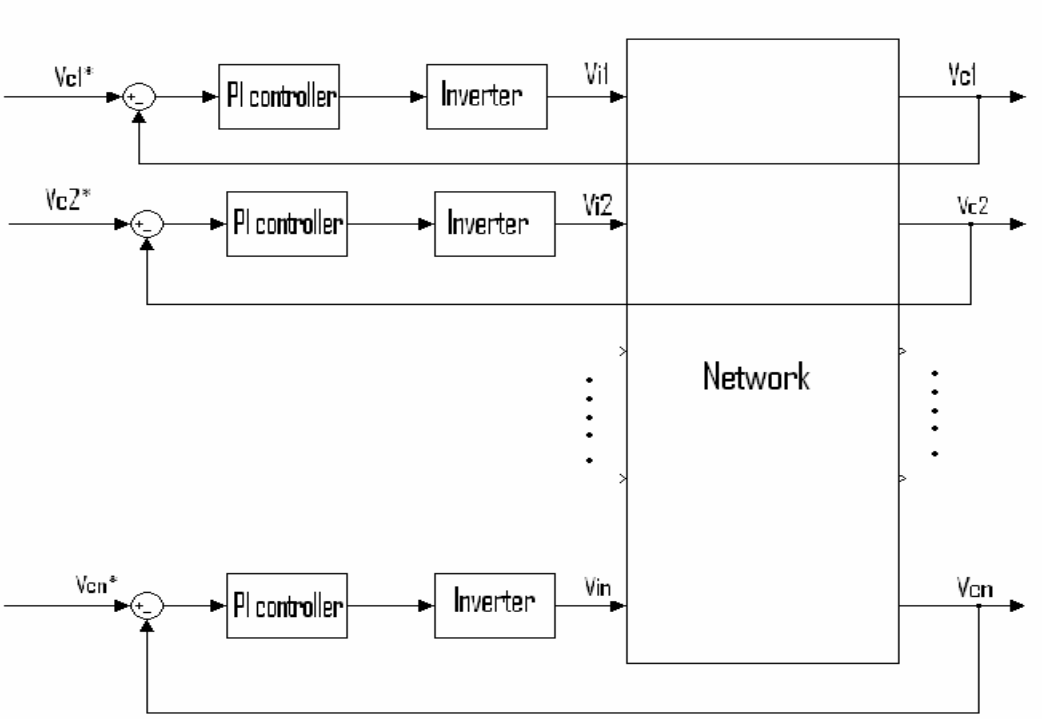


Figure 3.1. Simplified model of the distribution system with multiple controllable DEs interfaced to it.

$$\begin{bmatrix} I_G(S) \\ \underline{0} \end{bmatrix} = \begin{bmatrix} Y_{GG}(S) & Y_{GL}(S) \\ Y_{LG}(S) & Y_{LL}(S) \end{bmatrix} \begin{bmatrix} V_G(S) \\ V_L(S) \end{bmatrix} \tag{3.1}$$

where $I_G(S)$ is the vector of the current injection at the buses connected with the voltage sources; $V_G(S)$ is the corresponding voltage vector; $V_L(S)$ is the voltage vector of the load buses; and $Y_{GG}(S)$,$Y_{GL}(s)$,$Y_{LG}(S)$ and $Y_{LL}(S)$ are the sub matrix of the admittance matrix.

After network reduction, we acquire the voltages at the load buses as shown in Eq. (3.2), which includes the PCCs. It shows that the PCC voltages are a function of the network structure, line parameters and loads, and support from the voltage sources. Since the voltage at each PCC is the feedback signal, the parameters K_P, K_I of each PI controller are hence determined by those factors.

$$V_L(S) = -Y_{LL}^{-1}(S) * Y_{LG}(S) * V_G(S) \tag{3.2}$$

3.3. Simulations on Voltage Control with PE Interfaced DE

In this section the impact of K_P, K_I on the dynamic response of the voltage regulation and factors determining the range of K_P, K_I are tested in a radial distribution system with one DE and two DEs, respectively. The system diagram is shown in Figure 3.2. It is a typical radial distribution network with two DEs with a PE interface connected at bus 2 and bus 5, respectively. The only difference between the two cases is the omission of the DE at bus 5 for the single DE testing case.

3.3.1. Impact of KP and KI on Voltage Regulation

A. Single DE Test Case

The first case is the system shown in Figure 3.2 with only one DE at bus 2. Its PE controller was tested with different combinations of K_P and K_I. The different responses are shown in Figure 3.3. The straight green line is the reference voltage while the blue curve is the voltage at the PCC. The PCC voltage was 263 V before regulation and the reference voltage is set at 268 V for regulation. From 0 to 0.3s, there is no regulation and from 0.3s to 1.5s the compensation is performed. As shown in Figure 3.3, there is a stable range of K_P and K_I; Figure 3.3(a) shows a desirable dynamic response with a well designed K_P, K_I. If the systems is outside of this range, it becomes unstable, as is shown in Figure 3.3(b). Even in the stable range, inappropriate values for K_P and K_I may cause an undesired response; the compensation speed is too slow due to a too small value of K_I value as in Figure 3.3(d) or an overshoot and oscillation at the start, as shown in Figure 3.3(c).

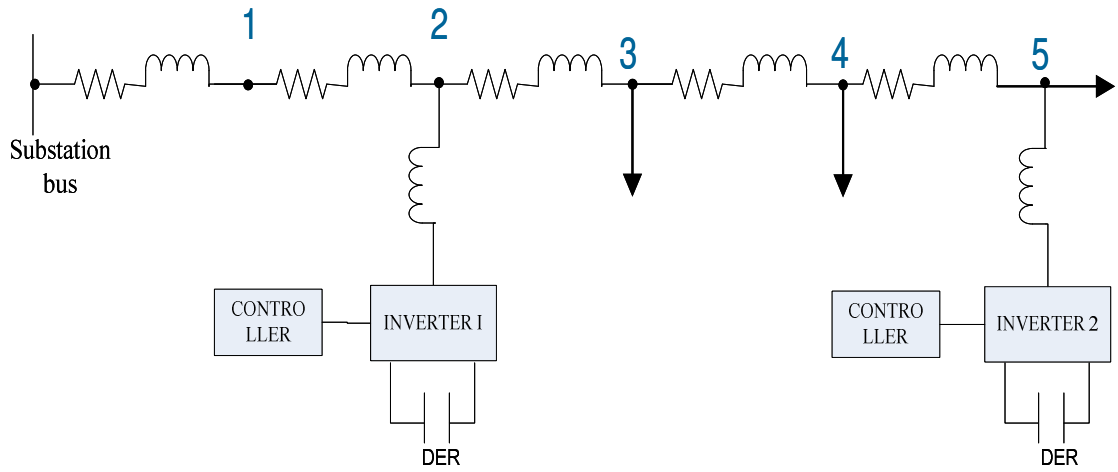
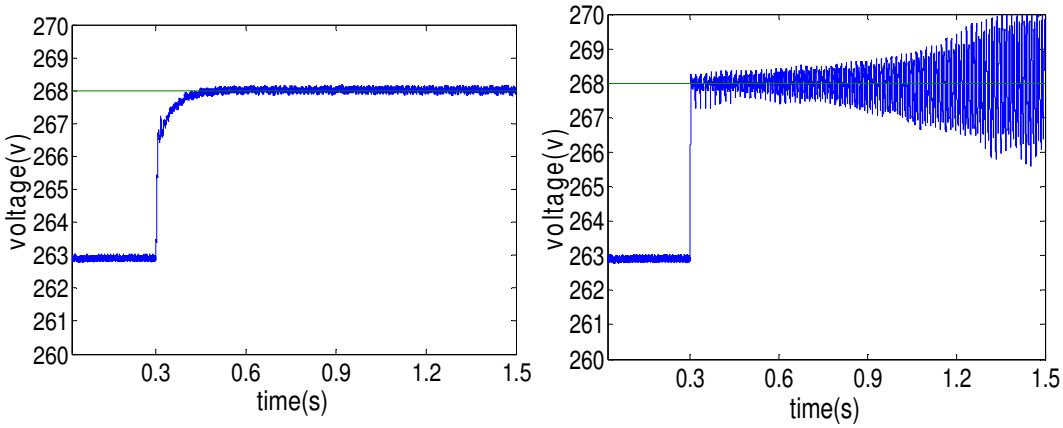
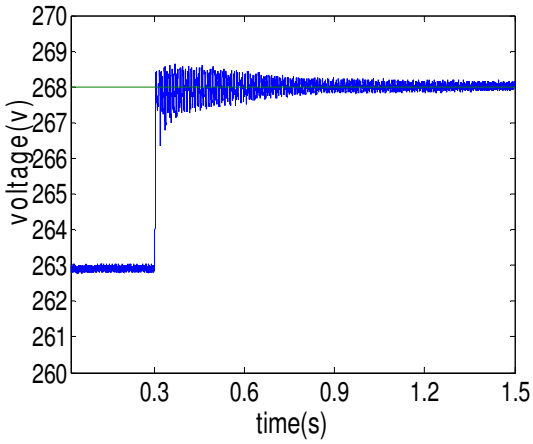


Figure 3.2. Single line diagram of the distribution system with DEs.

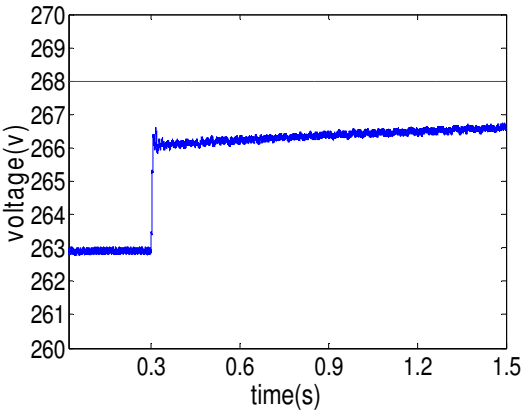


(a) K_P=0.03 K_I=0.8

(b) K_P=1 K_I=7



(c) K_P=0.2 K_I=3

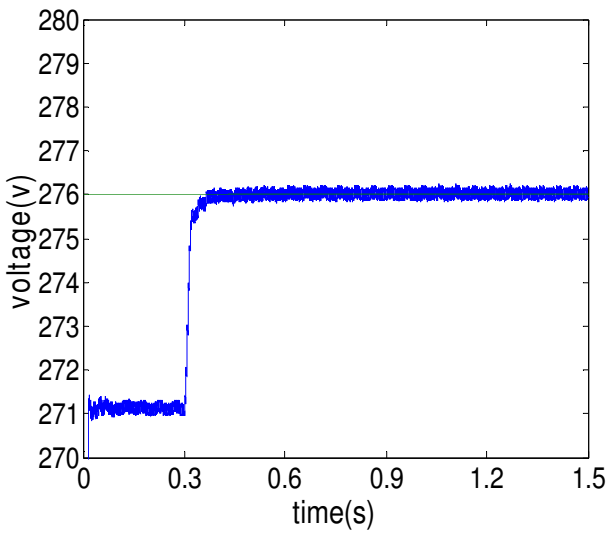


(d) K_P=0.01 K_I=0.1

Figure 3.3. Voltage regulation with different control parameters-single DE case.

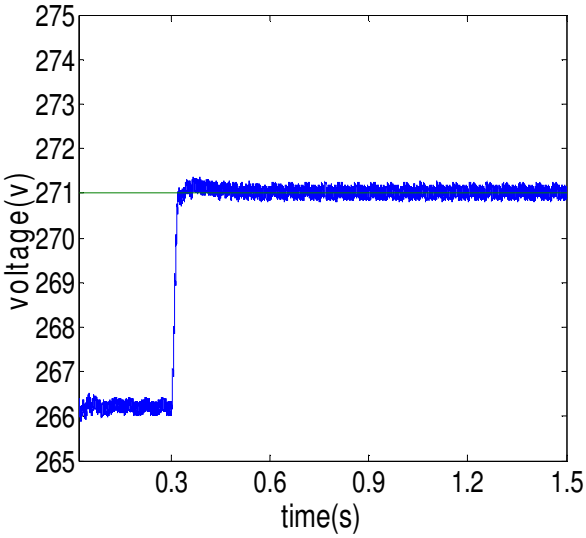
B. Two DEs Test Case

Next, the distribution system with two DEs was tested with different combinations of K_P and K_I. The test results are shown in Figure 3.4. The figures in the left column show the voltage response at bus 2 with respect to differing K_P and K_I while those in the right column show the voltage at bus 5 for the same changes in the gain parameters. Prior to 0.3s, there is no regulation and from 0.3s to 1.5s the compensation is performed. Similar to the single DE case, the value of K_P and K_I determines the response of the voltage regulation. However in the case with two DEs, the range of K_P and K_I becomes different, which is clearly demonstrated by comparing Figure 3.3(c) with Figure 3.4(b1) and Figure 3.4(b2). Even with the same value of K_P and K_I, the two DE case is unstable while the one DE case is stable. This suggests that the parameter range suited for a single DE case may not be directly used for voltage regulation with multiple DEs. In order for both cases to work together correctly, a coordinated design of the controller parameters for the multiple DEs is required.



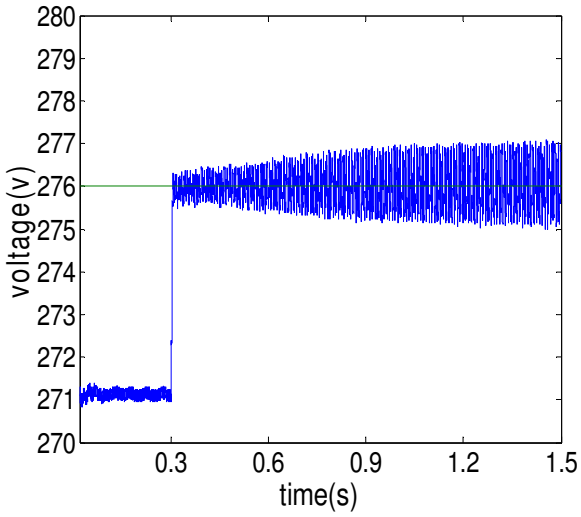
(a1) Voltage at bus 2 when

K_{P1}= K_{P2} =0.01, K_{I1}= K_{I2}=0.8



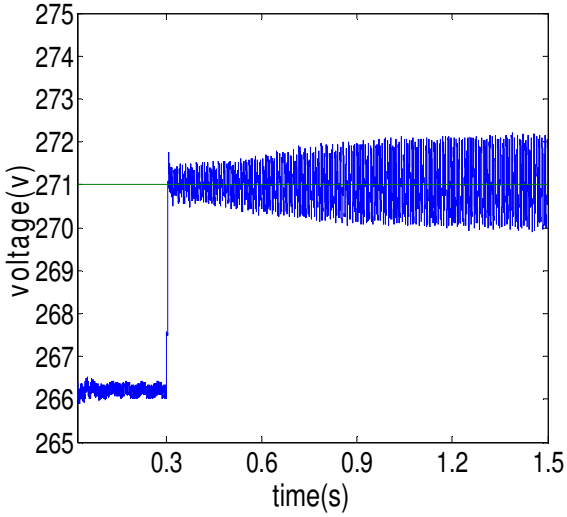
(a2) Voltage at bus 5 when

K_{P1}= K_{P2} =0.01, K_{I1}= K_{I2}=0.8



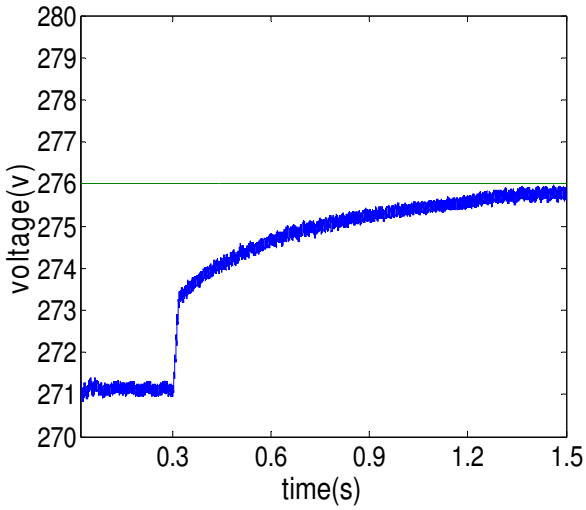
(b1) Voltage at bus 2 when

K_{P1}= K_{P2} =0.2, K_{I1}= K_{I2}=3



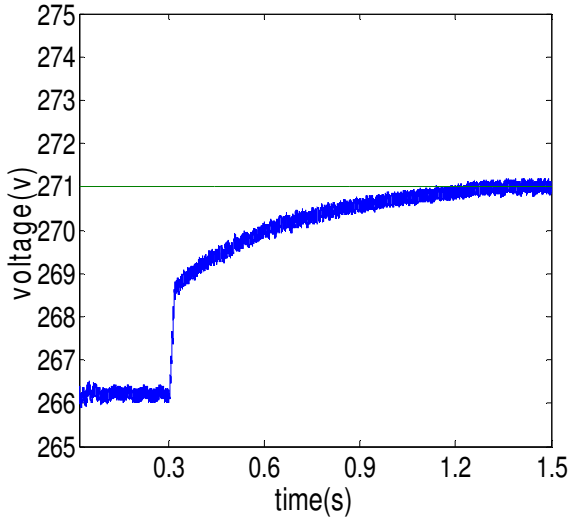
(b2) Voltage at bus 5 when

K_{P1}= K_{P2} =0.2, K_{I1}= K_{I2}=3



(c1) Voltage at bus 2 when

K_{P1}= K_{P2} =0.01, K_{I1}= K_{I2}=0.05



(c2) Voltage at bus 5 when

K_{P1}= K_{P2} =0.01, K_{I1}= K_{I2}=0.05

Figure 3.4. Voltage regulation with different control parameters-two DEs case.

3.3.2. Impact of DE Location on Voltage Regulation

From the previous analysis of the factors determining the controller parameters, we can see that the locations of the DEs affect the grouping of the buses; hence, they affect the structure of the reduced network and finally affect the appropriate range of the controller parameters. In this section, the results of the two cases with respect to DE location are investigated, respectively.

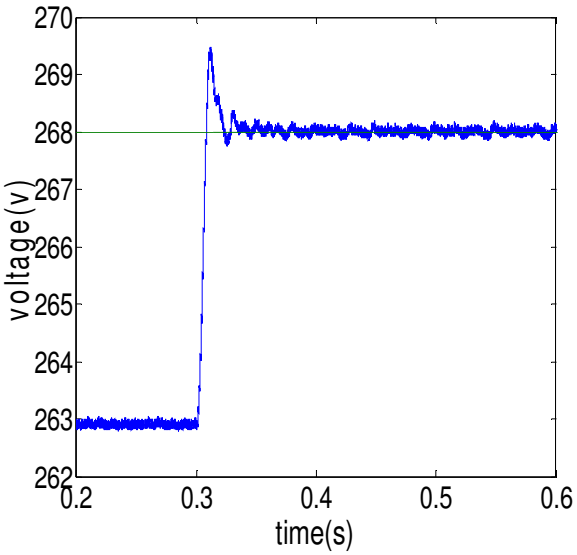
A. Single DE Test Case

Figure 3.5(a) and Figure 3.5(b) show the voltage responses corresponding to the DE at bus 2 and at bus 5, respectively. A more dynamic oscillation exists when the DE is connected at bus 5, although the responses are quite similar and both eventually reach the steady state.

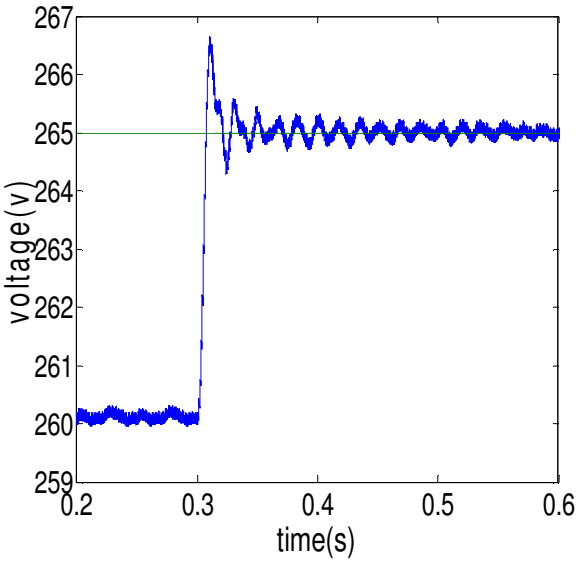
B. Two DE Test Case

In this case, the impact of the DE's location on voltage regulation dynamics is made more obvious by a comparison of Figure 3.6 and Figure 3.7. Figure 3.6 shows the voltage responses where the DEs are connected at bus 4 and bus 5. Figure 3.7 shows the voltage responses where DE1 is moved to bus 2 with all other conditions unchanged.

As is shown, the change of the DE1 location not only affects the voltage regulation of DE1itself, but also affects DE2 at bus5.

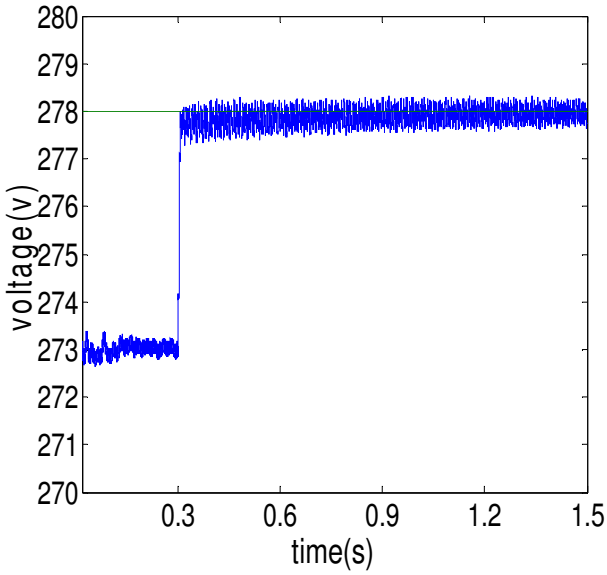


(a) DER at bus 2

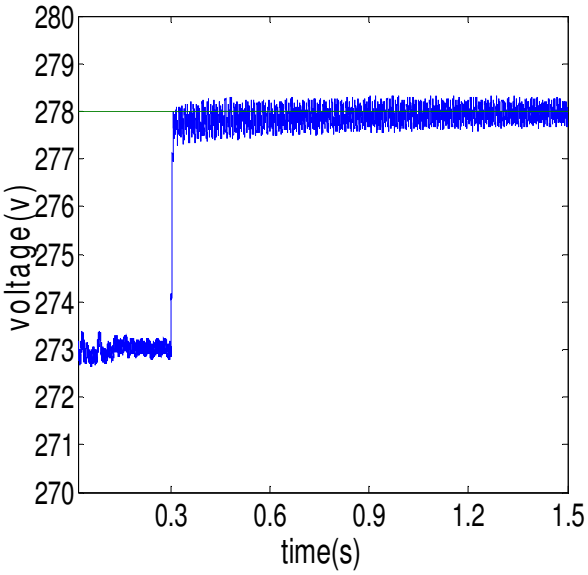


(b) DER at bus 5

Figure 3.5. Voltage regulation with different location of DE-single DE case.

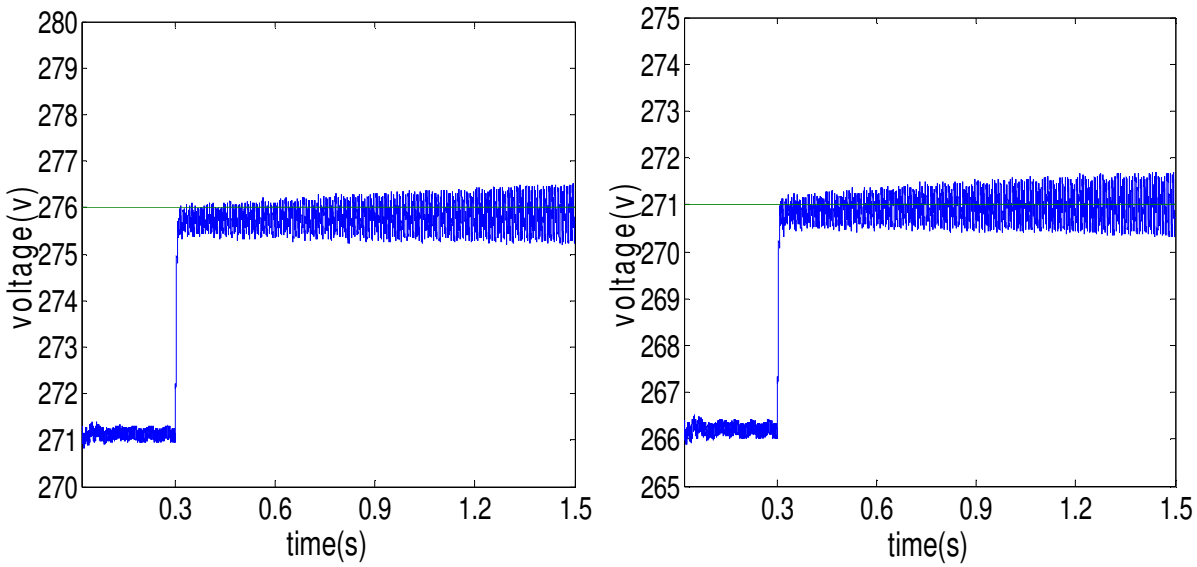


(a) Voltage response at bus 4



(b) Voltage response at bus 5

Figure 3.6. Voltage response when DE1 at bus 4 and DE2 at bus 5.



(a) Voltage response at bus 2

(b) Voltage response at bus 5

Figure 3.7. Voltage response when DE1 at bus 2 and DE2 at bus 5.

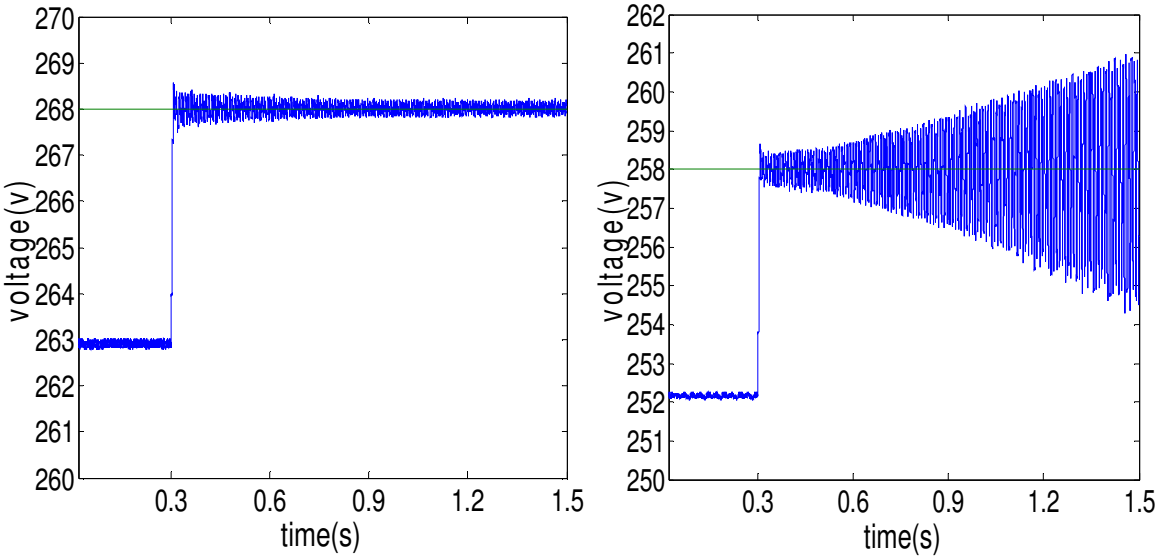
3.3.3. Impact of Loading Level on Voltage Regulation

The voltage regulation is also affected by the loading. In this study, the loads are modeled as constant impedances. Again the two cases with one DE and then two DEs are investigated to test the impact of the amount of the load, respectively.

A. Single DE Test Case

Figure 3.8 shows the impact of the load amount change on the voltage regulation response. For Figure 3.8(a), the load at bus 3 and bus 4 is 3.4kW+j2.2kVar and 50kW+j40kVar, respectively. For Figure 3.8(b) the load at bus 3 and bus 4 has been changed to 17kW+j0Var and 66.6kW+j40kVar. The difference caused by the load change is clear. In Figure 3.8(a) the voltage eventually reaches the desired steady state while, as shown in Figure. 3.8(b), the voltage oscillates into instability.

.



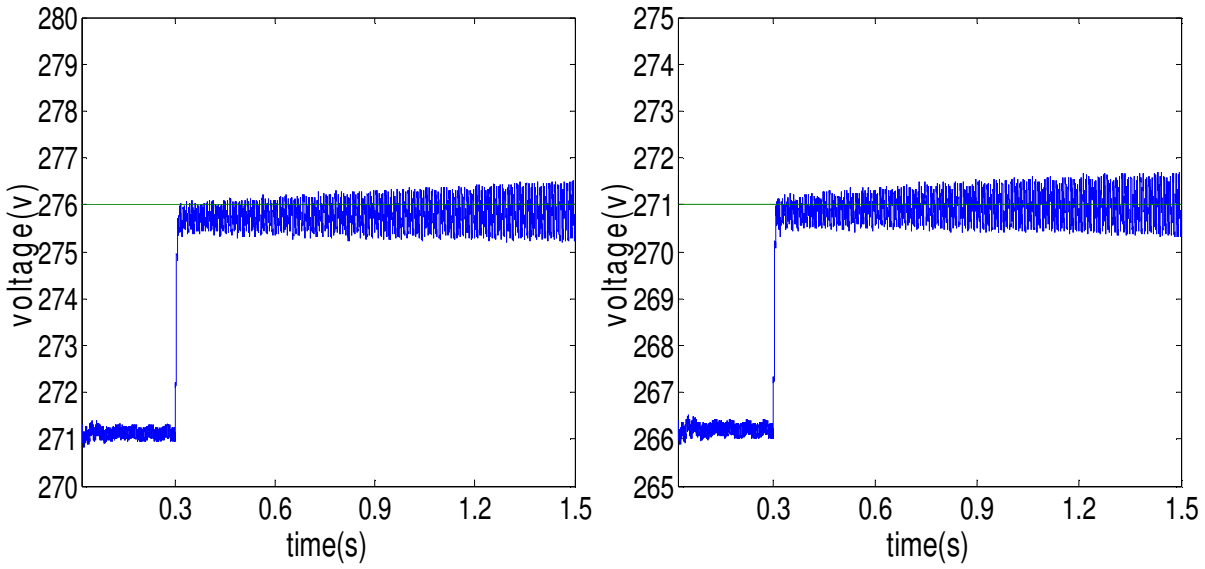
(a) Voltage response before load change

(b) Voltage response after load change

Figure 3.8. Voltage responses with different amount of load-single DE case.

B. Two DEs Test Case

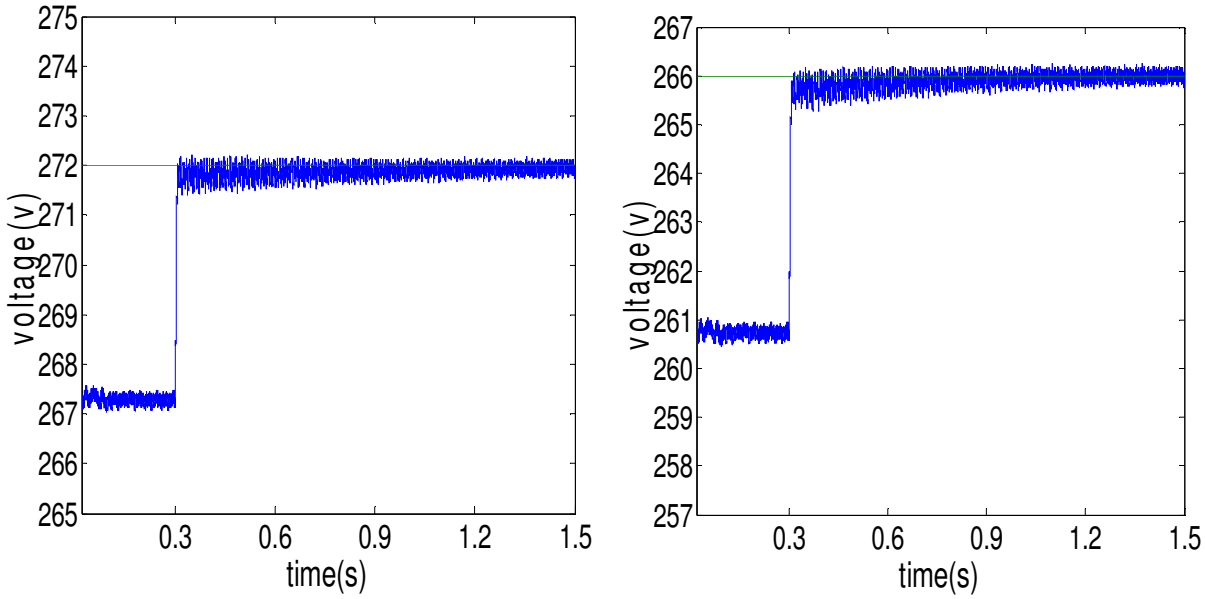
Figure 3.9 and Figure 3.10 show the voltage regulation responses before and after the real load at bus 3 increases by 13.6 kW. The gain parameters are the same for both load conditions: K_{P1}=0.21, K_{P2}=0.15, K_{I1}=0.15, K_{I2}=0.5. Comparing the voltage responses before and after the load change, the unstable system, before the load change, becomes stable after the load increases with the gain parameters fixed. The comparison clearly demonstrates that loading affects the voltage dynamic responses with DEs in the distribution system.



(a) Voltage at bus 2

(b) Voltage at bus 5

Figure 3.9. Voltage responses when load at bus 3 is 13.6kW+2.1kVar.



(a) Voltage at bus 2

(b) Voltage at bus 5

Figure 3.10. Voltage responses when load at bus 3 is 27.2kW+2.1kVar.

3.4. Chapter Summary and Discussion

The simulations clearly show that the PI controller parameters greatly affect the DE dynamic response for voltage regulation and that incorrect parameter settings may create an inefficient (slow), oscillatory, or worse, unstable response that can lead to system instability. Logically this raises an interesting issue, especially if a large amount of DEs with voltage regulating capabilities are deployed in the future:

How to ensure that control parameters for voltage-regulating DE work efficiently and effectively using a systematic approach?

It is not feasible for utility engineers to use a trial-and-error method to discern suitable parameters when a new DE is connected. Hence, an autonomous approach is needed. To address the parameter setting issue, a control scheme using intensive centralized communications may be possible such that commands from the substation are continuously sent to the DE for it to adjust its settings. Due to the uncertain and dispersed locations, and the expected high customer-based DE penetration, this centralized, intensive communication approach may be costly to install, maintain, and secure. Also, the contingency of a communications outage and how it impacts DE control, especially for major system conditions, would need to be considered. A stability analysis or optimal control based parameter tuning approach [30][45][46] may require detailed system parameters and real-time system information, and thus, fast communications. It may not be suitable for a real, large distribution system application.

Therefore, an autonomous and adaptive approach is much more advantageous for adjusting control parameters to regulate voltage with no or minimal communications (such as a voltage schedule provided with low-cost communications), especially for major system conditions, would need to be considered.

4 Adaptive Voltage Control with a Single DE

4.1. Chapter Introduction

An adaptive voltage control method, which does not require construction of a detailed dynamic model of the power system, is presented. Theoretic analysis, simulations, and field tests justify the proposed method.

4.2. Implementation of Adaptive Method for DE Controller

As shown in Chapter 3, if K_P or K_I is not chosen appropriately, the system response may be poor and at worst, create instability. So preventing a poor system response and optimizing the response speed are what is desired from the PI controller design. Thus the goal is to create an adaptive PI design that can dynamically adjust the PI controller in real-time based on the system's behavior and configuration. The proposed adaptive PI control method, inspired by the generic adaptive control method in [3][47][48], consists of three procedures:

- Determine the DC source voltage of the DE;
- Set the initial controller values, K_P and K_I; and
- Adaptively adjust the controller parameters according to real-time system conditions.

4.2.1. Determine the DC Source Voltage

The DE's PE interface with the utility is a VSI and the PWM method is used to convert the DC source voltage to an AC supply.

Figure 4.1 shows the relationship between $2V_c^p/V_{dc}$ and the modulation index m_a, where V_c^p is the peak voltage of the fundamental-frequency component of the compensator output voltage v_c and V_{dc} is the voltage of the DC supply.

As shown in Figure 4.1, for a given V_{dc}, V_c^p varies linearly with the modulation index m_a when it is 1.0 or less. It also shows that V_c^p should be less than $\frac{4}{\pi}\times\frac{V_{dc}}{2}$ for any m_a, even if it is under the saturated square-wave region. This means that V_{dc} determines the DE's ability to provide voltage regulation. To reduce the DE harmonic injection, m_a is chosen to be no greater than 1. Accordingly, we have:

$$V_{dc} \geq 2V_c^p = 2\sqrt{2}\times V_c \tag{4.1}$$

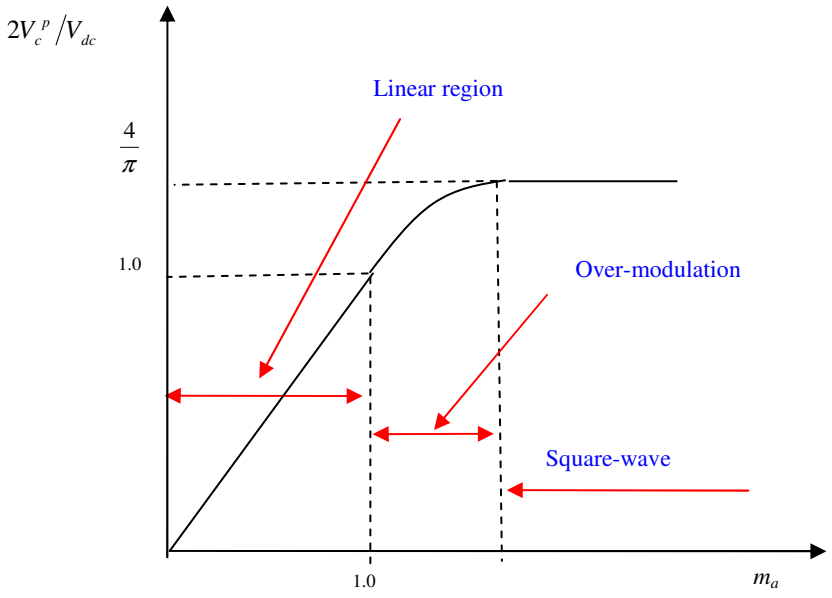


Figure 4.1. PWM voltage control by varying modulation index m_a.

Hence, if the DE needs to perform a voltage regulation to meet a certain scheduled voltage profile, there is a minimum DC supply voltage requirement. The requirement depends on the system requirement for V_c, i.e., the scheduled AC voltage profile. The approach to obtain an effective and acceptable voltage profile can be a separate research topic and will not be covered in this chapter. Instead, we simply assume that pre-defined, reasonable voltage schedules are available.

4.2.2. Set the Initial PI Controller Gains

Lower gain parameters, K_P and/or K_I, are typically chosen initially and only increased after confirming that they do not cause any of the above mentioned poor response and instability problems. In the following discussion, a method to initialize the gains is proposed.

A. Set the Initial K_P Value

At the initial time 0_+ (immediately after a voltage transient), the reference compensator output voltage v_c^* can be expressed as (4.2), since the contribution of the integral controller is 0:

$$v_c^* = v_t^0(t)[1 + K_P(V_t^*(t) - V_t^0(t))] \tag{4.2}$$

To keep the PWM modulation index, m_a, no greater than 1, the peak value of v_c^* needs to be less than the peak value of the triangle carrier signal, which is $0.5 \times V_{dc}$. Hence, we have:

$$K_P \le \frac{\frac{\frac{1}{2}V_{dc}}{V_t^{0,p}} - 1}{\Delta V_t^0} \tag{4.3}$$

where $\Delta V_t^0 = V_t^*(t) - V_t^0(t)$ is the initial RMS voltage deviation at time 0_+. This can be chosen as, and usually is, the maximum voltage deviation from the reference voltage at PCC.

Similarly, $V_t^{0,p}$ can be accordingly chosen as the peak value of the voltage, v_t, at time 0_+. Conservatively, the initial value of K_P, K_{P0}, can be empirically set to half of the RHS value defined by (4.3), when considering efficiency and error tolerance. Certainly, more research may be preformed regarding the choice of K_{P0} other than half of the RHS value in (4.3). Nevertheless, the initial value is only important for the initial transients and will be adjusted by the adaptive control when the system condition changes, as discussed next.

B. Setting the Initial K_I Value

The voltage response time of the controller for a voltage transient is set to 0.5 seconds in order to not interfere with the conventional utility voltage control. As can be seen from the simulation in Chapter 3, in an ideal voltage control process, the response of the control system to a step change can be approximated as an exponential decay curve, i.e., $\Delta V(t) = \Delta V_{t0} e^{-\frac{t}{\tau}}$ where τ is the time constant. Here a period of 5 times the time constant, 5τ, is chosen as the response time since this is normally the time needed to reach a new steady-state condition since e^{-5}=0.007≈0. Hence, we have $5\tau \approx 0.5s$ for the controller. When reaching the new steady state, the proportional part of the controller provides relatively no assistance and therefore we have:

$$v_c^* = v_t^{steady}(t)[1 + K_I \int_0^{5\tau} \Delta V_t(t)dt] \qquad (4.4)$$

Since in this study, PWM works only in the linear area, the amplitude of the triangle carrier signal is $0.5 \times V_{dc}$, so for the fundamental frequency component, the compensator output voltage v_c^* defined by Equation (1.7) should be equal to v_c. Replacing $\Delta V_t(t)$ with $\Delta V_{t0} e^{-\frac{t}{\tau}}$ and v_c^* with v_c we have:

$$K_I = \frac{\frac{V_c^{steady}}{V_t^{steady}} - 1}{\int_0^{5\tau} \Delta V_{t0} e^{-\frac{t}{\tau}} dt} \tag{4.5}$$

where $\frac{V_c^{steady}}{V_t^{steady}}$ is the ratio of converter output voltage to the voltage at the PCC which equals V_t^* in the steady state. V_c^{steady} can be calculated in the worst-case situation, which assumes a maximum voltage variation ΔV_{t0} such as the under peak load condition. The initial value of K_I, K_{I0}, is set to half of the RHS value in (4.5) to be conservative for the same reason as K_{P0}.

4.2.3. Adaptively Adjusting the PI Controller Gain Parameters

The controller with a fixed K_P and K_I may not always reach the desired and acceptable response in power systems since system load and other conditions are constantly changing. Without a centralized communication and control system, the controller has to utilize a self-learning capability to adjust K_P and K_I dynamically. Using the case of local voltage requiring an increase as an example, if the control logic shows that the voltage has increased too rapidly, then K_P and K_I will be adjusted to lower values. On the contrary for when it is too slow, K_P and K_I will be adjusted to higher values. Certainly, this needs additional logic to check the present voltage response with respect to the desired voltage response.

Figure 4.2 shows the overall logic of the adaptive control method. The key processes of this approach are:

- The voltage deviation of the ideal response $\Delta V_t(t) = \Delta V_{t0} e^{-\frac{t}{\tau}}$ is used as the reference. In every step, the actual voltage deviation and desired voltage deviation are monitored and a scaling factor $r_v = \frac{actual\ voltage\ deviation}{ideal\ voltage\ deviation}$ is calculated. Here the

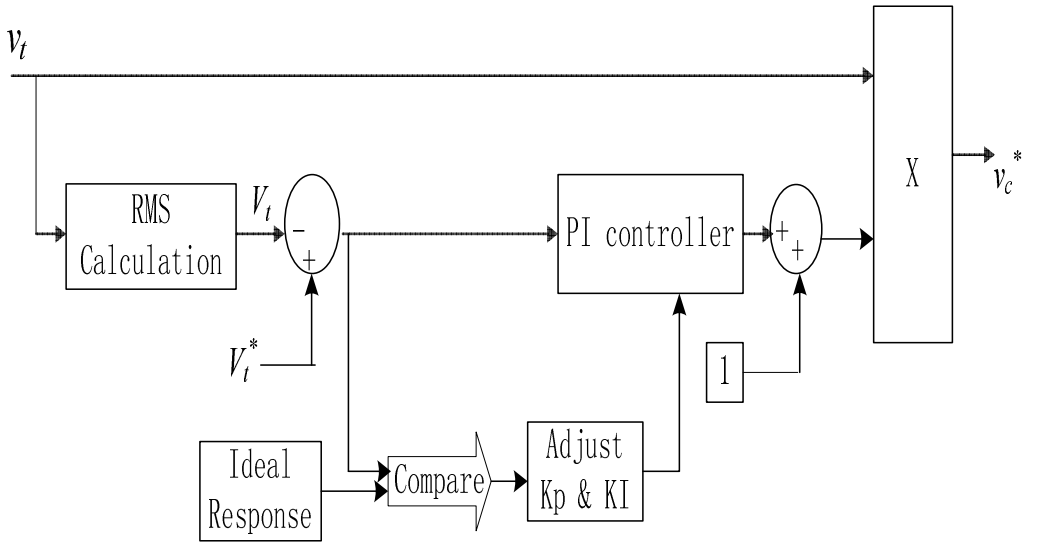


Figure 4.2. Adaptive Control of the Voltage Regulation.

actual voltage deviation is the voltage difference between the measured V_t and reference V_t^*; and the *ideal voltage deviation* is the difference between the exponential voltage curve and the reference V_t^*.

- Next, K_P and K_I are multiplied by the scaling factor r_v. When the actual response is faster than the desired exponential curve, it will be slowed when K_P and K_I are multiplied by $r_v<1$. Similarly, when the actual response is slower than the desired exponential curve, it will speed up when K_P and K_I are multiplied by $r_v>1$. This approach avoids the possible issues of slow response, overshoot, oscillation, or instability.

The method of adaptive control is illustrated in Figure 4.3. Certainly, a threshold can be applied when scaling K_P and K_I to avoid having too frequent updates. For instance, if the scaling factor r_v is very close to 1.0, no updating is needed and thus the controller can impose the maximum and minimum limits for r_v to avoid unnecessary updates.

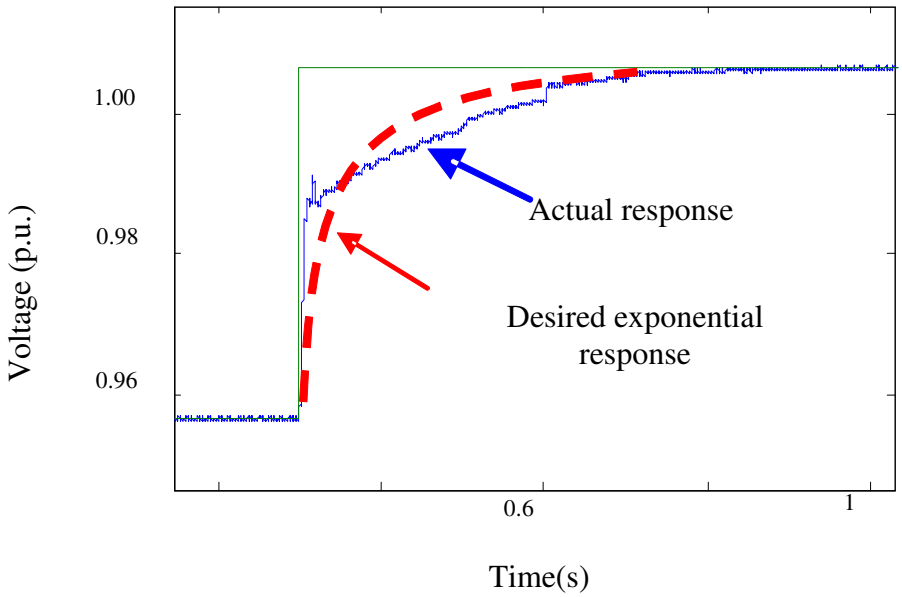


Figure 4.3. The desired and actual response of the controller.

The first feature of this algorithm is the dynamic adjustment of the control parameters K_P and K_I for voltage regulation. Another advantage in addition to performance is the elimination of an extensive and expensive centralized communications system because the parameters track the locally defined ideal voltage response curve. The high frequency sampling rate of modern power electronics and sensors ensures this as demonstrated in the simulations and field testing. Hence, the approach is termed “adaptive voltage control”.

4.3. Analytical Formulation of the Adaptive Method

The previous section presented the fundamental idea and algorithm for a dynamic K_P and K_I adjustment based on a desired exponential response. Because of the fast data sampling rate, such as 12.5 kHz, in the PI control implementation, this adaptive approach can be very effective, as shown in the following simulation and field experiments in Sections 4.4 and 4.5, respectively.

The adaptive method in Section 4.2 may raise the issue of its validity and thus the question: *Can the adaptive algorithm be expressed in an analytical formulation to provide a theoretical foundation?* If so, it can be generalized to work in other systems. This section will present a theoretical approach for the rigorous formulation of K_P and K_I as functions of time or time-dynamics. The dynamic K_P and K_I values can be calculated from equations and thus the heuristic approach of the adaptive method of the previous section can be benchmarked for verification and validity.

Figure 4.4 shows a system with a single DE regulating its terminal voltage.

First, the DE source, v_c, is modeled as a voltage source connected to Bus i, as shown in Figure 4.4. Without losing generality, it is assumed there may be a voltage source (substation) at each bus. The voltage source, v_{sl} $(l=1\sim n)$, can be set to 0 if no source exists. In the Laplace (S) domain, the nodal voltage equations can be expressed as:

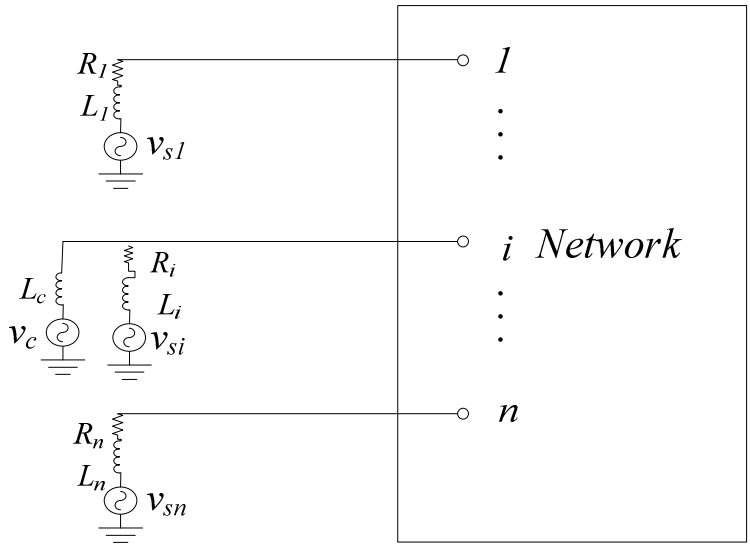


Figure 4.4. A schematic diagram of a network and sources.

$$Y(s)\begin{bmatrix} v_{t1}(s) \\ \vdots \\ v_{ti}(s) \\ \vdots \\ v_{tn}(s) \end{bmatrix} = \begin{bmatrix} \dfrac{v_{s1}(s)}{R_1 + sL_1} \\ \vdots \\ \dfrac{v_c(s)}{sL_c} + \dfrac{v_{si}(s)}{R_i + sL_i} \\ \vdots \\ \dfrac{v_{sn}(s)}{R_n + sL_n} \end{bmatrix} \tag{4.6}$$

where $Y(s)$ is the admittance matrix of the system; $v_{ti}(s)$ is the voltage at Bus i; $v_{sl}(s)$ is the voltage source at Bus l $(l=1\sim n)$, excluding the DE source; R_l+L_l is the equivalent impedance for the electrical connection from the voltage source v_{sl} to the terminal buses l; $v_c(s)$ is the DE source; and L_c is the inductance for the DE to the terminal Bus i connection. From Equation (4.6), we can derive the voltage's vector as:

$$\begin{bmatrix} v_{t1}(s) \\ \vdots \\ v_{ti}(s) \\ \vdots \\ v_{tn}(s) \end{bmatrix} = Z(s)\begin{bmatrix} \dfrac{v_{s1}(s)}{R_1 + sL_1} \\ \vdots \\ \dfrac{v_c(s)}{sL_c} + \dfrac{v_{si}(s)}{R_i + sL_i} \\ \vdots \\ \dfrac{v_{sn}(s)}{R_n + sL_n} \end{bmatrix} \tag{4.7}$$

where the impedance matrix is $Z(S) = [Y(S)]^{-1}$. From Eq. (4.7), we can obtain the regulated voltage at Bus i as follows:

$$v_{ti}(s) = Z_{ii}(s)\frac{v_c(s)}{sL_c} + \sum_{l=1}^{n} Z_{il}(s)\frac{v_{sl}(s)}{R_l + sL_l} \tag{4.8}$$

where $Z_{ii}(S)$ and $Z_{il}(S)$ are the corresponding elements of the matrix $Z(S)$, which only depends on the network parameters.

Given the desired voltage at Bus i, we can calculate the support voltage requirement for the DE from (4.8) as:

$$v_c(s) = \frac{v_{ti}(s) - \sum_{l=1}^{n} Z_{il}(s) \frac{v_{sl}(s)}{R_l + sL_l}}{Z_{ii}(s)} \cdot sL_c \tag{4.9}$$

And v_c^* defined by (1.7) should be equal to v_c, that is:

$$v_{ti}(s) \cdot [1 + (K_P(s) + \frac{K_I(s)}{s})\Delta V_{ti}(s)] = v_c(s) \tag{4.10}$$

where $\Delta V_{ti}(s)$ is the deviation of the RMS value of the voltage at Bus *i* from the reference RMS value $V_{ti}^*(s)$. The PI controller gains are time variant, so they are expressed as $K_P(s)$ and $K_I(s)$.

Since in the adaptive approach, $K_P(s)$ and $K_I(s)$ follow the same pattern for adjustment, we let $K_I(s) = mK_P(s)$, where *m* is K_{I0}/K_{P0}, the ratio of the initial values of K_I and K_P. When we substitute this into (4.10), we have:

$$v_{ti}(s) \cdot [1 + (K_P(s) + \frac{mK_P(s)}{s})\Delta V_{ti}(s)] = v_c(s) \tag{4.11}$$

Hence:

$$K_P(s) = \frac{\frac{v_c(s)}{v_{ti}(s)} - 1}{\Delta V_{ti}(s)(1 + \frac{m}{s})} \tag{4.12}$$

Since $v_{ti}(s)$ has a zero-crossing value, the ratio of the RMS values of $v_c(s)$ over $v_{ti}(s)$ is used to replace the ratio of the instantaneous values. This is reasonable as we only have the fundamental element. Thus, Eq. (4.12) can be rewritten as:

$$K_P(s) = \frac{\frac{\mathrm{V}_c(s)}{\mathrm{V}_{ti}(s)} - 1}{\Delta V_{ti}(s)(1 + \frac{m}{s})} \tag{4.13}$$

Based on the assumption that the ideal voltage response is an exponential response, we have:

$$\Delta V_{ti}(s) = \frac{\Delta V_{\max}}{s + 1/\tau} \tag{4.14}$$

where $\Delta V_{\max}$ is the magnitude of the voltage step change and τ is the time constant, which can be defined according to the users' requirement for response speed.

Hence, the voltage at Bus i can be derived as:

$$v_{ti}(t) = (V_{ti}^{*} - \Delta V_{\max} e^{-\frac{t}{\tau}}) \cos(2\pi f t + \phi) \tag{4.15}$$

and

$$V_{ti}(s) = (V_{ti}^{*} - \frac{\Delta V_{\max}}{s + 1/\tau}) \tag{4.16}$$

where ϕ is the phase angle of the voltage at terminal Bus *i*, and f is the fundamental frequency.

By substituting Eqs. (4.9), (4.14), and (4.16) into (4.13), we can finally calculate $K_P(s)$ and hence, $K_I(s)$. They are given as:

$$K_P(s) = \frac{\frac{\mathrm{RMS}(\frac{A}{Z_{ii}(S)} \cdot sL_c)}{(V_{ti}^{*} - \frac{\Delta V_{\max}}{s + 1/\tau})} - 1}{\frac{\Delta V_{\max}}{s + 1/\tau} \cdot (1 + \frac{m}{s})} \tag{4.17}$$

$$K_I(s) = m\frac{\frac{\mathrm{RMS}(\frac{A}{Z_{ii}(S)} \cdot sL_c)}{(V_{ti}^{*} - \frac{\Delta V_{\max}}{s + 1/\tau})} - 1}{\frac{\Delta V_{\max}}{s + 1/\tau} \cdot (1 + \frac{m}{s})} \tag{4.18}$$

where:
$$A = v_{ti}(s) - \sum_{l=1}^{n} Z_{il}(s)\frac{v_{sl}(s)}{R_l + sL_l} \tag{4.19}$$
$$= (V_{ti}^{*} - \Delta V_{\max} e^{-\frac{t}{\tau}})\cos(2\pi ft + \phi) - \sum_{l=1}^{n} Z_{il}(s)\frac{v_{sl}(s)}{R_l + sL_l}$$

Thus, we have proven that theoretical formulations for both $K_P(s)$ and $K_I(s)$ exist for the ideal, exponential response of the voltage regulation. These formulations will be used to confirm that the heuristic approach for adaptive control is equivalent to using $K_P(s)$ and $K_I(s)$ in Eqs. (4.17) and (4.18).

However, in most application cases, we do not have enough data to calculate $K_P(s)$ and $K_I(s)$. Even if we do, it is tedious and error-prone work to perform since multiple distribution system parameters are involved. However, given the reference voltage and the desired response speed, K_P and K_I can be automatically adjusted, as shown in the adaptive algorithm in Section 4.2, to track the defined ideal response.

Figure 4.6 shows a comparison of the value of KP calculated by the theoretical equation (4.17) and by the adaptive algorithm in Section 4.2. The simulation is performed on the system as shown in Figure 4.5 with the DE modeled as an ideally controlled voltage source. A load increase is applied at 0.2s to mimic voltage sag. The desired compensator response time is 0.5s so it must reach the original voltage schedule at 0.7s. The solid blue line

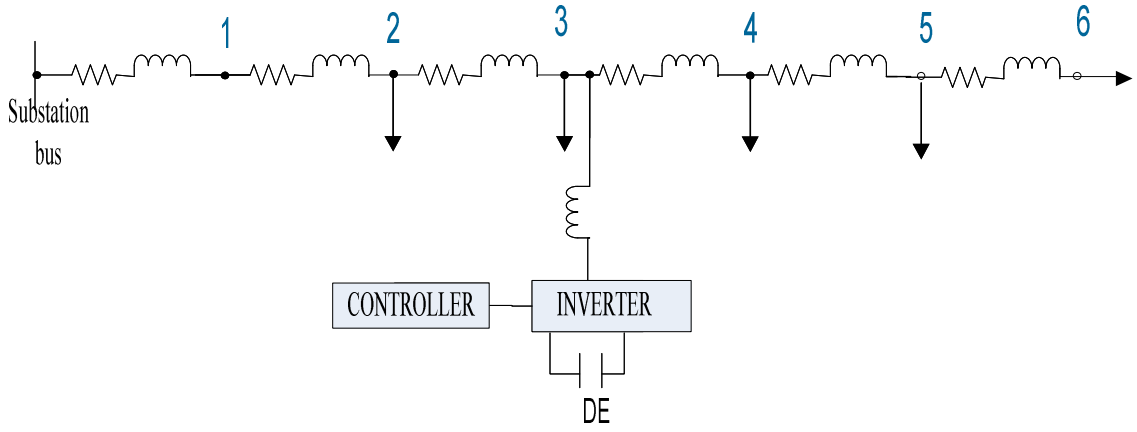


Figure 4.5. A radial test system.

is K_P calculated theoretically using (4.17) and the dashed red curve is K_P generated by the adaptive control approach. As can be seen, these two curves are extremely close, thus verifying the heuristic approach with the theoretical formulations. Similarly, Figure 4.7 shows the comparison of K_I for the two methods, which again shows an extremely close match. In addition, Figure 4.8 shows the voltage regulation results by adjusting K_P and K_I with the two methods. The dashed red line is the defined ideal response. The solid blue line is the voltage response of the adaptive control approach and the dash-dot black line is the voltage response with K_P and K_I calculated using Eqs. (4.17-4.18). The dotted red (flat) line is the reference voltage.

The results in Figures 4.6-4.8 verify the equivalence of Equations (4.17-4.18) with the adaptive algorithm of Section4.2, thus verifying the heuristic approach with a theoretical foundation. The ideal response, defined as an exponential response, can be achieved by dynamically adjusting K_P and K_I.

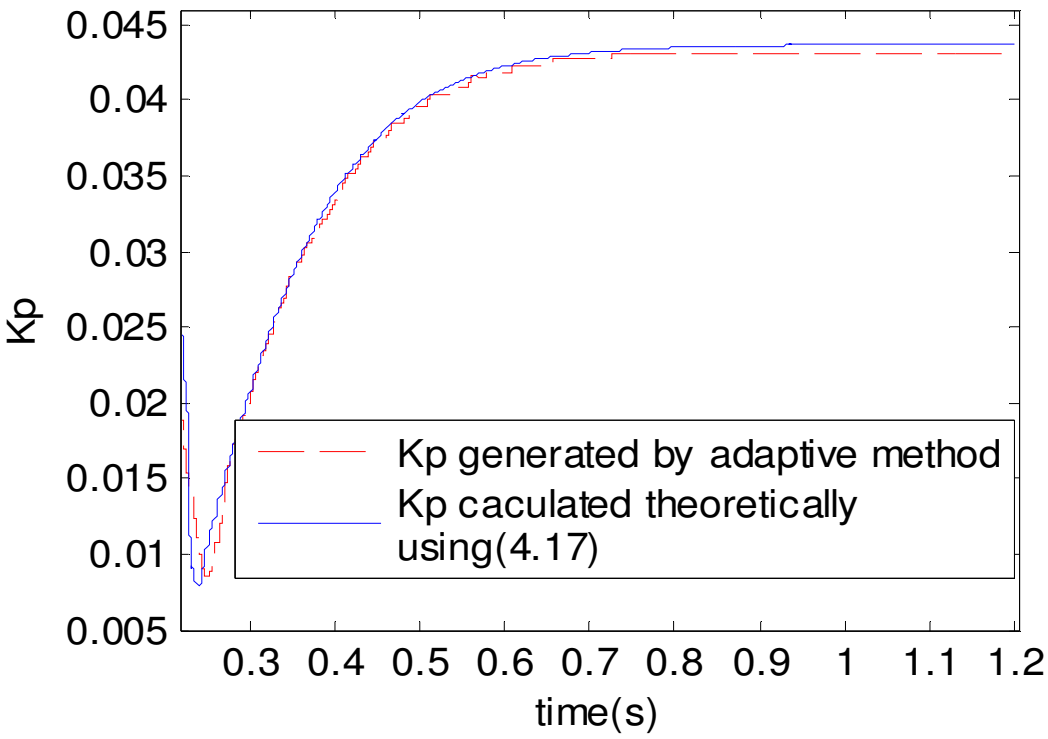


Figure 4.6. Comparison of the value of K_P generated by the two methods.

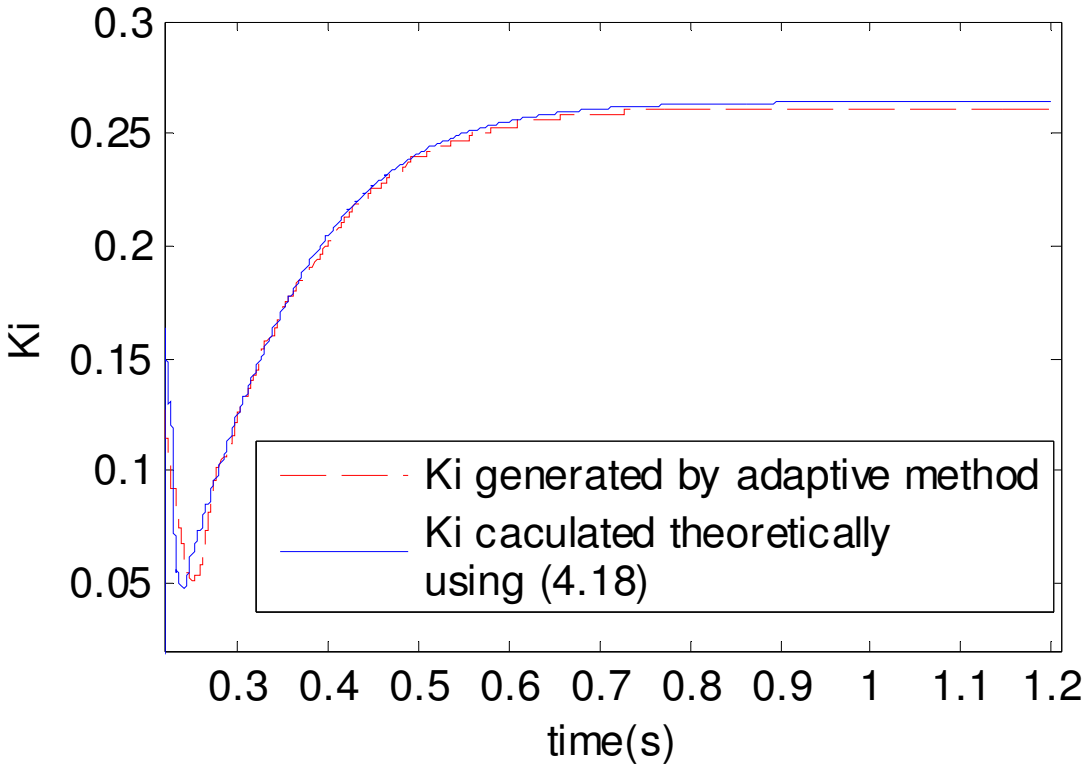


Figure 4.7. Comparison of the value of K_I generated by the two methods.

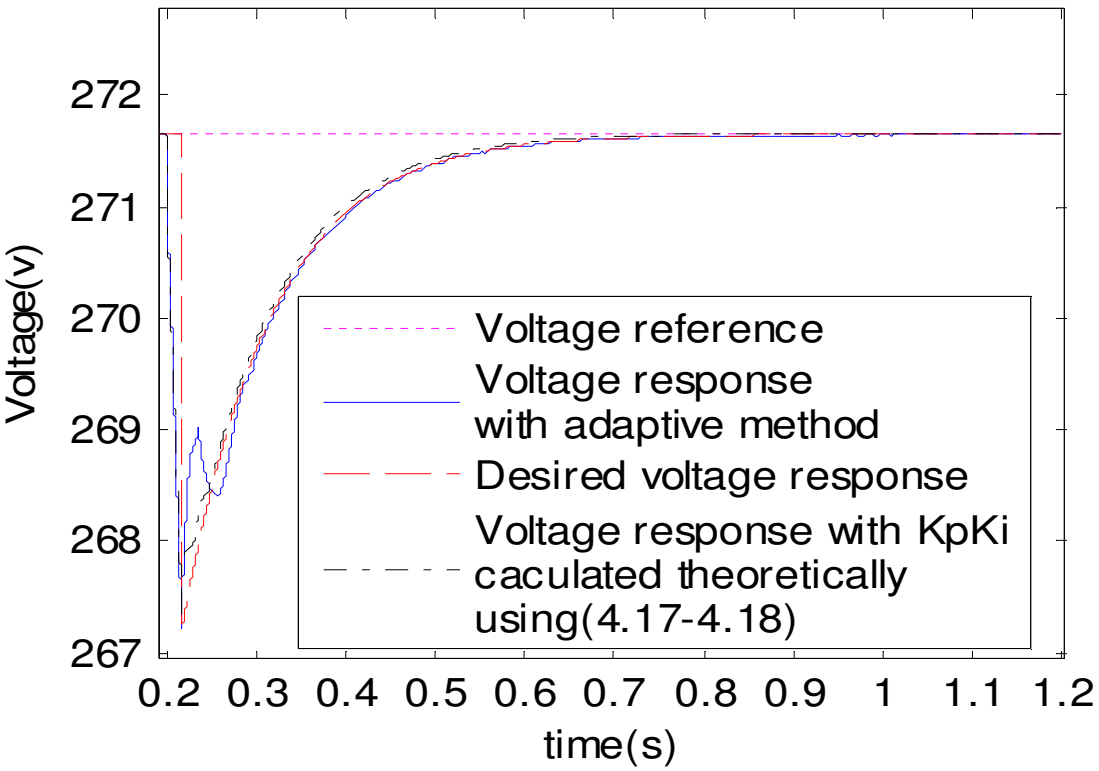


Figure 4.8. Tracking ideal response by adjusting K_P and K_I with the two methods.

4.4. Simulation Results

In this section, a step-by-step example is shown to illustrate how to implement the heuristic adaptive algorithm for voltage regulation as discussed in Section 4.2. The system in Figure 4.5 is used again for illustration.

4.4.1. Initial Parameter Setting

As before, the DE is connected at Bus 3. The line-to-line voltage on the consumer side of the infinite bus is assumed to be 480 V (RMS). The total load of the system is 70.18kVA (59 kW, 38kVar). We assume that the heaviest load condition is when the loads at Bus 4 and Bus 6 increase by 20.93kVA (20.3 kW, 5.08 kVar) and 27.94kVA (27.1 kW, 6.8 kVar), respectively. The desired phase voltage profile at Bus 3 is 271.65 V (line-to-neutral, RMS); however, the phase voltage at Bus 3 for the peak load condition is 267.2 V. From this information, we can determine the DE requirements for voltage regulation.

1) Calculate the DC voltage requirement of the DE (V_{dc}).

Here the DE and substation bus can be viewed as the voltage resources. Hence, the voltage at the load buses, such as Bus 3, can be expressed as follows:

$$\overline{V}_3 = a_{3,sub}\overline{V}_{sub} + a_{3,DE}\overline{V}_c \tag{4.20}$$

where $\overline{V}_3$ is the voltage at Bus 3; $\overline{V}_{sub}$ is the voltage at the substation bus, which can be viewed as a constant; $\overline{V}_c$ is the output voltage of the DE; and the coupling coefficients $a_{3,sub}$ and $a_{3,DE}$ represent the sensitivity between the two bus voltages (i.e., $\frac{\partial \overline{V}_3}{\partial \overline{V}_{sub}}$ and $\frac{\partial \overline{V}_3}{\partial \overline{V}_c}$, respectively), which can be calculated with network parameters.

In this case, we have:

$$\overline{V}_3 = (0.8359 + 0.022i)\overline{V}_{sub} + (0.1278 - 0.0559i)\overline{V}_c \tag{4.21}$$

and

$$P = \frac{V_3 V_c}{\omega L_c} \sin(\alpha_c - \alpha_3) \tag{4.22}$$

where α_c and α_3 are the phase angles of $\overline{V}_c$ and $\overline{V}_3$ respectively. Since the regulation goal is to maintain a voltage schedule at $V_3 = 271.65$ V, we calculate $V_c = 286.9$ V.

Then, considering $V_{dc} \geq 2V_c^p = 2\sqrt{2} \times V_c$ as shown in Equation (4.1), we can determine that the DC voltage for the DE should be no less than 811V, thus we choose 900 V.

2) Initialize K_P.

The initial value of K_P can be calculated based on Equation (4.3):

$$K_{P0} = 0.5 \times \frac{\frac{1}{2}V_{dc} - 1}{\frac{V_t^{0,p}}{\Delta V_t^0}} = 0.5 \times \frac{\frac{900/2}{\sqrt{2} \times 267.2} - 1}{271.65 - 267.2} = 0.021 \tag{4.23}$$

3) Initialize K_I.

The initial value of K_I can be calculated based on (4.5):

$$K_{I0} = 0.5 \times \frac{\frac{V_c^{steady}}{V_t^{steady}} - 1}{\int_0^{5\tau} \Delta V_{t0} e^{-\frac{t}{\tau}} dt} = 0.5 \times \frac{286.9/271.65 - 1}{\int_0^{0.5} (271.65 - 267.2) e^{-\frac{t}{0.1}} dt} = 0.127 \tag{4.24}$$

4.4.2. Simulation Results of the Adaptive control Approach.

The adaptive control approach is tested on a DE with an inverter interface. After detecting a large voltage deviation at 0.2s, the difference of the two voltages is checked at every quarter cycle for the possible adjustment of K_P and K_I.

Figure 4.9 shows the voltage regulation with an adaptive adjustment of K_P and K_I. The dotted blue line is the desired voltage response while the solid red line is the actual

voltage response. As indicated, the actual voltage tracks the desired voltage response and satisfies the 0.5s response time requirement. Figure 4.10 shows the comparison of the desired and actual voltage deviations. The actual voltage response matches the reference voltage except at the very beginning of the adjustment. The reason for the relatively large difference at the very beginning is due to the initial high sensitivity of the voltage and the dominance of the proportional part in Eq. (1.7) over the integral part. Hence, any small inaccuracy tends to lead to a relatively large difference. However, when time approaches 0.3s, the proportional part has less weight and the integral part has more effect. Therefore, the actual voltage response curve is controlled very close to the desired curve.

In addition, Figures 4.11 and 4.12 are the real and reactive power injections, respectively, during the voltage regulation. It should be noted that the P injection in Figure 4.11 remains constant except for small ripples around 0.2-0.4 s. These occur simply because of the terminal voltage dynamics.

For verification purposes, Figure 4.13 shows the non-adaptive voltage regulation with gains fixed to their initial values of K_{P0} and K_{I0}. The response is much slower when compared to the adaptive control approach. Instead of 0.5s, it takes more than 1s to reach the voltage reference. Thus, the proposed adaptive control approach provides greater response efficiency.

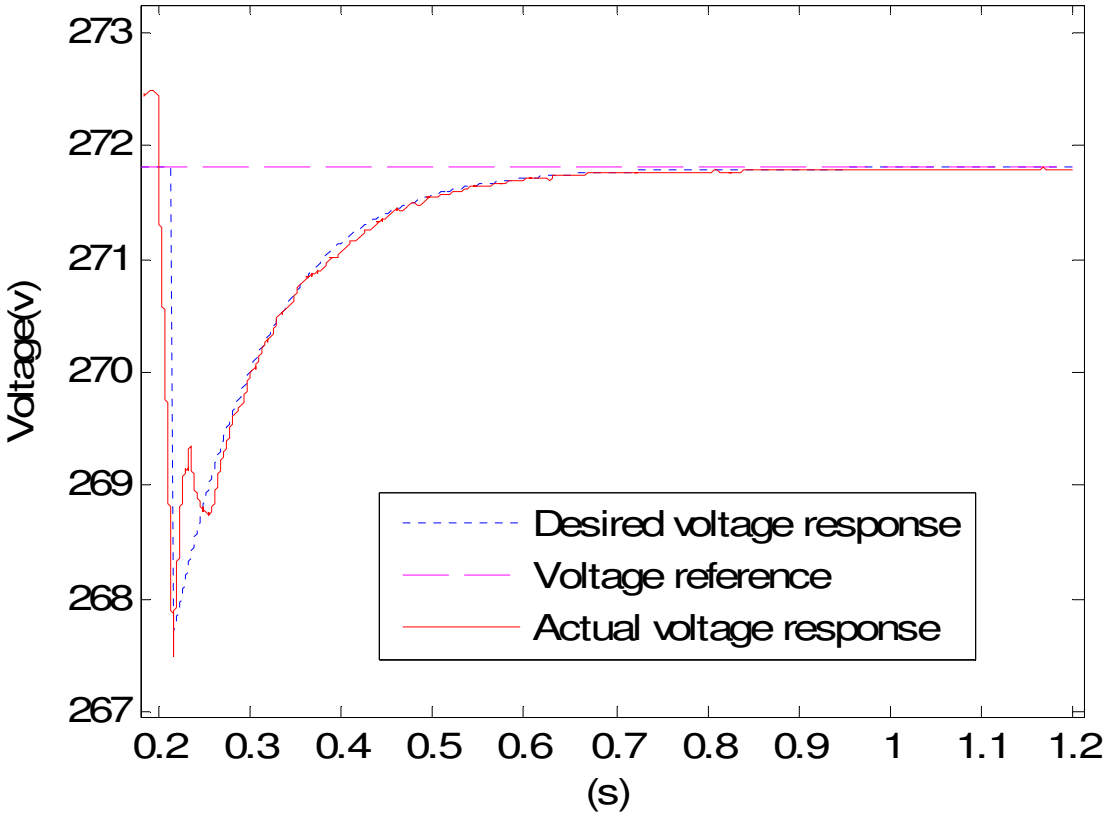


Figure 4.9. Voltage regulation with adaptive adjustment of K_P and K_I.

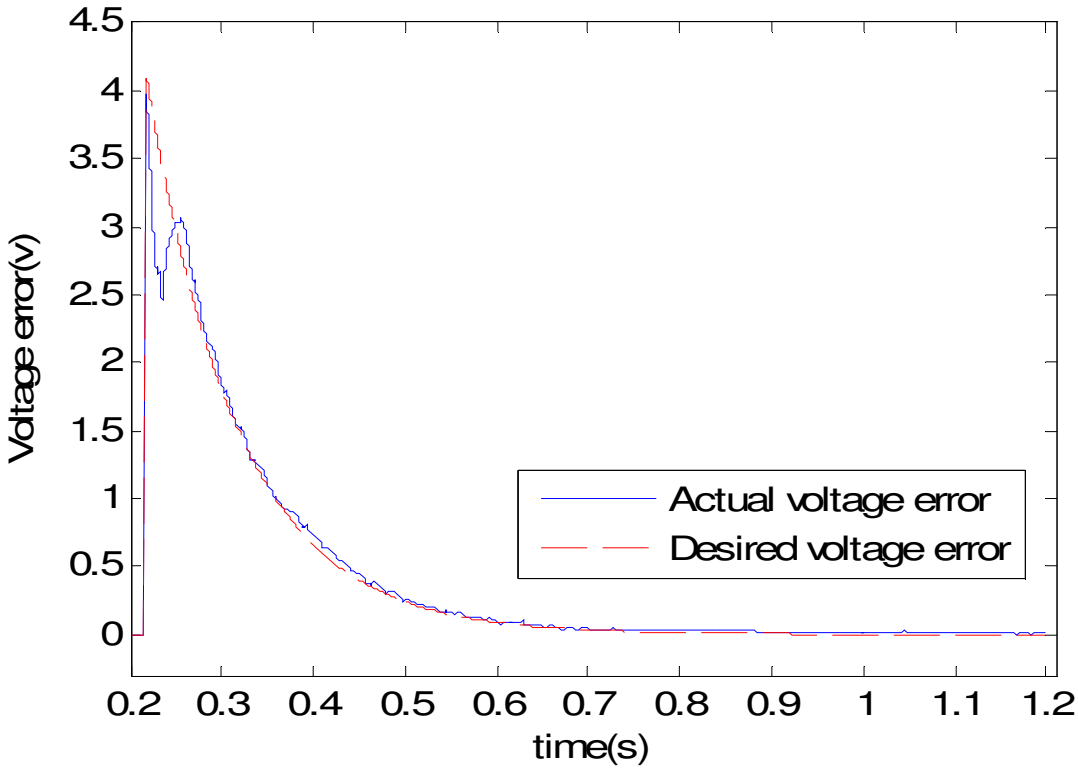


Figure 4.10. Comparing the desired and actual voltage deviations.

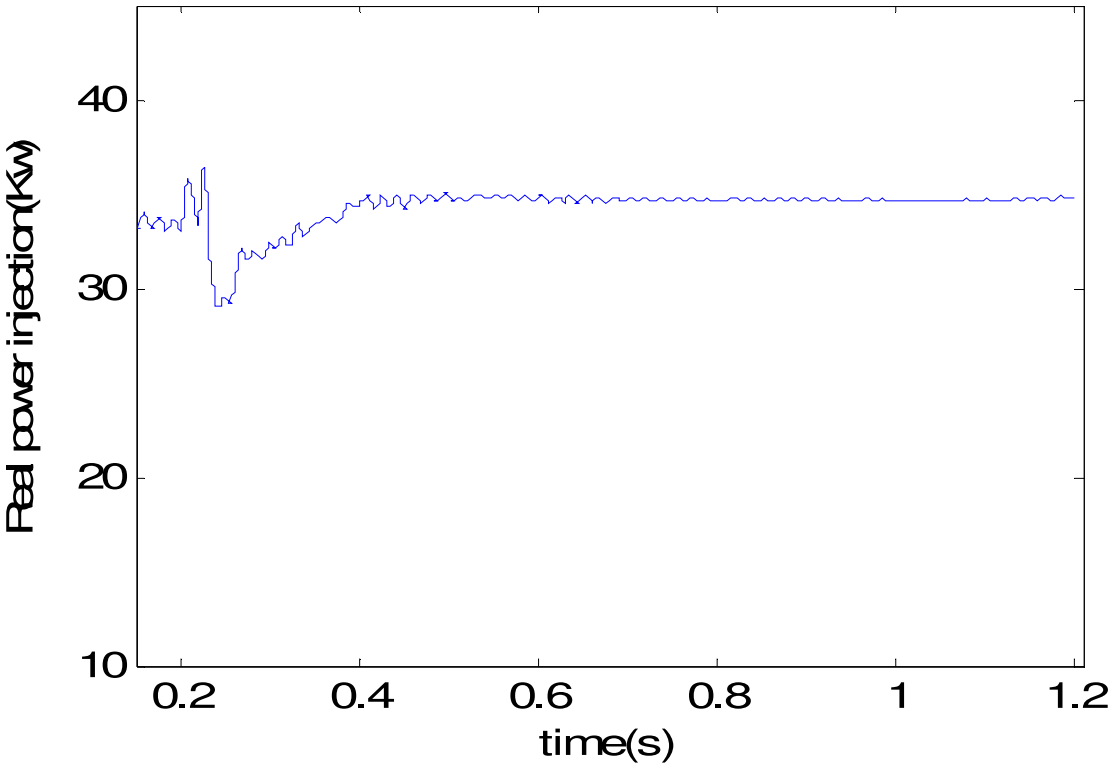


Figure 4.11. Real power injection.

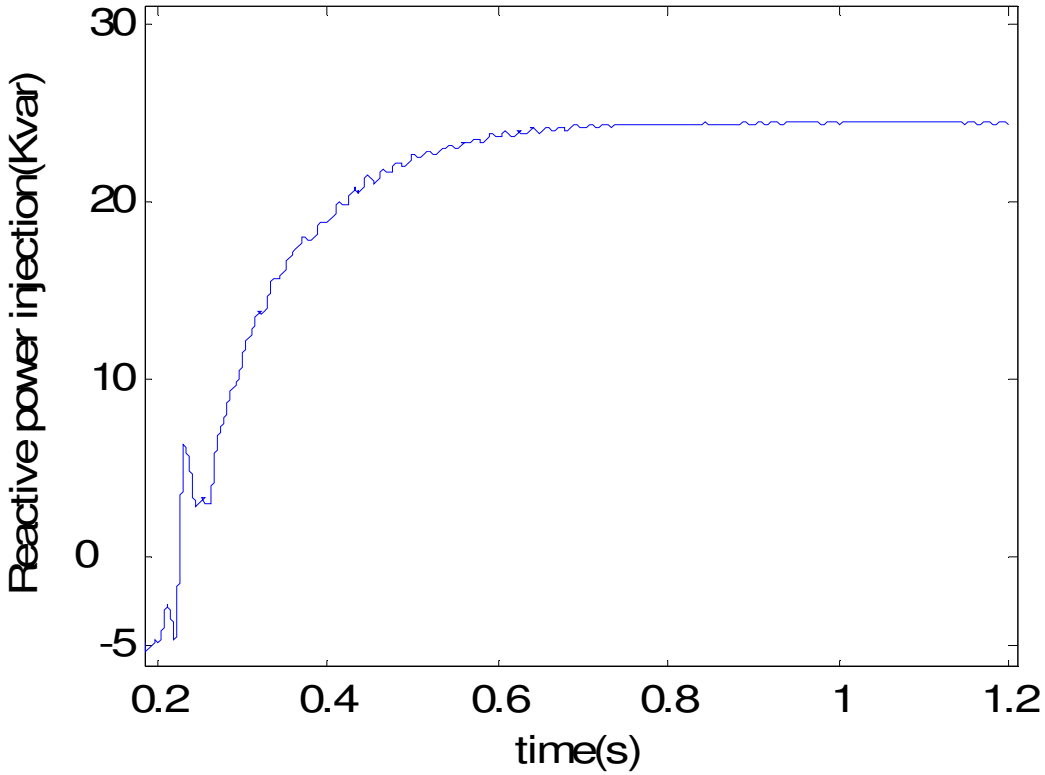


Figure 4.12. Reactive power injection.

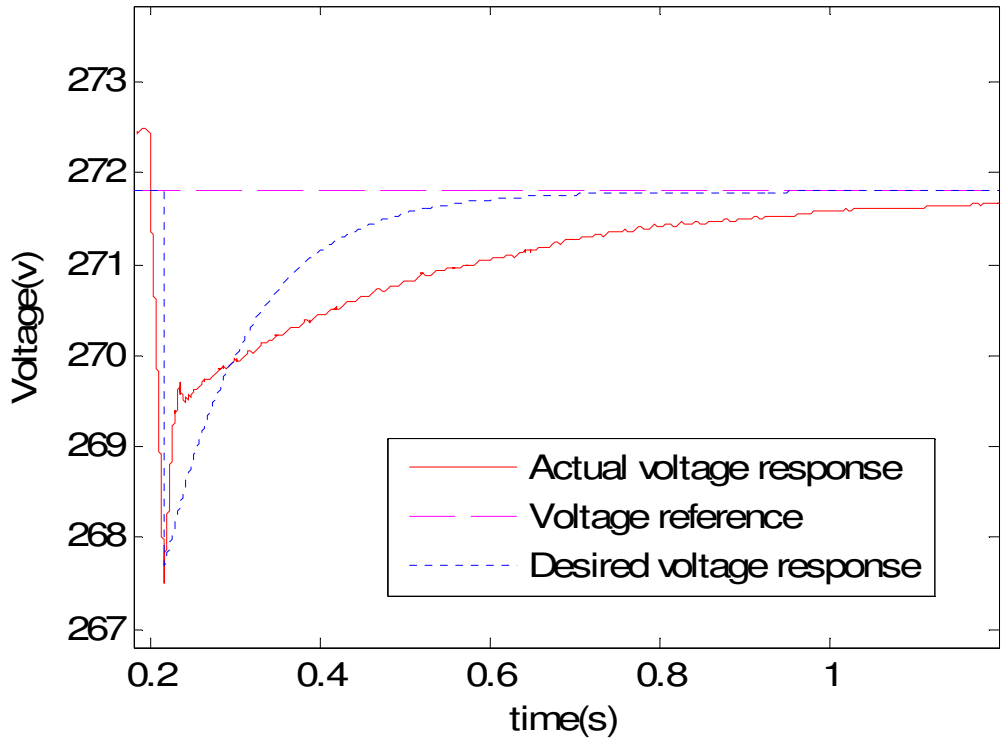


Figure 4.13. Non-adaptive voltage regulation with K_P and K_I fixed at the initial values.

4.5. Field Experiment Results at ORNL

The field experiment in this subsection is performed primarily by researchers at ORNL including Dr. Yan Xu, Mr. D. Tom Rizy, and Mr. John D. Kueck. The results are included here for the completeness of this dissertation, while credit should be attributed to them.

Field tests were conducted at the Oak Ridge National Laboratory (ORNL)'s Distributed Energy Communications & Controls (DECC) Laboratory, which is interfaced to the ORNL distribution system and receives its power from the Tennessee Valley Authority (TVA)'s bulk transmission system, as shown in Figure 4.14. The inverter of the DE test system, which is rated at 150A, is connected to a 480V/600A power panel fed from circuit #2 of the 3000 substation of the ORNL distribution system.

A sudden load change of 20 kW (from 80 to 100 kW) and 37.5 kVar (from 37.5 to 75 kVar) is applied which causes a voltage sag in the system. The load change results in a sustained voltage drop if there is no voltage regulation. The PCC voltage of the inverter (an average RMS of all three phases) is shown in Figure 4.15 and occurs when there is no voltage regulation. The voltage drops 1.5V because of the load increase.

Figure 4.16 shows the PCC voltage (at Panel PP3 in Figure 4.14) using the DE to provide voltage regulation with the non-adaptive approach. The same load change is applied during the voltage regulation test and the response time is 2.42s. By applying the same sudden load change as shown in Figure 4.15, the adaptive voltage regulation control is implemented and the test results are shown in Figure 4.17.

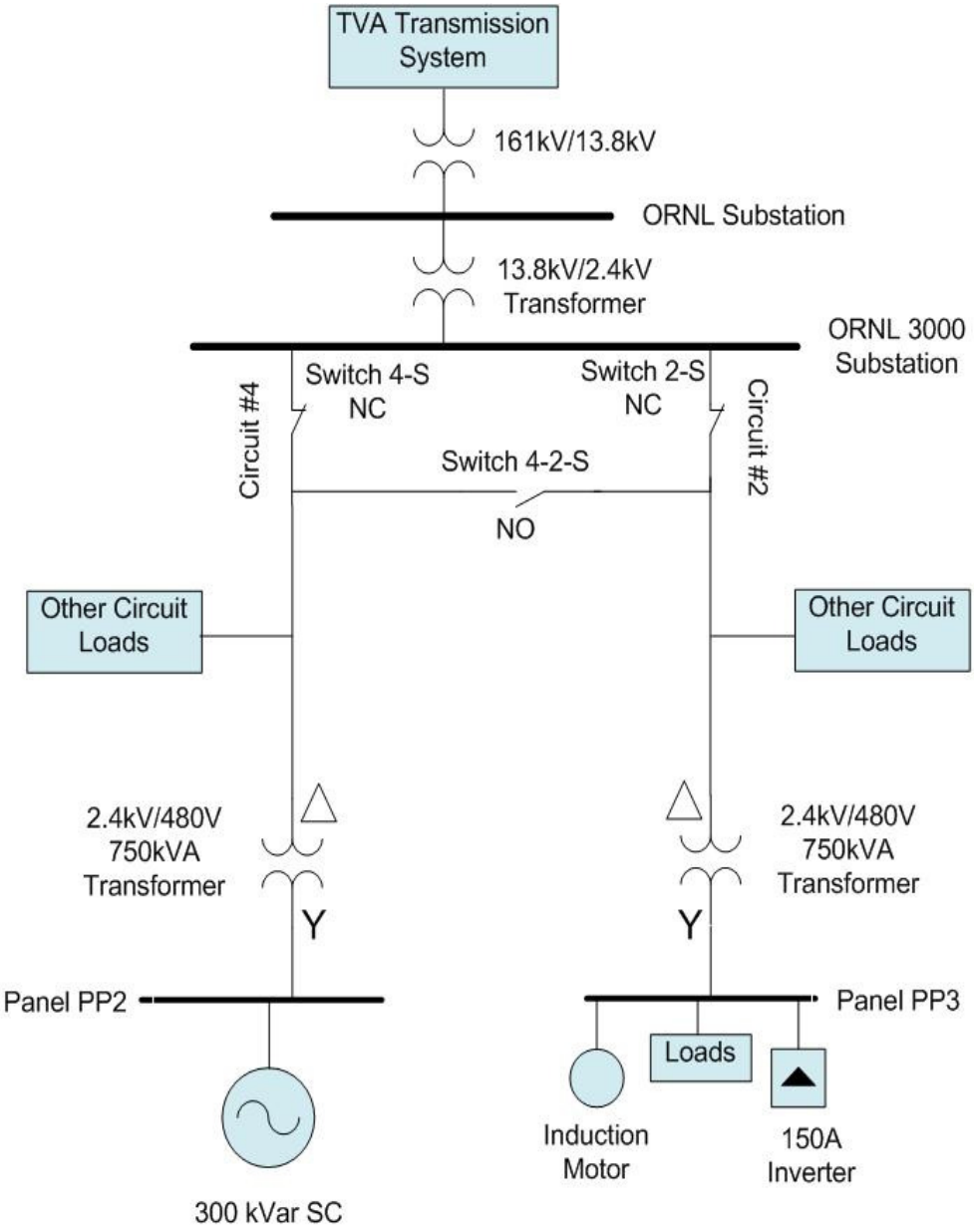


Figure 4.14. ORNL's DECC Laboratory.

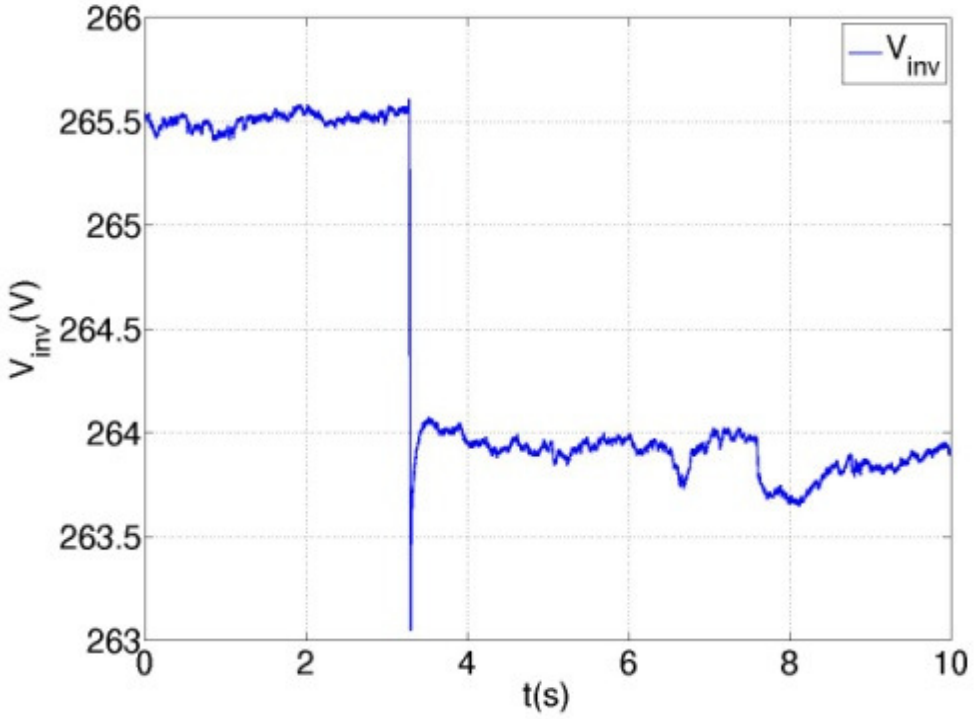


Figure 4.15. PCC voltage at the inverter without voltage regulation.

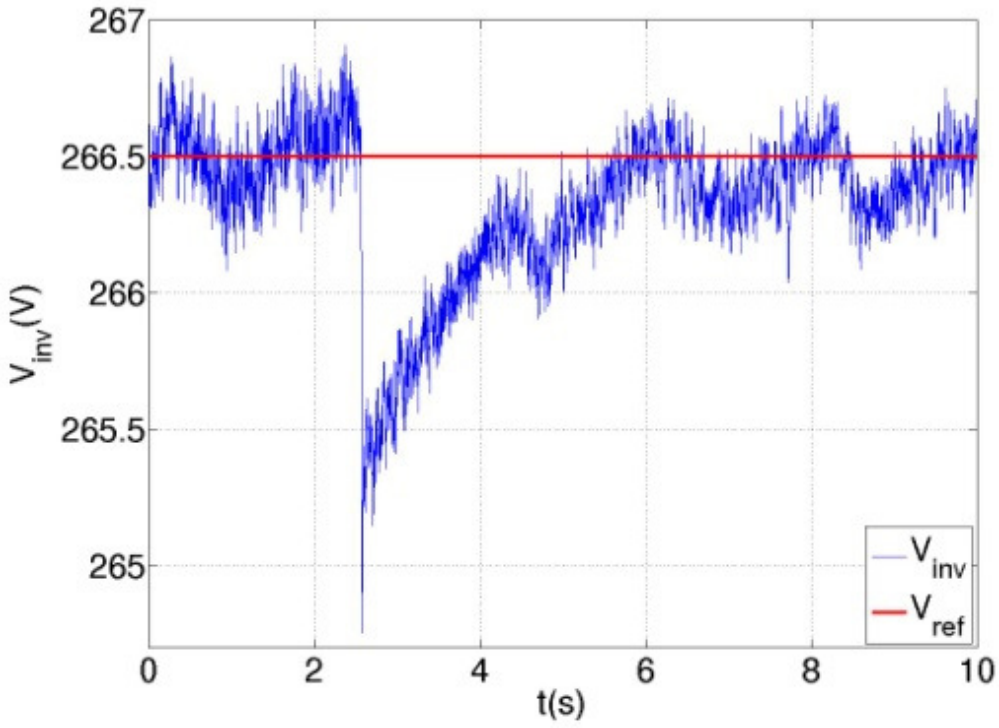


Figure 4.16. PCC voltage (in RMS) with non-adaptive voltage regulation.

The response time is significantly shortened to 0.44*s* without any overshoot or oscillation, or instability problem. Figure 4.18 shows the actual voltage deviation from the experiment (the blue line with ripples) and the desired voltage deviation under the ideal exponential response (the smooth red line). The actual deviation decay time closely matches the 5τ decay time of the ideal curve (0.5 s). The experimental result verifies the advantage of the adaptive control approach.

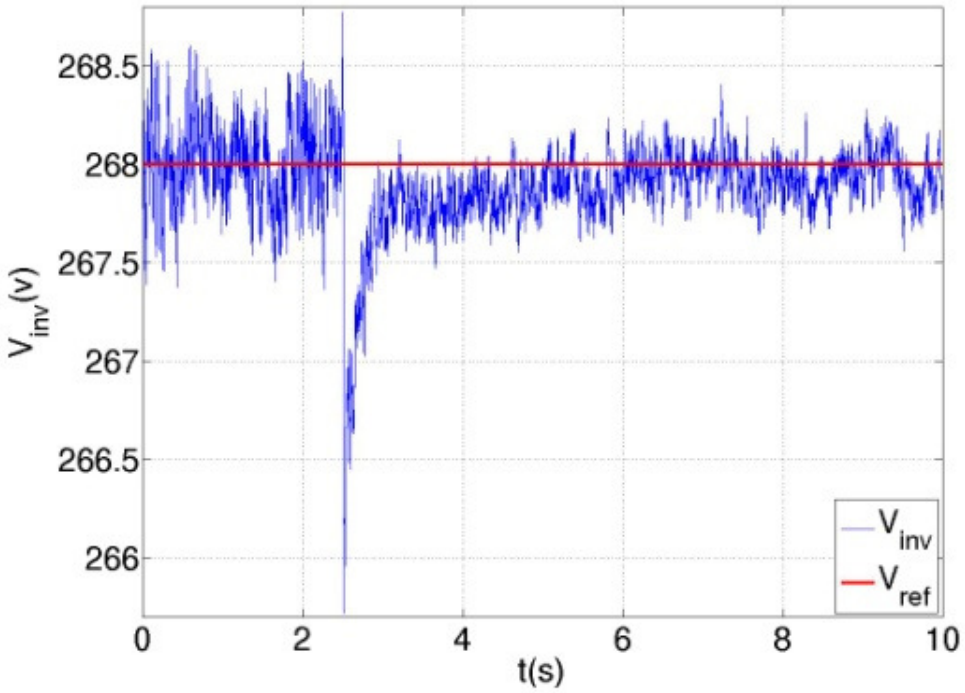


Figure 4.17. PCC voltage (in RMS) with adaptive voltage regulation.

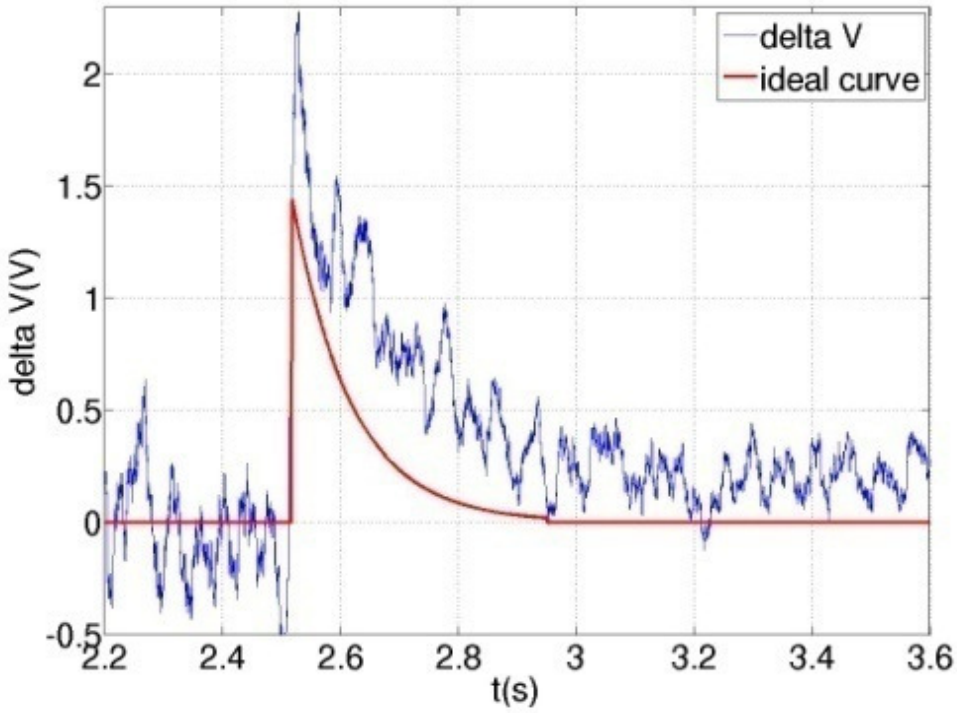


Figure 4.18. Comparison of the desired and actual voltage deviations.

4.6. Chapter Conclusion

An adaptive voltage control approach using PI feedback control, which is based on the local voltage variation and non-active power theory [10], is developed. The approach has a wide adaptability and is easy to implement by practicing engineers since it does not require detailed system data. Simulations and field experiments both show that the adaptive approach satisfies the rapid response and performance requirements needed for integration with existing system equipment.

5. Voltage Regulation with Multiple DEs

5.1. Chapter Introduction

In this chapter, the challenges of voltage regulation with multiple DEs are discussed. A theoretical calculation of the controller parameters of the adaptive method in multiple DEs voltage regulation is presented. Based on the availability of the communications among the voltage regulating DEs, a high-end with communication implementation and low-end without communication implementation of the adaptive control method are proposed, respectively. Simulation results show that in both implementations, DEs can track the desired response curve closely and yield satisfactory regulation results.

5.2. Challenges in Voltage Control with Multiple DEs

When multiple DEs connected in the systems participate in the voltage regulation, the interference among these DEs makes the voltage control process more complicated. As shown in the simulations in Chapter 3, the controller parameters suited for voltage regulation with a single DE may fail to generate satisfactory performance in voltage regulation in the two DEs case. The problem of coordination among all the DE controllers needs to be considered as the DEs have similar response time that may cause them to chase each other which could lead to instability or oscillations.

Note that in a practical operation, we may choose only a limited number of DEs for voltage control, similar to the practice in AGC control. DEs with voltage regulation ability can bid for providing this service such as in the ancillary service market. This should reduce complexity while maintaining an acceptable efficiency. However, the exploration of how to implement the process of choosing voltage regulating DEs in a large distribution system is

beyond the scope of this research and therefore will not be discussed in this dissertation. Instead, it is assumed that the locations of the voltage regulating DEs are known.

In the following simulations, it is assumed that two DEs are installed at bus 3 (DE1) and bus 6 (DE2), respectively, as shown in Figure 5.1. The five simulation scenarios can be categorized into two types: only one DE offers the voltage regulation (Scenarios 1 and 4) or both DEs participate in voltage regulation (Scenarios 2, 3, and 5). In all the scenarios, the voltage reference at the PCC of DE2 remains fixed and the voltage reference setting of DE1 is varied in order to investigate the impact of the voltage regulation of DE1 on that of DE2. The simulation conditions of each scenario are listed in Table 5.1.

Figure 5.2 shows the voltage responses of bus 6, where DE2 is connected, when the voltage regulation settings of DE1 are varied. The controller parameters remain fixed with K_P=0.04 and K_I=1.2 for both DEs in all the simulation scenarios. The red solid flat line is the

Table 5-1. Simulation conditions of the test scenarios.

Scenario No.	If participating in voltage regulation		Terminal voltage reference (v)	
	DE1	DE2	DE1	DE2
1	No	Yes		270.2
2	Yes	Yes	270.6	270.2
3	Yes	Yes	271.0	270.2
4	Yes	No	271.2	
5	Yes	Yes	271.2	270.2

voltage reference of DE2. The blue curve is the voltage response of DE2 in Scenario 1. The magenta dash curve is the voltage response of DE2 in Scenario 2 and the green dot curve shows the voltage response of DE2 in Scenarios 3. A comparison of voltage responses of DE2 in the three scenarios shows that the voltage regulation behavior of DE1 affects the terminal voltage response of DE2.

Figures 5.3 and 5.4 show the voltage responses of DE1 in Scenarios 2 and 3, respectively. As seen in Figures 5.2 to 5.4, when the voltage reference of DE1 is set to 271v, both DEs try to bring the voltage up and inject reactive power, which make the regulation process of DE2 faster than the case when there is only one DE to regulate the voltage; while the voltage reference of DE1 is set to 270.6 v in Figure 5.3, DE1 reduces the voltage, which is the opposite direction to the voltage change of DE2. This slows down the regulation process.

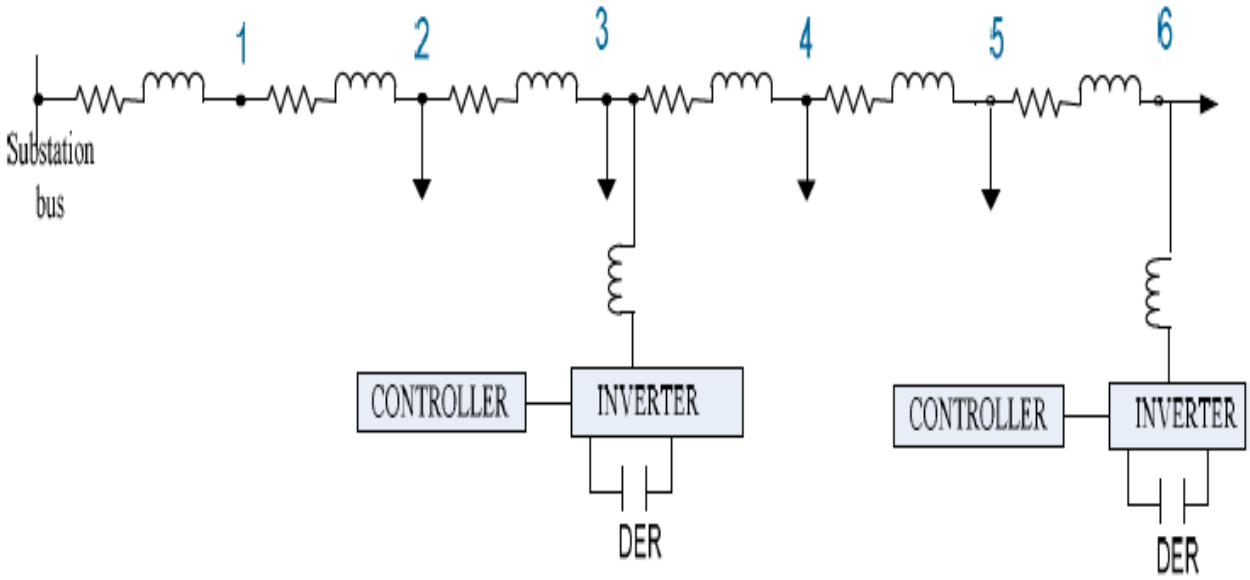


Figure 5.1. A radial test system installed with two DEs.

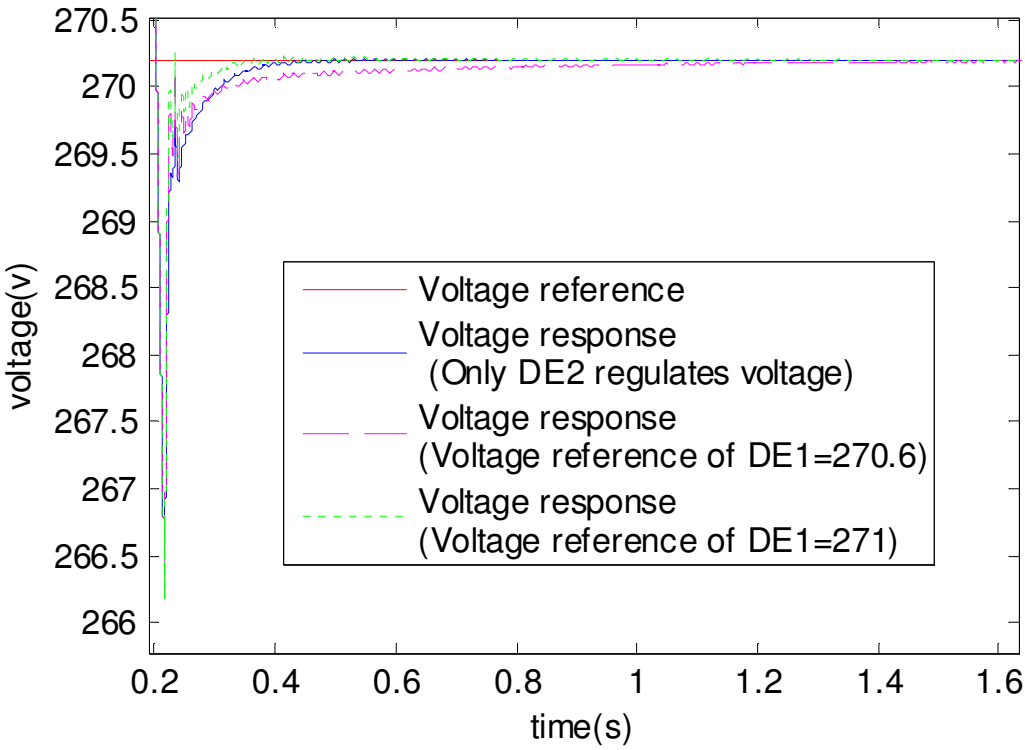


Figure 5.2. Voltage responses of DE2 in Scenarios 1, 2, and 3.

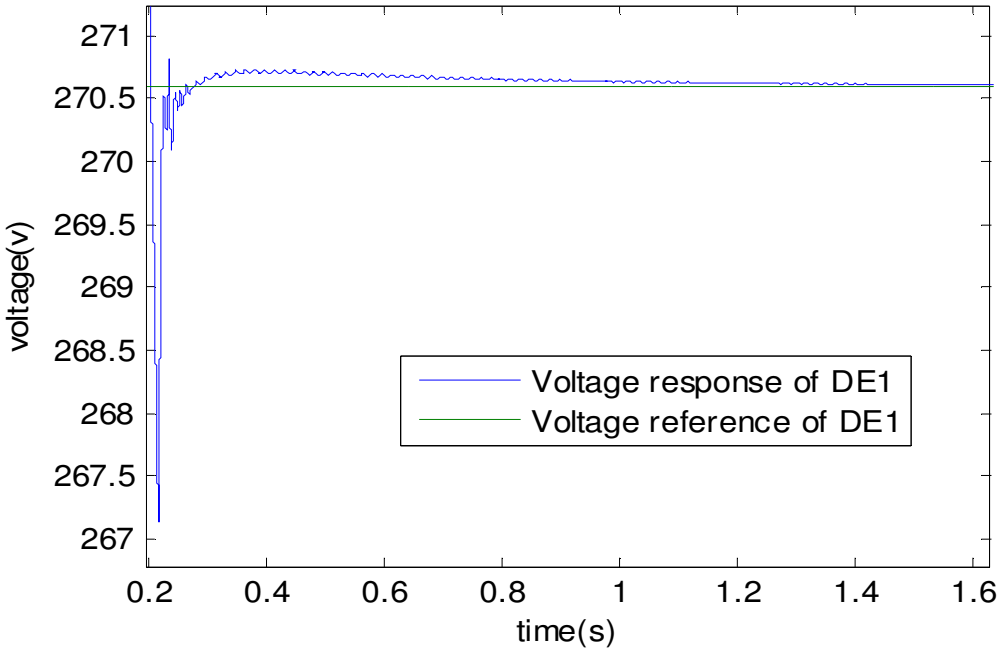


Figure 5.3. Voltage regulation of DE1 in Scenario 2.

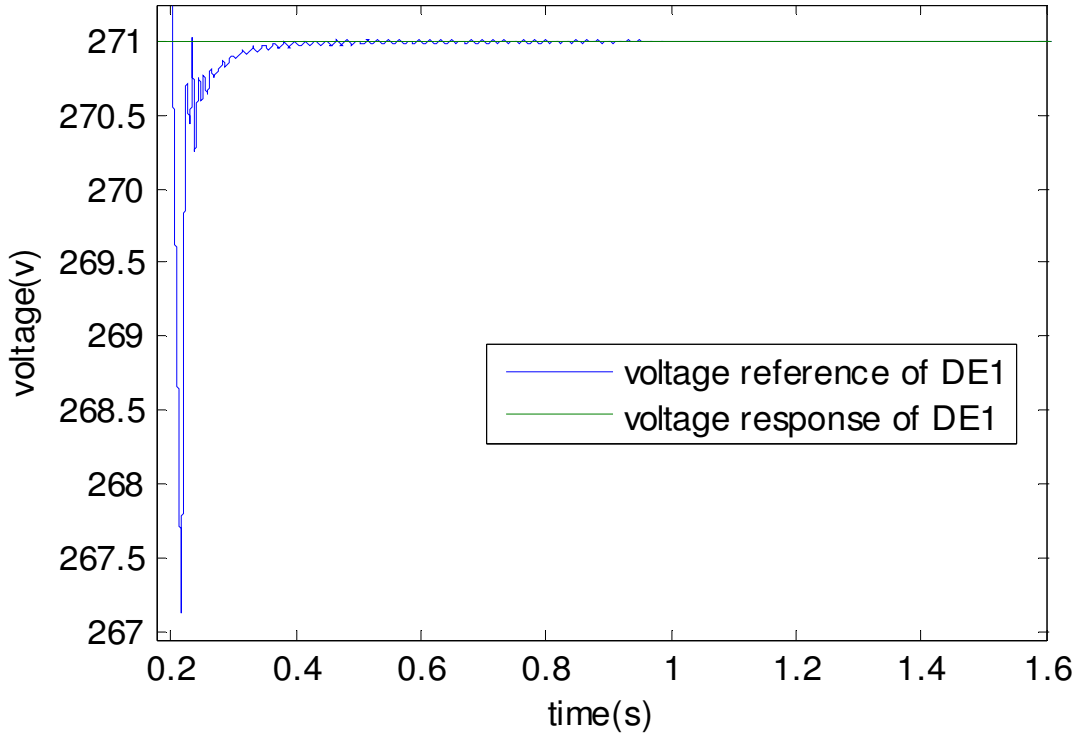


Figure 5.4. Voltage regulation of DE1 in Scenario 3.

Besides changing the response speed of the other DEs, the voltage regulation behavior of one DE may cause the wrong regulation direction problem of the other DEs. This is demonstrated in the following discussion.

Recall that

$$v_c^* = v_t(t)[1 + K_p(V_t^*(t) - V_t(t)) + K_I \int_0^t (V_t^*(t) - V_t(t))dt]. \quad (5.1)$$

This is the reference voltage required for a DE to produce during the regulation process. For fixed control parameters K_P and K_I with a positive value (usually K_I is greater than K_P), if the reference voltage $V_t^*(t)$ is higher than the terminal voltage $V_t(t)$, the DE will increase its output voltage and attempt to bring the voltage up to the reference. On the other hand, if $V_t^*(t)$ is less than $V_t(t)$, the DE will reduce its output voltage and reduce the actual voltage. When only a single DE regulates the voltage, the positive or negative sign of the

error between $V_t^*(t)$ and $V_t(t)$ provides a correct regulation direction for the DE. However, in the case of multiple DEs participating in the voltage regulation, due to the other DEs' simultaneous compensation, the sign of the error between $V_t^*(t)$ and $V_t(t)$ may not produce correct information on which direction to move.

In Figure 5.5, the blue solid curve shows the terminal voltage response of DE2 in Scenario 4, when only DE1 regulates its own terminal voltage. As can be seen, it exceeds the voltage reference (the red flat line) and DE2 needs to reduce the voltage to bring it down to the voltage reference if DE2 also participated in the regulation. However, the magenta dashed curve shows that in Scenario 5 when both DEs regulate the voltages, DE2 still tries to increase the voltage before reaching the reference at 0.3 *s* and only after the overshoot happens begins to reduce the voltage. The reason is that it begins to absorb the reactive power and bring the terminal voltage down only when the terminal voltage is higher than the reference voltage. Therefore, the overshoot is inevitable in this case.

In short, in the case of multiple DEs regulating voltages, one DE may be required to absorb reactive power to offset the excessive compensation from the other DEs, even when its terminal voltage is less than the reference voltage. In this situation, the sign of the error between the reference voltage and actual voltage fails to provide the right direction on whether the DE should increase the voltage output or decrease it, and accordingly, the overshoot occurs.

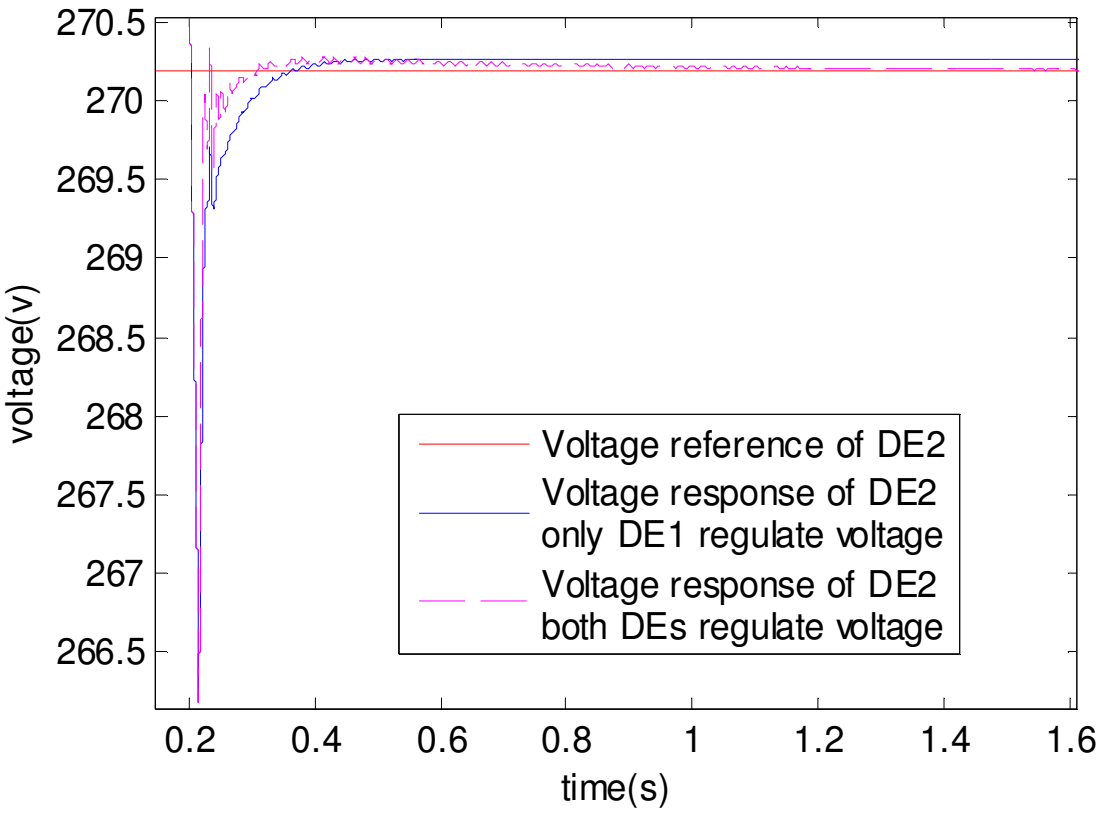


Figure 5.5. Voltage response of DE2 in scenario 4 and scenario 5.

From the simulation results of the five scenarios, we can conclude that:

- When multiple DEs participate in the voltage regulation, they interact with one another. The terminal voltage response of each DE is the result of all the DE's regulation behavior, and therefore, its speed may be increased or decreased by the other participating DEs.
- The voltage correction of the other DEs may result in excessive compensation at one DE's terminal bus, which makes the sign of the error between the reference voltage and actual voltage fail to indicate whether the DE should increase output voltage or decrease it without a voltage overshoot. To avoid this problem, a new signal should be introduced to provide the correct regulation direction for the DE.

The interaction among the DEs raises additional challenges for voltage control. The control algorithm needs to consider the impact from the other DEs and avoid the overshoot problem caused by the misleading information from the voltage error signal. However, we also can observe from the simulation results that the local terminal voltage measurement reflects the impacts of the other DEs' regulation on one specific DE. This information can still be used as the feedback to adjust the controller parameters.

5.3. Theoretical Formulation of the Parameters for Multiple Voltage-Regulating DEs with Adaptive Control Method

In Chapter 4, the formulation of the controller parameters in the case of a single voltage-regulating DE with the adaptive algorithm has been explained. When multiple DEs participate in the voltage regulation, as shown in Figure 5.6, it is interesting to investigate whether the adaptive control algorithm can still be applied to each voltage-regulating DE and the desired voltage response curve of each DE can be defined independently. This section will answer these questions and present a theoretical formulation of the controller parameters for multiple DEs with an adaptive algorithm.

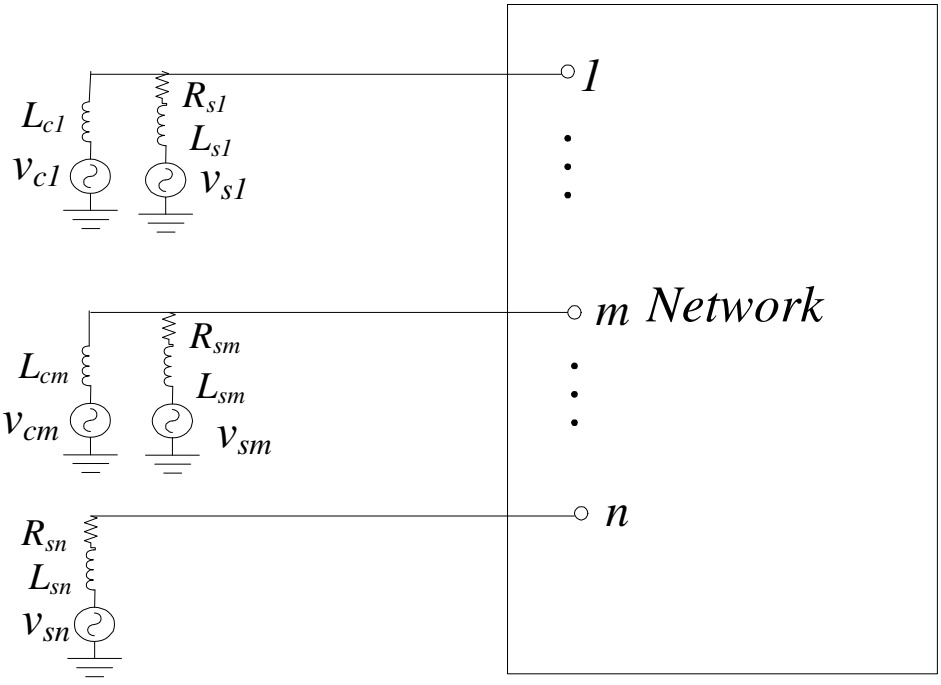


Figure 5.6. A schematic diagram of a network and with multiple DE sources.

Assume the DEs are connected at bus 1 through bus *m*, as shown in Figure 5.6. The nodal voltage equation can be expressed as

$$Y(s)\begin{bmatrix} v_{t1}(s) \\ \vdots \\ v_{tm}(s) \\ v_{tm+1}(s) \\ \vdots \\ v_{tn}(s) \end{bmatrix} = \begin{bmatrix} \dfrac{v_{c1}(s)}{sL_{c1}} + \dfrac{v_{s1}(s)}{R_1 + sL_1} \\ \vdots \\ \dfrac{v_{cm}(s)}{sL_{cm}} + \dfrac{v_{sm}(s)}{R_m + sL_m} \\ \dfrac{v_{sm+1}(s)}{R_{m+1} + sL_{m+1}} \\ \vdots \\ \dfrac{v_{sn}(s)}{R_n + sL_n} \end{bmatrix} \tag{5.2}$$

where $Y(s)$ is the admittance matrix of the system; $v_{ti}(s)$ is the voltage at bus i; $v_{sl}(s)$ is the voltage source at bus l $(l=1\sim n)$, excluding the DE source; R_l+L_l is the equivalent impedance for the electrical connection from the voltage source v_{sl} to the terminal buses l; $v_{ck}(s)$ is the output voltage of the DE source connected at bus k $(k=1\sim m)$; and L_{cl} is the inductance for the

DE to the terminal bus *k* connection. From Equation (5.2), we can derive the voltages vector as

$$\begin{bmatrix} v_{t1}(s) \\ \vdots \\ v_{tm}(s) \\ v_{tm+1}(s) \\ \vdots \\ v_{tn}(s) \end{bmatrix} = Z(s) \begin{bmatrix} \frac{v_{c1}(s)}{sL_{c1}} + \frac{v_{s1}(s)}{R_1 + sL_1} \\ \vdots \\ \frac{v_{cm}(s)}{sL_{cm}} + \frac{v_{sm}(s)}{R_m + sL_m} \\ \frac{v_{sm+1}(s)}{R_{m+1} + sL_{m+1}} \\ \vdots \\ \frac{v_{sn}(s)}{R_n + sL_n} \end{bmatrix} \tag{5.3}$$

where the impedance matrix $Z(S) = [Y(S)]^{-1}$. From Equation (5.3), we can obtain the vector of the regulated voltage as follows

$$\begin{bmatrix} v_{t1}(s) \\ \vdots \\ v_{ti}(s) \\ \vdots \\ v_{tm}(s) \end{bmatrix} = Z_1(s) \begin{bmatrix} \frac{v_{s1}(s)}{R_1 + sL_1} \\ \vdots \\ \frac{v_{si}(s)}{R_i + sL_i} \\ \vdots \\ \frac{v_{sn}(s)}{R_n + sL_n} \end{bmatrix} + Z_2(s) \cdot A(s) \begin{bmatrix} v_{c1}(s) \\ \vdots \\ v_{c2}(s) \\ \vdots \\ v_{cm}(s) \end{bmatrix} \tag{5.4}$$

where $Z_1(S)$ is the sub-matrix of $Z(S)$ formed by rows *1* to *m*; $Z_2(S)$ is an additional sub-matrix of $Z(S)$ formed by rows *1* to *m* and columns *1* to *m*; and $A(S)$ is the diagonal matrix defined in Equation (5.5)

$$A(s) = \begin{bmatrix} 1/sL_{c1} & & 0 \\ & \ddots & \\ 0 & & 1/sL_{cm} \end{bmatrix} \tag{5.5}$$

From Equation (5.4), the vector of the DE output voltages can be expressed as

$$\begin{bmatrix} v_{c1}(s) \\ \vdots \\ v_{ci}(s) \\ \vdots \\ v_{cm}(s) \end{bmatrix} = A(s)^{-1} Z_2(s)^{-1} \cdot \left[\begin{bmatrix} v_{t1}(s) \\ \vdots \\ v_{ti}(s) \\ \vdots \\ v_{tm}(s) \end{bmatrix} - Z_1(s) \begin{bmatrix} \frac{v_{s1}(s)}{R_1 + sL_1} \\ \vdots \\ \frac{v_{si}(s)}{R_i + sL_i} \\ \vdots \\ \frac{v_{sn}(s)}{R_n + sL_n} \end{bmatrix} \right] \tag{5.6}$$

Based on the assumption of the adaptive control method, we have

$$\Delta V_{ti}(s) = \frac{\Delta V_{ti_\max}}{s + 1/\tau} \text{ and} \tag{5.7}$$

$$V_{ti}(s) = (V_{ti}^{*} - \frac{\Delta V_{ti_\max}}{s + 1/\tau}) . \tag{5.8}$$

Therefore, we have

$$v_{ti}(t) = (V_{ti}^{*} - \Delta V_{ti_\max} e^{-\frac{t}{\tau}}) \cos(2\pi ft + \phi_i) \tag{5.9}$$

where $V_{ti}(s)$ is the RMS of the voltage at bus i; $\Delta V_{ti}(s)$ is the error between V_{ti}^{*}, the reference voltage at bus i, and $V_{ti}(s)$; Φ_i is the phase angle of the voltage at the terminal Bus i, and f is the fundamental frequency. Φ_i is known as the pre-disturbance condition or what can be obtained by the steady-state power flow calculation in the simulation.

By substituting Equation (5.9) into Equation (5.6), we can obtain

$$\begin{bmatrix} v_{c1}(s) \\ \vdots \\ v_{ci}(s) \\ \vdots \\ v_{cm}(s) \end{bmatrix} = A(s)^{-1} Z_2(s)^{-1} \cdot \left[\begin{bmatrix} (V_{t1}^{*} - \Delta V_{t1_\max} e^{-\frac{t}{\tau}}) \cos(2\pi ft + \phi_1) \\ \vdots \\ (V_{ti}^{*} - \Delta V_{ti_\max} e^{-\frac{t}{\tau}}) \cos(2\pi ft + \phi_i) \\ \vdots \\ (V_{tm}^{*} - \Delta V_{tm_\max} e^{-\frac{t}{\tau}}) \cos(2\pi ft + \phi_m) \end{bmatrix} - Z_1(s) \begin{bmatrix} \frac{v_{s1}(s)}{R_1 + sL_1} \\ \vdots \\ \frac{v_{si}(s)}{R_i + sL_i} \\ \vdots \\ \frac{v_{sn}(s)}{R_n + sL_n} \end{bmatrix} \right] \tag{5.10}$$

For any bus i $(i=1\sim m)$, where the DE is connected, we have

$$v_{ci}(s) = sL_{ci} \cdot \sum_{j=1}^{m} T_{ij} \left[(V_{tj} - \Delta V_{tj_\max} e^{-\frac{t}{\tau}}) \cos(2\pi ft + \phi_j) - \sum_{l=1}^{n} Z_{jl} \frac{v_{sl}(s)}{R_l + sL_l} \right] \tag{5.11}$$

where T_{ij} is the element at row i and column j in $Z_2(S)^{-1}$ and Z_{jl} is the element of row j and column l of $Z(S)$.

From Section 4.3, recall that

$$K_{Pi}(s) = \frac{\frac{\mathrm{V}_{ci}(s)}{\mathrm{V}_{ti}(s)} - 1}{\Delta V_{ti}(s)(1 + \frac{m}{s})} \tag{5.12}$$

where m is K_{I0}/K_{P0}, the calculation of which has been discussed in Section 4.2. For the DEs having the same DC voltage ratings, it can be assumed that the values of m are the same for simplicity.

By substituting Equation (5.7), (5.8) and (5.11) into (5.12), we have

$$K_{Pi}(s) = \frac{\frac{RMS(sL_{ci} \sum_{j=1}^{m} T_{ij} \left[(V_{tj} - \Delta V_{tj_\max} e^{-\frac{t}{\tau}}) \cos(2\pi ft + \phi_j) - \sum_{l=1}^{n} Z_{jl} \frac{v_{sl}(s)}{R_l + sL_l} \right])}{(V_{ti}^{*} - \frac{\Delta V_{ti_\max}}{s + 1/\tau})} - 1}{\frac{\Delta V_{ti_\max}}{s + 1/\tau}(1 + \frac{m}{s})} \tag{5.13}$$

and

$$K_{Ii}(s) = \frac{\frac{mRMS(sL_{ci} \sum_{j=1}^{m} T_{ij} \left[(V_{tj} - \Delta V_{tj_\max} e^{-\frac{t}{\tau}}) \cos(2\pi ft + \phi_j) - \sum_{l=1}^{n} Z_{jl} \frac{v_{sl}(s)}{R_l + sL_l} \right])}{(V_{ti}^{*} - \frac{\Delta V_{ti_\max}}{s + 1/\tau})} - 1}{\frac{\Delta V_{ti_\max}}{s + 1/\tau}(1 + \frac{m}{s})} \tag{5.14}$$

Equations (5.13) and (5.14) provide the formulations to calculate the parameters of the adaptive voltage controller when multiple DEs participate in the voltage regulation. If

only one voltage-regulating DE exists in the system and we assume it is connected at bus i, T_{ij} should be equal to $1/Z_{ii}$ then Equations (5.13) and (5.14) are the same as Equations (4.17) and (4.18).

We can calculate the controller parameters with which the terminal voltage follows the exponential decay pattern, provided that the network parameters are known, using Equations (5.13) and (5.14). In the situation that one of the DEs needs to absorb the reactive power in advance when its voltage is still below the reference to prevent the voltage overshoot, and it is highly interesting to investigate what the controller parameters would be. To investigate this phenomenon, the controller parameters in Scenario 5, listed in Table 5.1, are calculated by Equations (5.13) and (5.14). The results are shown in Figures 5.7 ~5.12.

Figures 5.7 and 5.8 depict the terminal voltage responses of DE1 and DE2, respectively. From the two figures, we can observe that after a disturbance occurs at 0.2 *sec* which causes the voltage drop, the voltage at both buses follows the exponential decay pattern to reach the reference voltages. Different from the response of the fixed parameters control, no overshoot occurs at the terminal bus of DE2. This means that the timely regulation direction information can be achieved by following the defined ideal voltage response (i.e., the exponential decay pattern), instead of comparing the actual voltage with the fixed reference voltage. The K_P and K_I parameters of the controllers will change during the regulation process to generate the exponential-decay-pattern response. Those parameters are shown in Figures 5.9 ~ 5.12. It should be noted that both DEs are assumed to have the same DC voltage rating, and therefore, have the same value of K_I/K_P, which is calculated in Section 4.4. The K_P and K_I of the controller of DE1 are shown in Figures 5.9 and 5.10. They vary with respect to time during the entire regulation process. Similar to what we observed in the simulation results of the single DE case, both of the K_P and K_I parameters increase

gradually to reach a stable positive value. However, from the K_P and K_I values of the DE2 controller, shown in Figures 5.11 and 5.12, we can observe that the values of the parameters K_P and K_I reduce to negative. It should be noted that the sign of the values of K_P and K_I reflect the voltage regulation direction. To avoid voltage overshoot at the terminal bus of DE2, the voltage output of DE2 needs to be reduced to absorb reactive power, even when the actual voltage is lower than the reference voltage. Therefore, the K_P and K_I values have to be negative to reduce the voltage output of the DE2.

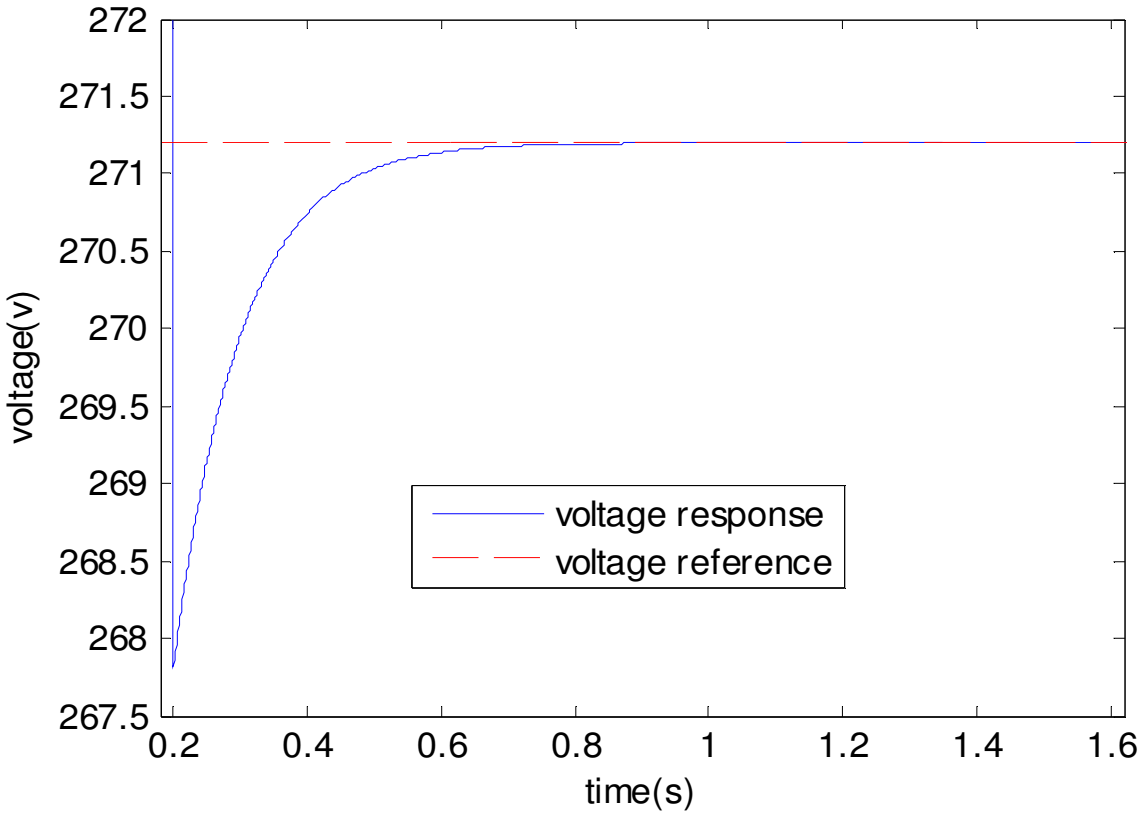


Figure 5.7. Terminal voltage of DE1 - Scenario 5.

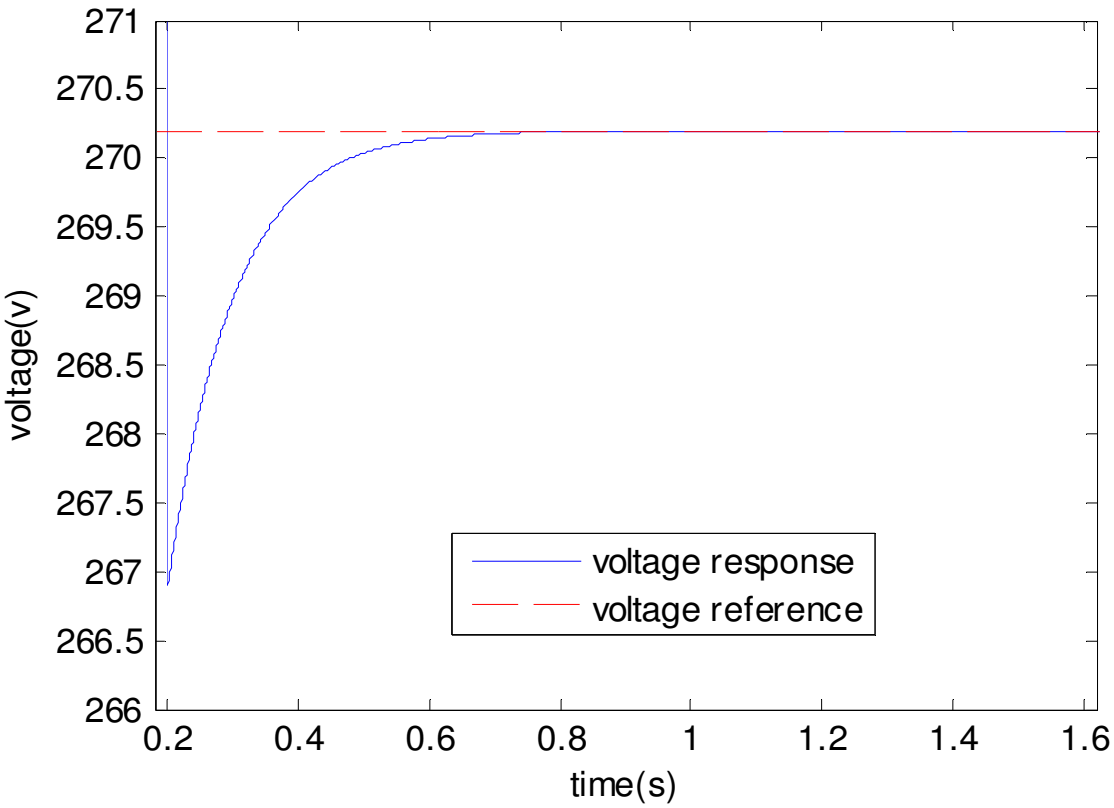


Figure 5.8. Terminal voltage of DE2 – Scenario 5.

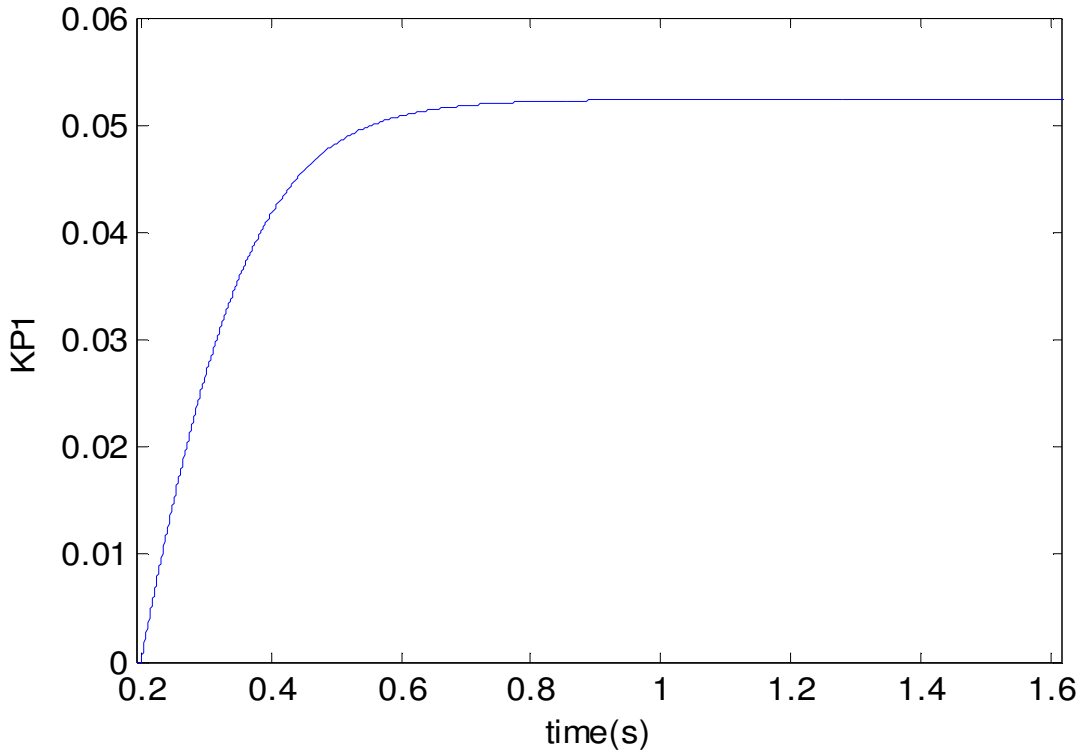


Figure 5.9. The calculated value of K_P of DE1 in adaptive control - Scenario 5.

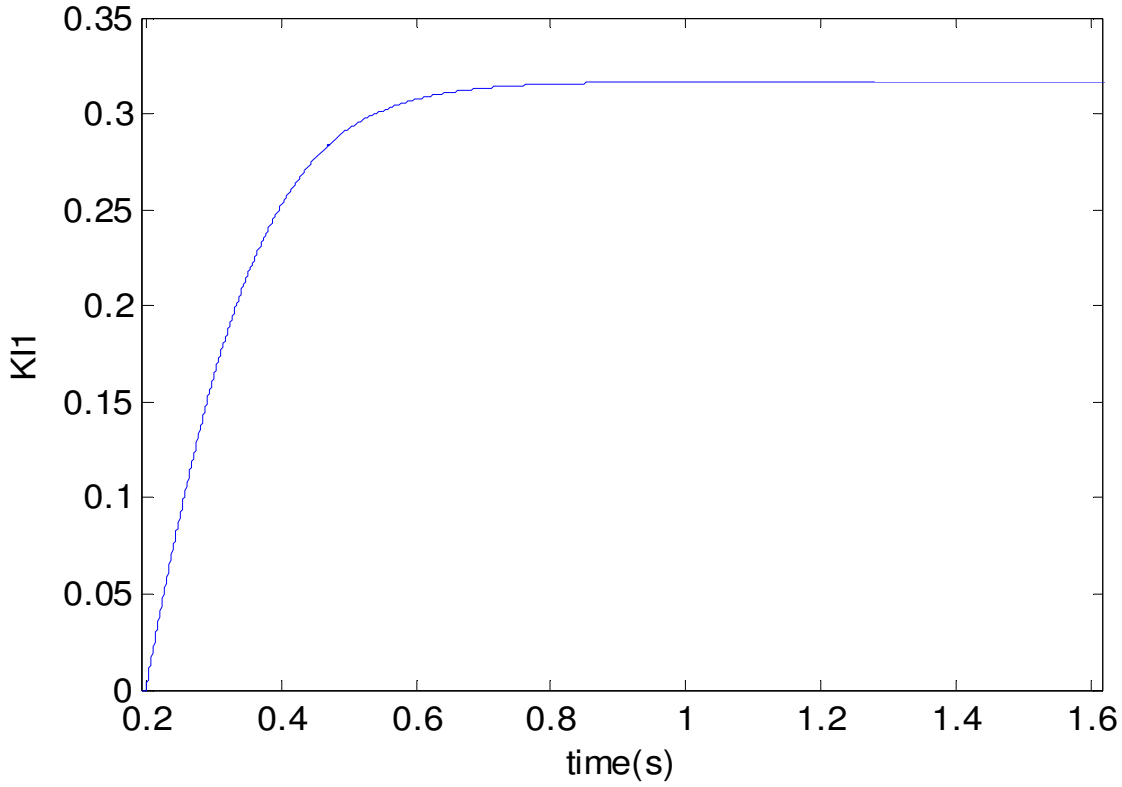


Figure 5.10. The calculated value of K_I of DE1 in adaptive control - Scenario 5.

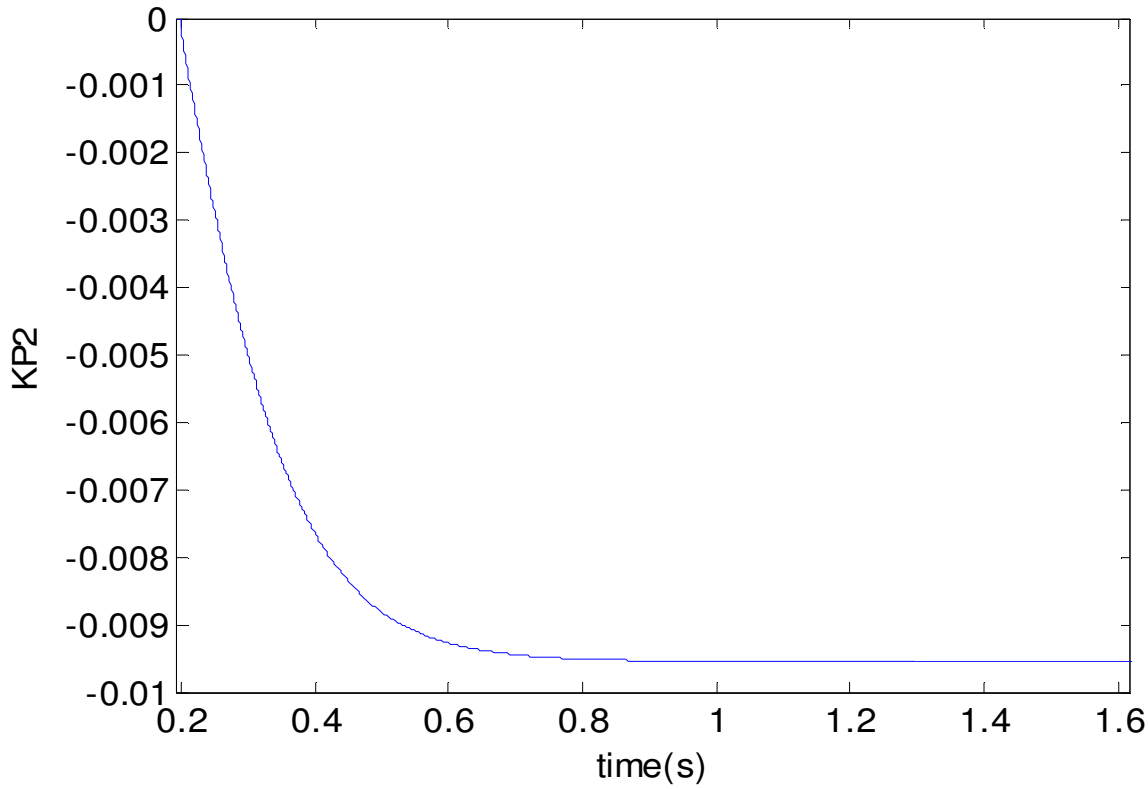


Figure 5.11. The calculated value of K_P of DE2 in adaptive control - Scenario 5.

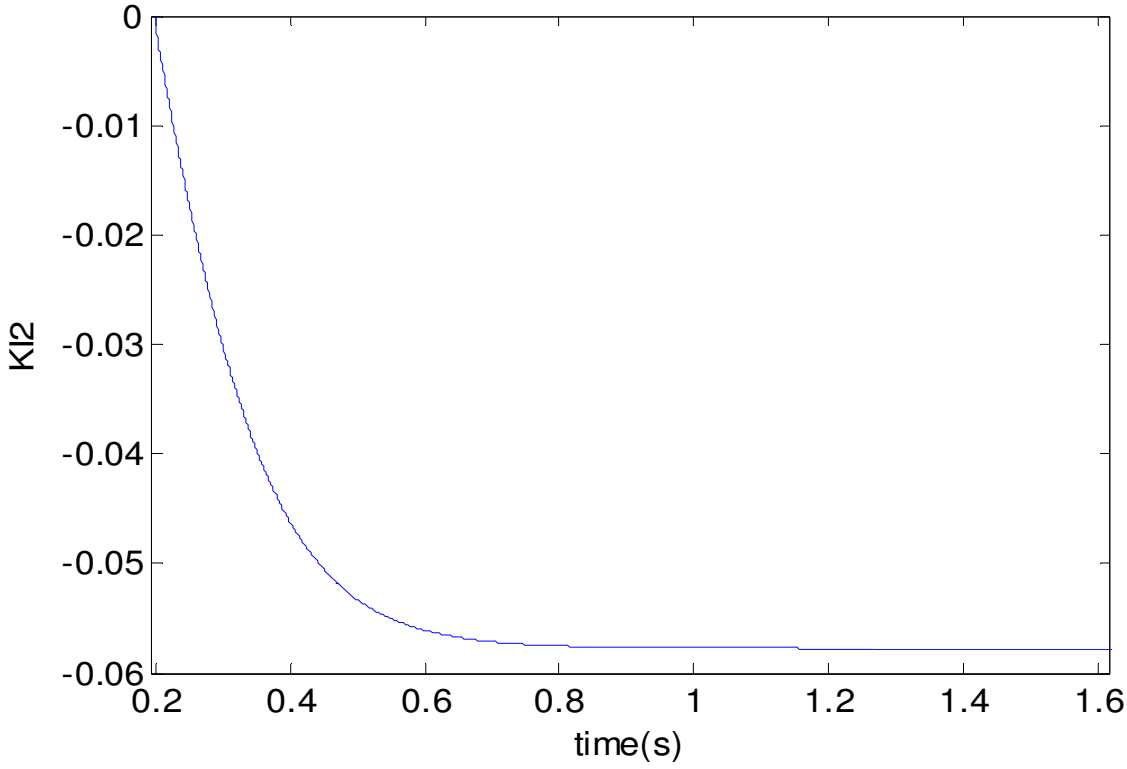


Figure 5.12. The calculated value of K_I of DE2 in adaptive control - Scenario 5.

The previous analysis and simulations prove that a unique solution for the control parameters under any specific operation condition exists. They also prove the existence of a unique solution of the dynamic, time-varying control parameters that will lead to the ideal voltage response.

To control the voltage regulation behavior of multiple voltage-regulating DEs in the grid, two possible solutions exist: control with communication or control without communication.

1. **A high-end, with communication solution:** Communications among the DEs enable each voltage-regulating DE to have the necessary information to make the control decision. The terminal voltage of each DE which participates in the voltage regulation is broadcast among the voltage regulation DE groups or is

reported to the control center. Then each DE voltage controller or the control center has sufficient information to make the right control decision. This high-end solution requires a continuous communication that may incur additional cost and create reliability issues. It should be noted that this work assumes the communication is ideal. Hence, the discussion of the actual communication is ignored while the focus is on the investigation of the control method.

2. **A low-end solution with no communication**: Methods with or without light communication are more preferable. In section 5.2, we have observed that the voltage at one DE's terminal bus also reflects the simultaneous impact from the other DEs' voltage regulation behavior. So, when compared with the desired response pattern, the local voltage measurement can still provide accurate and timely information of the regulation direction. With the suitable adjusting step size and timely adjustment, it is still possible for each DE to track its desired voltage response pattern closely and finally reach the reference voltage.

In the following subsections of this chapter, both the voltage regulation approaches, with and without communication, will be investigated and the results will be compared. Features of each approach are discussed.

5.4. Voltage Regulation with Communication

The communication among the voltage-regulating DEs or with the control center provides the real time information of the whole system, including the terminal voltage at the other DE buses and the output voltage of every DE.

At any time *t*, we have

$$Y\begin{bmatrix} \dot{V}_{t1}(t) \\ \vdots \\ \dot{V}_{tm}(t) \\ \dot{V}_{t(m+1)}(t) \\ \vdots \\ \dot{V}_{t1tn}(t) \end{bmatrix} = \begin{bmatrix} \dfrac{\dot{V}_{c1}(t)}{jX_{c1}} + \dfrac{\dot{V}_{s1}(t)}{R_{s1}+jX_{s1}} \\ \vdots \\ \dfrac{\dot{V}_{cm}(t)}{jX_{cm}} + \dfrac{\dot{V}_{sm}(t)}{R_{sm}+jX_{sm}} \\ \dfrac{\dot{V}_{sm+1}(t)}{R_{s(m+1)}+jX_{s(m+1)}} \\ \vdots \\ \dfrac{\dot{V}_{sn}(t)}{R_{sn}+jX_{sn}} \end{bmatrix} \tag{5.15}$$

where Y is the admittance matrix Y_{ij}=G_{ij}+jB_{ij} and $\dot{V}_{ti} = V_{ti}\angle\delta_{ti}$, ($i$=1~$n$).

Equation (5.15) is the discretization of function (5.2). For any bus, i, which is connected with DE, from Equation (5.15) we can obtain

$$\begin{aligned} &\sum_{j=1}^{n}(G_{ij}+jB_{ij})V_{tj}(t)\angle\delta_j(t) = \frac{V_{ci}(t)\angle\delta_{ci}(t)}{jX_{ci}} + \frac{V_{si}(t)\angle\delta_{si}(t)}{R_{si}+jX_{si}}, \quad i=1\sim m. \\ &\sum_{j=1}^{n}(G_{ij}+jB_{j})V_{tj}(t)\angle\delta_j(t) = \frac{V_{si}(t)\angle\delta_{si}(t)}{R_{si}+jX_{si}}, \qquad i=(m+1)\sim n. \end{aligned} \tag{5.16}$$

By splitting Equation (5.16) into real part and imaginary parts, we have

$$\begin{aligned} &\sum_{j=1}^{n}G_{ij}V_{tj}(t)\cos(\delta_j(t)) - B_{ij}V_{tj}(t)\sin(\delta_j(t)) = \frac{V_{ci}(t)\sin(\delta_{ci}(t))}{X_{ci}} + source_r_i(t), \\ &\qquad\qquad i=1\sim m. \\ &\sum_{j=1}^{n}G_{ij}V_{tj}(t)\sin(\delta_j(t)) + B_{ij}V_{tj}(t)\cos(\delta_j(t)) = \frac{-V_{ci}(t)\cos(\delta_{ci}(t))}{X_{ci}} + source_i_i(t), \\ &\qquad\qquad i=1\sim m. \\ &\sum_{j=1}^{n}G_{ij}V_{tj}(t)\cos(\delta_j(t)) - B_{ij}V_{tj}(t)\sin(\delta_j(t)) = source_r_i(t), \quad i=m+1\sim n. \\ &\sum_{j=1}^{n}G_{ij}V_{tj}(t)\cos(\delta_j(t)) - B_{ij}V_{tj}(t)\sin(\delta_j(t)) = source_i_i(t), \quad i=m+1\sim n. \end{aligned} \tag{5.17}$$

where $source_r_i(t)$ and $source_i_i(t)$ are the real and imaginary parts of $\frac{V_{si}(t)\angle\delta_{si}(t)}{R_{si}+jX_{si}}$, respectively. They are constants because the voltage sources from the substations are known, as is typically assumed.

Considering the real power output of DEs, we have

$$\frac{V_{ci}(t)V_{ti}(t)}{X_{ci}}\sin(\delta_{ci}(t)-\delta_i(t))=P_i(t),\quad i=1\sim m. \tag{5.18}$$

In the adaptive control method, the terminal voltage response of each DE, $V_i(t)$, i=1~m, is predefined, so we have $2n+m$ unknown variables remaining. These $2n+m$ unknowns include:

- The phase angles of the bus voltage $\delta_i(t)$, i=1~n;
- The magnitudes of the voltage at the other buses, excluding DE terminal buses, $V_i(t)$, i=m+1~n;
- The phase angles of the DE output voltages, $\delta_{ci}(t)$, i=1~m; and
- The magnitude of DEs output voltages, $V_{ci}(t)$, i=1~m.

There are total of $2n+m$ equations in (5.17) and (5.18), which matches the total number of the unknown variables. Hence, at any moment t, given the terminal voltage of DEs, $V_i(t)$, i=1~m, there are corresponding DE output voltages $V_{ci}(t)$, i=1~m.

$$V_{ci}(t)=f_i(V_1(t),\cdots V_m(t)),\ i=1\sim m. \tag{5.19}$$

From t_0 to $t_0+\Delta t$, if $\Delta V_i(t)$ is very small and Function (5.19) can be linearized to acquire the approximation of $V_{ci}(t_0+\Delta t)$ as

$$V_{ci}(t_0+\Delta t)=V_{ci}(t_0)+\sum_{j=1}^{m}\frac{\partial f_i}{\partial V_j}\Big|_{t=t_0}(V_j(t_0+\Delta t)-V_j(t_0)),\ i=1\sim m. \tag{5.20}$$

where $\left.\frac{\partial f_i}{\partial V_j}\right|_{t=t_0}$ is assumed to be constant in the small range and can be calculated by the local measurement in real time.

At t_0, $t_0+\Delta t$, $t_0+2\Delta t$, …, $t_0+m\Delta t$, without the loss of generality, we can set the output voltages of DE at bus i are $V_{ci}(t_0)$, $V_{ci}(t_0+\Delta t)$, $V_{ci}(t_0+2\Delta t)$, …, $V_{ci}(t_0+m\Delta t)$, respectively, where $i=1\sim m$. The corresponding terminal voltages, $V_j(t_0)$, $V_j(t_0+\Delta t)$, $V_j(t_0+2\Delta t)$, …, $V_j(t_0+m\Delta t)$, where $j=1\sim m$, at the buses which have DE connections can be measured. Hence, for any bus i which has a DE connection, we have the following equations

$$\begin{aligned}
\Delta V_{ci}^{(1)} &= V_{ci}(t_0+\Delta t)-V_{ci}(t_0)=\sum_{j=1}^{m}\frac{\partial f_i}{\partial V_j}\Delta V_j^{(1)} \\
\Delta V_{ci}^{(2)} &= V_{ci}(t_0+2\Delta t)-V_{ci}(t_0+\Delta t)=\sum_{j=1}^{m}\frac{\partial f_i}{\partial V_j}\Delta V_j^{(2)} \\
&\vdots \\
\Delta V_{ci}^{(m)} &= V_{ci}(t_0+m\Delta t)-V_{ci}(t_0+(m-1)\Delta t)=\sum_{j=1}^{m}\frac{\partial f_i}{\partial V_j}\Delta V_j^{(m)}
\end{aligned} \tag{5.21}$$

where $\Delta V_j^{(k)} = V_j(t_0+k\Delta t)-V_j(t_0+(k-1)\Delta t),\ k=1\sim m,\ i=1\sim m,\ j=1\sim m$.

Equation (5.21) can also be expressed in matrix form as

$$\begin{bmatrix} \Delta V_{ci}^{(1)} \\ \Delta V_{ci}^{(2)} \\ \vdots \\ \Delta V_{ci}^{(m)} \end{bmatrix} = \begin{bmatrix} \Delta V_1^{(1)} & \Delta V_2^{(1)} & \cdots & \Delta V_m^{(1)} \\ \Delta V_1^{(2)} & \Delta V_2^{(2)} & \cdots & \Delta V_m^{(2)} \\ \vdots & \vdots & \vdots & \vdots \\ \Delta V_1^{(m)} & \Delta V_2^{(m)} & \cdots & \Delta V_m^{(m)} \end{bmatrix} \begin{bmatrix} \frac{\partial f_i}{\partial V_1} \\ \frac{\partial f_i}{\partial V_2} \\ \vdots \\ \frac{\partial f_i}{\partial V_m} \end{bmatrix} \tag{5.22}$$

We can derive the coefficient vector as

$$\begin{bmatrix} \frac{\partial f_i}{\partial V_1} \\ \frac{\partial f_i}{\partial V_2} \\ \vdots \\ \frac{\partial f_i}{\partial V_m} \end{bmatrix} = \begin{bmatrix} \Delta V_1^{(1)} & \Delta V_2^{(1)} & \cdots & \Delta V_m^{(1)} \\ \Delta V_1^{(2)} & \Delta V_2^{(2)} & \cdots & \Delta V_m^{(2)} \\ \vdots & \vdots & \vdots & \vdots \\ \Delta V_1^{(m)} & \Delta V_2^{(m)} & \cdots & \Delta V_m^{(m)} \end{bmatrix}^{-1} \begin{bmatrix} \Delta V_{ci}^{(1)} \\ \Delta V_{ci}^{(2)} \\ \vdots \\ \Delta V_{ci}^{(m)} \end{bmatrix} \tag{5.23}$$

By Equation (5.23), we can obtain the linearized relation in a small range between all DE output voltages and the voltages at all the DE terminals.

In the adjustment process, once the coefficient vectors have been calculated by (5.23), we can easily calculate how much the DE output voltage needs to be for the next adjustment step based on Equation (5.20) in order to achieve the voltage response matching the desired response. When the voltage matches the desired response, it follows the pattern below

$$\begin{aligned} \Delta V_j^{(1)} &= V_j(t_0 + \Delta t) - V_j(t_0) \\ &= (V_{tj}^* - \Delta V_{tj_\max} e^{-\frac{t+\Delta t}{\tau}}) - (V_{tj}^* - \Delta V_{tj_\max} e^{-\frac{t}{\tau}}) \\ &= \Delta V_{j_\max} (e^{-\frac{t}{\tau}} - e^{-\frac{t+\Delta t}{\tau}}) \end{aligned} \tag{5.24}$$

from t_0 to $t_0+\Delta t$; and

$$\Delta V_j^{(2)} = V_j(t_0 + 2\Delta t) - V_j(t_0 + \Delta t) = \Delta V_{tj_\max} (e^{-\frac{t+\Delta t}{\tau}} - e^{-\frac{t+2\Delta t}{\tau}}) \tag{5.25}$$

from $t_0+\Delta t$ to $t_0+2\Delta t$.

For two consecutive voltage changes, we can obtain the ratio of the two by dividing (5.25) by (5.24),

$$r = \frac{\Delta V_j^{(2)}}{\Delta V_j^{(1)}} = \frac{\Delta V_{tj_\max} (e^{-\frac{t+\Delta t}{\tau}} - e^{-\frac{t+2\Delta t}{\tau}})}{\Delta V_{tj_\max} (e^{-\frac{t}{\tau}} - e^{-\frac{t+\Delta t}{\tau}})} = \frac{e^{-\frac{\Delta t}{\tau}} - e^{-\frac{2\Delta t}{\tau}}}{1 - e^{-\frac{\Delta t}{\tau}}}, \; j = 1 \sim m. \tag{5.26}$$

Provided that the fixed step size, Δt, of the parameter-adjusting process, the ratio is constant and remains the same for each DE terminal voltage. Therefore, from Equation (5.20), we have

$$\begin{aligned}\Delta V_{ci}^{(2)} &= V_{ci}(t_0 + 2\Delta t) - V_{ci}(t_0 + \Delta t) \\ &= \sum_{j=1}^{m} \frac{\partial f}{\partial V_j}\Big|_{t=t_0+\Delta t} \Delta V_j^{(2)} \approx \sum_{j=1}^{m} \frac{\partial f}{\partial V_j}\Big|_{t=t_0} r\Delta V_j^{(1)} \\ &= r\sum_{j=1}^{m} \frac{\partial f}{\partial V_j}\Big|_{t=t_0} \Delta V_j^{(1)} = r\Delta V_{ci}^{(1)}\end{aligned} . \qquad (5.27)$$

We can conclude that the DE output voltage required to generate the desired response should follow the following rule:

The ratio of two consecutive adjustments is constant and equal to the ratio of the corresponding two consecutive terminal voltage changes.

So, after the terminal voltage response matches the desired response, the DE output voltage can be adjusted according to this rule to make the voltage response follow the desired response. In the following adjusting process, the coefficient vector $\left[\frac{\partial f_i}{\partial V_1}, \frac{\partial f_i}{\partial V_2}, \cdots, \frac{\partial f_i}{\partial V_m}\right]^T$ does not need to be calculated, and actually, Equation (5.23) does not exist when the voltage follows the desired exponential decay paten because $\begin{bmatrix} \Delta V_1^{(1)} & \Delta V_2^{(1)} & \cdots & \Delta V_m^{(1)} \\ \Delta V_1^{(2)} & \Delta V_2^{(2)} & \cdots & \Delta V_m^{(2)} \\ \vdots & \vdots & \vdots & \vdots \\ \Delta V_1^{(m)} & \Delta V_2^{(m)} & \cdots & \Delta V_m^{(m)} \end{bmatrix}$ will become singular in this condition.

The regulating algorithm discussed so far can be generalized into three steps:

1. Increasing the DEs voltage output by a fixed step to calculate the coefficient vector $\left[\frac{\partial f_i}{\partial V_1}, \frac{\partial f_i}{\partial V_2}, \cdots, \frac{\partial f_i}{\partial V_m}\right]^T$.

2. Setting the DE voltage outputs according to Equation (5.20) to ensure each DE terminal voltage to match the desired response.
3. Updating the DEs voltage output according to Equation (5.27).

A more detailed algorithm flow chart is shown in Figure 5.13.

In the following discussion, the simulation results of the adaptive voltage control method with communication on the system in Figure 5.1 will be shown. The real power injection of DE1 and DE2 is 30 kW and 10 kW, respectively, and remains constant. The voltage references for bus 3 and bus 6 are 275.85 v and 275.70 v. Assume after a load increase, the voltages at bus 3 and bus 6 drop to 270.85 v and 270.70 v, respectively. The adjustment cycle is 1/60 s (i.e., the adjustment frequency is aligned with the electricity frequency).

1. Calculating the coefficient vector $\left[\frac{\partial f_i}{\partial V_1}, \frac{\partial f_i}{\partial V_2}, \cdots, \frac{\partial f_i}{\partial V_m}\right]^T$.

$V^{(0)}=[270.85,\ 270.5]^{\mathrm{T}}$, $V_c^{(0)}=[271.1726,\ 270.1228]^{\mathrm{T}}$. Increase DE output voltage by $\Delta V_c^{(1)}=[0.1,0.1]^{\mathrm{T}}$ and $\Delta V_c^{(2)}=[0.1,0.15]^{\mathrm{T}}$ in two consecutive adjustment processes. Then, we have $V_c^{(1)}=[271.2726,\ 270.2228]^{\mathrm{T}}$ and $V_c^{(2)}=[271.3726,\ 270.3728]^{\mathrm{T}}$. The corresponding terminal voltages are $V^{(1)}=[270.8758,\ 270.5267]^{\mathrm{T}}$ and $V^{(2)}=[270.9074,\ 270.5598]^{\mathrm{T}}$. According to Equation (5.23), for DE1 we have

$$\begin{bmatrix} \frac{\partial f_1}{\partial V_3} \\ \frac{\partial f_1}{\partial V_6} \end{bmatrix} = \begin{bmatrix} \Delta V_3^{(1)} & \Delta V_6^{(1)} \\ \Delta V_3^{(2)} & \Delta V_6^{(2)} \end{bmatrix}^{-1} \begin{bmatrix} \Delta V_{c1}^{(1)} \\ \Delta V_{c1}^{(2)} \end{bmatrix}$$

$$= \begin{bmatrix} 270.8758 - 270.85 & 270.5267 - 270.5 \\ 270.9074 - 270.8758 & 270.5598 - 270.5267 \end{bmatrix}^{-1} \begin{bmatrix} 0.1 \\ 0.1 \end{bmatrix}$$

$$= \begin{bmatrix} 66.7170 \\ -60.7167 \end{bmatrix}$$

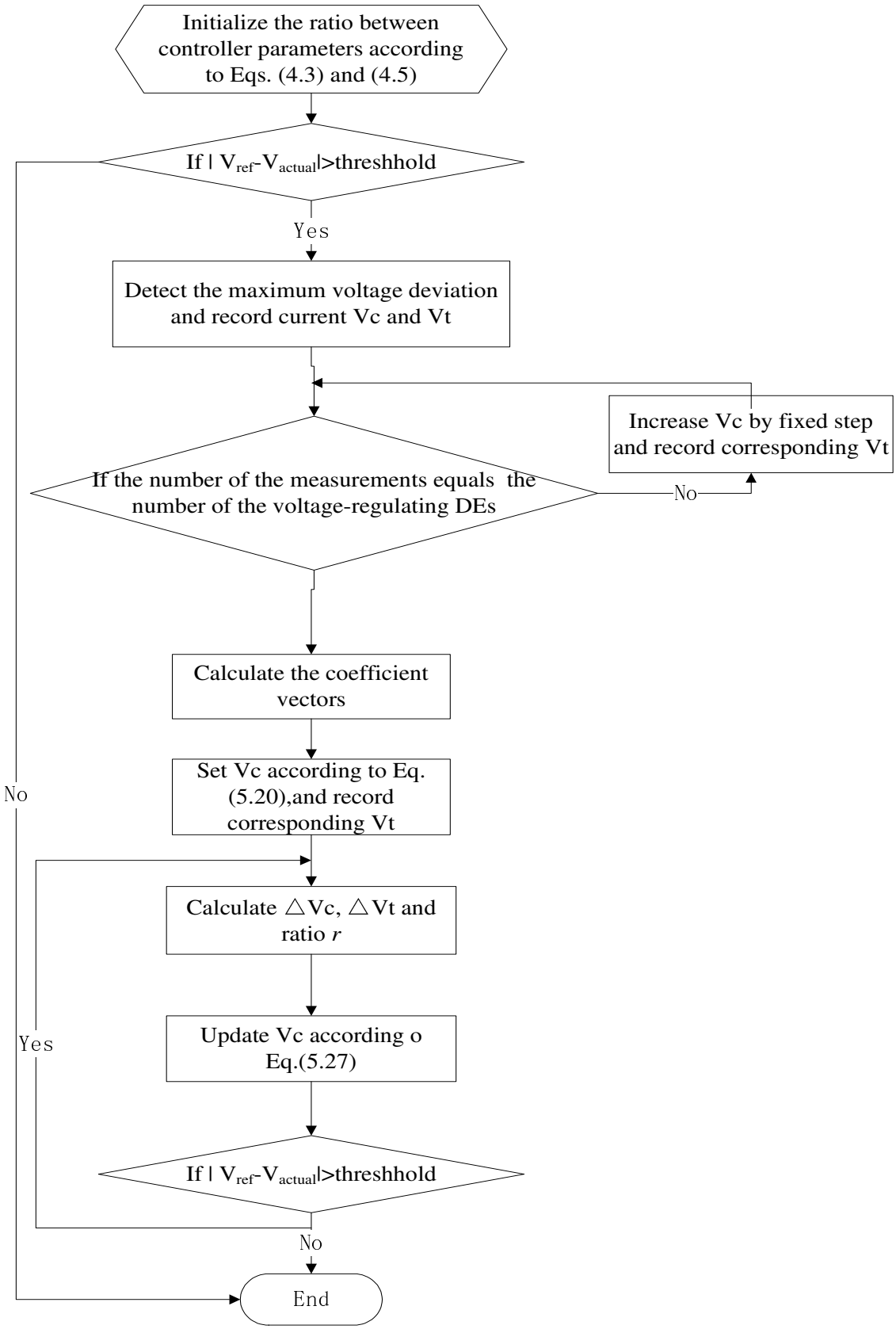


Figure 5.13. Adaptive voltage adjusting algorithm with communication.

For DE2, we have

$$\begin{bmatrix} \frac{\partial f_2}{\partial V_3} \\ \frac{\partial f_2}{\partial V_6} \end{bmatrix} = \begin{bmatrix} \Delta V_3^{(1)} & \Delta V_6^{(1)} \\ \Delta V_3^{(2)} & \Delta V_6^{(2)} \end{bmatrix}^{-1} \begin{bmatrix} \Delta V_{c2}^{(1)} \\ \Delta V_{c2}^{2} \end{bmatrix}$$

$$= \begin{bmatrix} 270.8758 - 270.85 & 270.5267 - 270.5 \\ 270.9074 - 270.8758 & 270.5598 - 270.5267 \end{bmatrix}^{-1} \begin{bmatrix} 0.1 \\ 0.15 \end{bmatrix}$$

$$= \begin{bmatrix} -70.8723 \\ 72.2351 \end{bmatrix}$$

2. Adjusting DE output voltages to make terminal voltage match the desired response.

The desired voltage at bus 3 is $275.85 - 5e^{-\frac{3\times 1/60}{0.1}} = 272.8173$ V, and at bus 6 is $275.7 - 5.2e^{-\frac{3\times 1/60}{0.1}} = 272.5460$ V. According to Equation (5.20), the voltage adjustments need to be

$$\begin{bmatrix} \Delta V_{c1}^{(3)} \\ \Delta V_{c2}^{(3)} \end{bmatrix} = \begin{bmatrix} \frac{\partial f_1}{\partial V_3} & \frac{\partial f_1}{\partial V_6} \\ \frac{\partial f_2}{\partial V_3} & \frac{\partial f_2}{\partial V_6} \end{bmatrix} \begin{bmatrix} \Delta V_{3_desired}^{(3)} \\ \Delta V_{6_desired}^{(3)} \end{bmatrix}$$

$$= \begin{bmatrix} 66.7170 & -60.7167 \\ -70.8723 & 72.2351 \end{bmatrix} \begin{bmatrix} 272.8173 - 270.9074 \\ 272.5460 - 270.5598 \end{bmatrix}$$

$$= \begin{bmatrix} 6.8265 \\ 8.1155 \end{bmatrix}$$

After the adjustments, the output voltages of two DEs are

$$\begin{bmatrix} V_{c1}^{(3)} \\ V_{c2}^{(3)} \end{bmatrix} = \begin{bmatrix} 271.3726 + 6.8265 \\ 270.3728 + 8.1155 \end{bmatrix} = \begin{bmatrix} 278.1991 \\ 278.4883 \end{bmatrix}.$$

The corresponding terminal voltages are $V^{(3)}$=[272.8061, 272.5350]^T, which are very close to the desired response.

For the next adjusting process, we have the desired response as

$$V_{desired}^{(4)} = \begin{bmatrix} 275.85 - 5e^{-\frac{4\times 1/60}{0.1}} \\ 275.7 - 5.2e^{-\frac{4\times 1/60}{0.1}} \end{bmatrix} = \begin{bmatrix} 273.2829 \\ 273.0302 \end{bmatrix}$$

To match the desired response, the DEs output voltages need to be

$$\begin{bmatrix} V_{c1}^{(4)} \\ V_{c2}^{(4)} \end{bmatrix} = \begin{bmatrix} V_{c1}^{(3)} \\ V_{c2}^{(3)} \end{bmatrix} + \begin{bmatrix} \frac{\partial f_1}{\partial V_3} & \frac{\partial f_1}{\partial V_6} \\ \frac{\partial f_2}{\partial V_3} & \frac{\partial f_2}{\partial V_6} \end{bmatrix} \begin{bmatrix} \Delta V_{3_desired}^{(4)} \\ \Delta V_{6_desired}^{(4)} \end{bmatrix}$$

$$= \begin{bmatrix} 278.1991 \\ 278.4883 \end{bmatrix} + \begin{bmatrix} 66.7170 & -60.7167 \\ -70.8723 & 72.2351 \end{bmatrix} \begin{bmatrix} 273.2829 - 272.8061 \\ 273.0302 - 272.5350 \end{bmatrix}$$

$$= \begin{bmatrix} 279.9373 \\ 280.4736 \end{bmatrix}$$

The actual voltages are $V_t^{(4)}$=[273.2768, 273.0242]$^{\mathrm{T}}$. The voltage responses at both buses follow the desired response.

Similar patterns will be repeated for the following processes.

3. Adjusting DE output based on the ratio of voltage change between two consecutive adjusting steps.

If the voltage responses perfectly follow the desired responses without any error, the ratio of the two consecutive voltage changes can be calculated by applying equation (5.26) as

$$r = \frac{e^{-\frac{\Delta t}{\tau}} - e^{-\frac{2\Delta t}{\tau}}}{1 - e^{-\frac{\Delta t}{\tau}}} = \frac{e^{-\frac{1/60}{0.1}} - e^{-\frac{2/60}{0.1}}}{1 - e^{-\frac{1/60}{0.1}}} = 0.8465 .$$

The actual needed ratio can be calculated as: $r = \frac{\Delta V_{desired}^{\,i}}{\Delta V^{\,i-1}}$. For multiple DEs, we can take the average value of all the DEs to neutralize the random errors. In this case, we have

$$r = \left(\frac{273.6770 - 273.2768}{273.2768 - 272.8061} + \frac{273.4401 - 273.0242}{273.0242 - 272.5350} \right) / 2 = 0.8502 .$$

And hence, the DE output for this step should be

$$\begin{bmatrix} V_{c1}^{(5)} \\ V_{c2}^{(5)} \end{bmatrix} = \begin{bmatrix} V_{c1}^{(4)} \\ V_{c2}^{(4)} \end{bmatrix} + r \begin{bmatrix} \Delta V_{c1}^{(4)} \\ \Delta V_{c2}^{(4)} \end{bmatrix} = \begin{bmatrix} 279.9373 \\ 280.4736 \end{bmatrix} + 0.8502 \begin{bmatrix} 1.7383 \\ 1.9853 \end{bmatrix} = \begin{bmatrix} 281.4152 \\ 282.1614 \end{bmatrix}.$$

The corresponding terminal voltages are $V_t^{(5)}$=[273.6760, 273.4392]$^{\mathrm{T}}$. The actual voltages closely follow the desired responses. For the following adjusting steps, this operation will be repeated until the actual responses reach the voltage references.

Figures 5.14 and 5.15 show the comparison of the actual voltage responses and desired voltage responses in the whole process. The voltage drop occurs at 0.2 *sec*. At the beginning of the regulation process, the voltage response does not follow the ideal response because the DEs' output voltages are controlled to increase in the fixed step size to calculate the coefficients between the DEs' output voltage changes and the terminal voltage changes. After obtaining the coefficients, the voltage responses successfully catch the ideal responses and going forward follow the ideal responses very closely until reaching the reference voltages. The maximum difference of the ideal voltage and actual voltage is 0.0112 V for DE1 and 0.0111 V for DE2 in the process. Figures 5.16~5.19 show the values of the K_P and K_I parameters of the DE1 and DE2 controllers, respectively, in the adjustment process. Figure 5.20 shows the average value of the ratio of the two consecutive voltage changes, which is close to the ideal value 0.8465.

This method is also tested in the case that one DE needs to absorb reactive power. Figures 5.21 and 5.22 show the voltage responses at terminals DE1 and DE2, respectively, when only DE1 regulates its terminal voltage. The terminal voltage of DE2 finally reaches 275.48 V. If the reference voltage at the terminal of DE2 is set to 271.10 V, DE2 needs to absorb reactive power. Figures 5.23~5.29 show the simulation results when both DEs

regulate the voltage, when the reference voltages of DE1 and DE2 are 275.85 V and 275.10 V, respectively. The terminal voltage responses of DE1 and DE2 can closely track the ideal responses except at the very beginning, as shown in Figures 5.23 and 5.24. After obtaining the coefficient vector, the maximum tracking errors are 0.0576 V and 0.0566 V, respectively. The values of K_P in the DE1 and DE2 controllers are shown in Figures 5.25 and 5.27, respectively. The K_P of DE2 decreases to a negative value to make the output voltage of DE2 less than the terminal voltage and therefore, DE2 absorbs the reactive power while its terminal voltage is still below the reference. The average value of the ratio of the two consecutive voltage changes during the regulation process, shown in Figure 5.29, is close to the ideal value 0.8465 as well. These simulation results show that this tracking method can also work well in the case where the DE needs to absorb reactive power even when its reference voltage is higher than its terminal voltage.

The control approach with the communication can directly calculate how much the DEs output voltages need to be in order to match the desired response curve and hence can track the desired response quite closely.

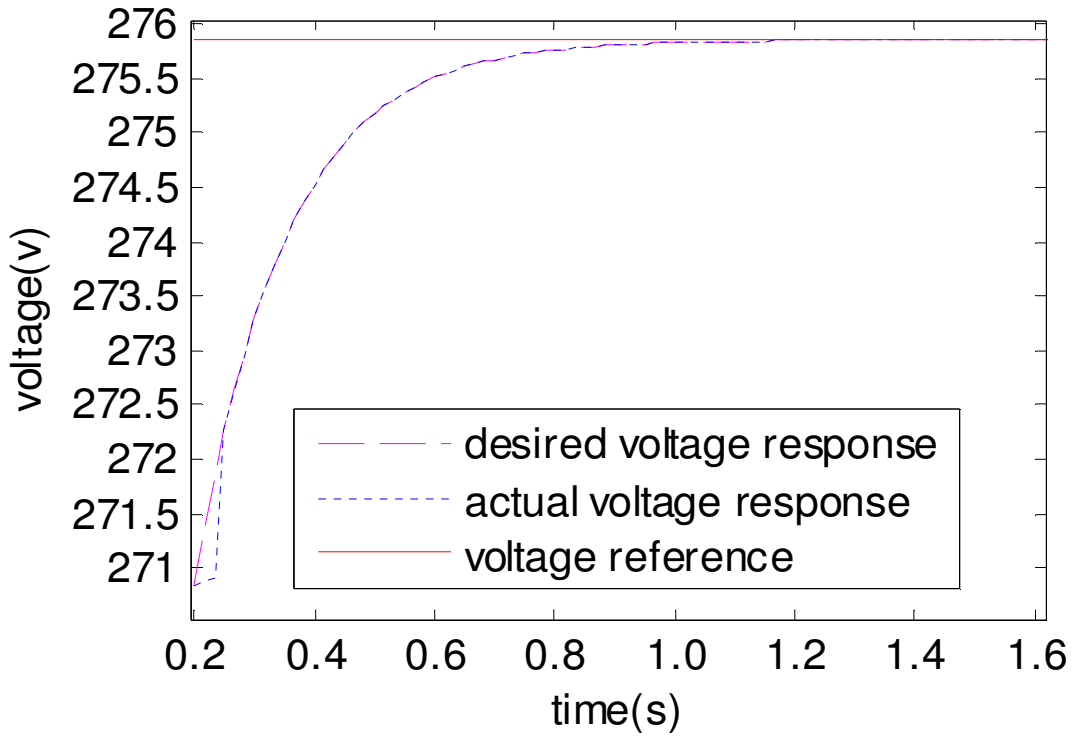


Figure 5.14 Voltage response of DE1 using the with-communication method when the reference voltages of DE1 and DE2 are 275.85 V and 275.70 V, respectively.

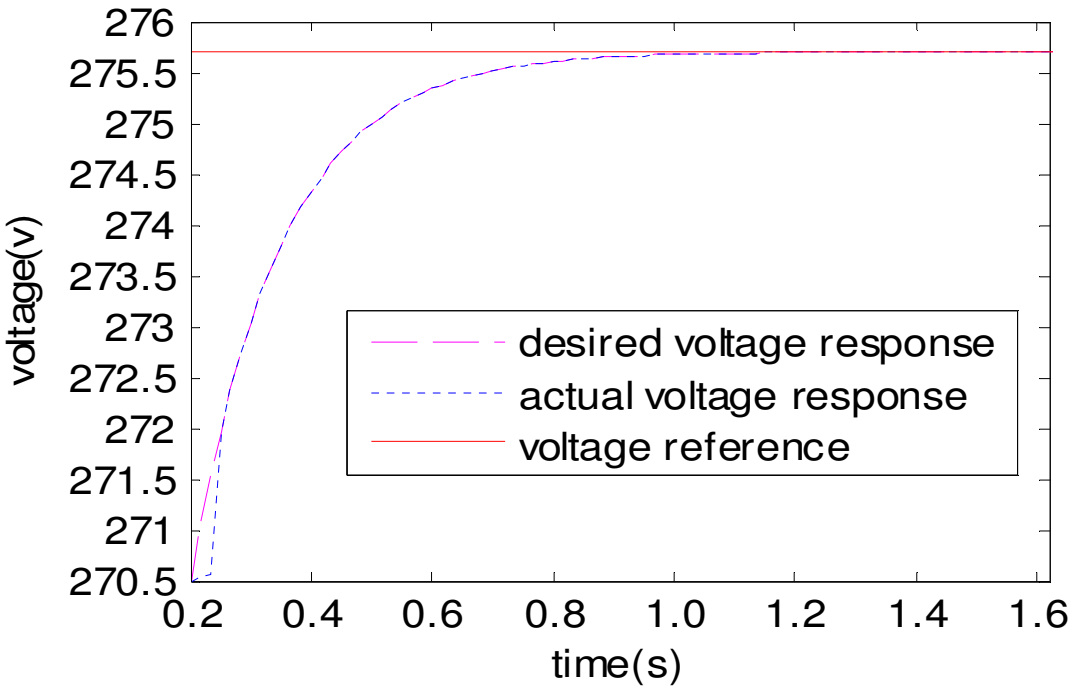


Figure 5.15. Voltage response of DE2 using the with-communication method when the reference voltages of DE1 and DE2 are 275.85 V and 275.70 V, respectively.

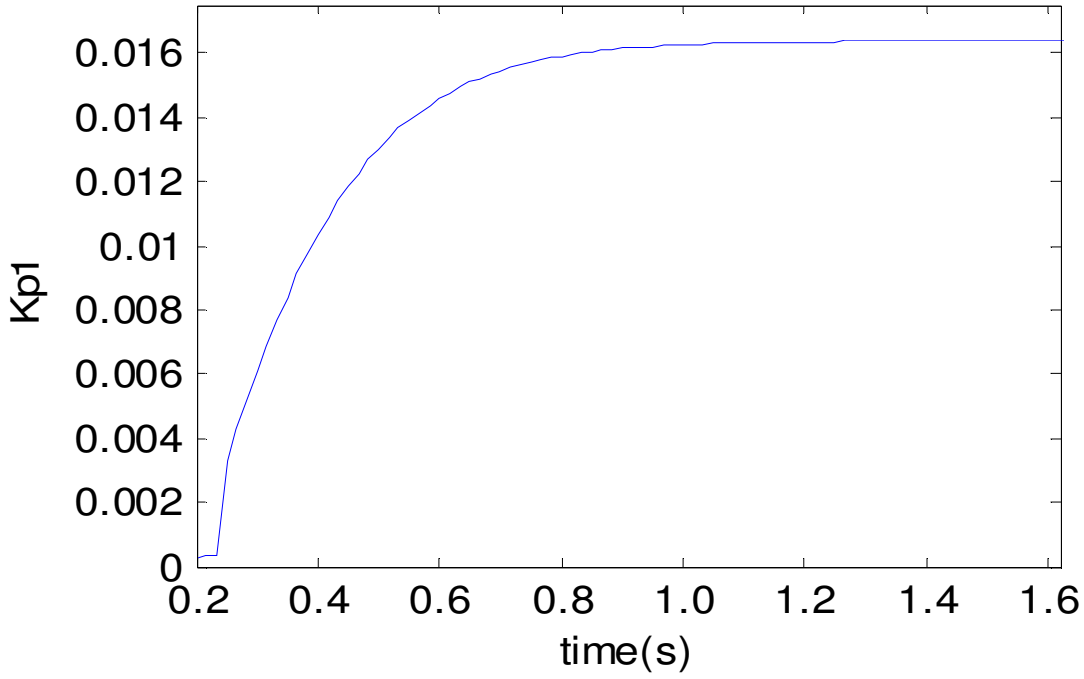


Figure 5.16. K_P of DE1 using the with-communication method when the reference voltages of DE1 and DE2 are 275.85 V and 275.70 V, respectively.

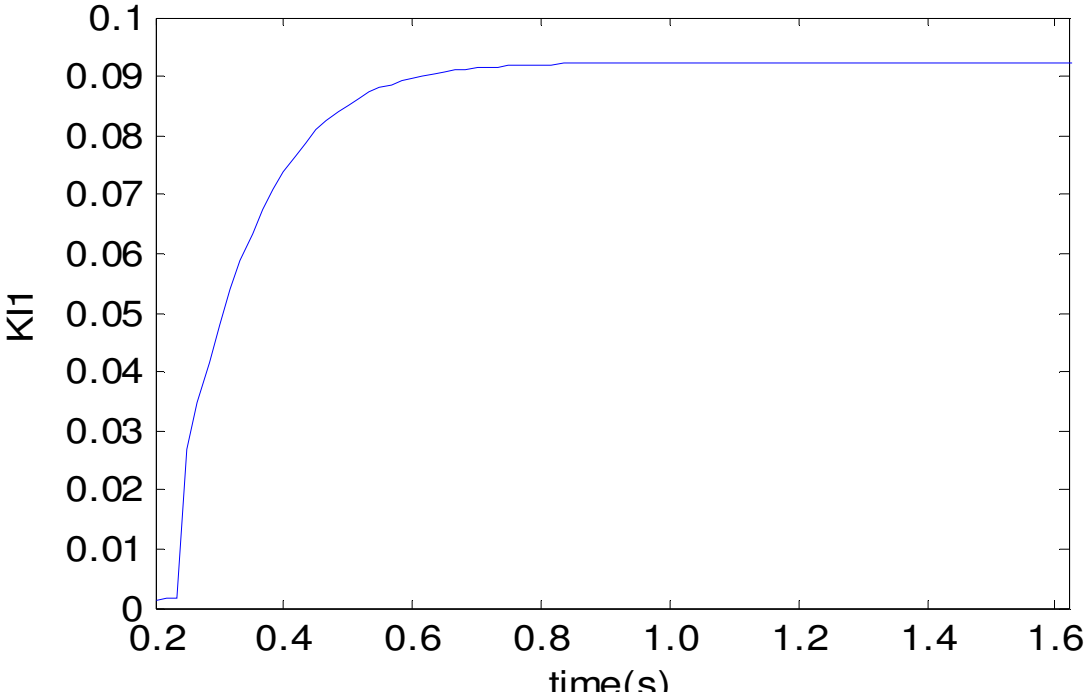


Figure 5.17. K_I of DE1 using the with-communication method when the reference voltages of DE1 and DE2 are 275.85 V and 275.70 V, respectively.

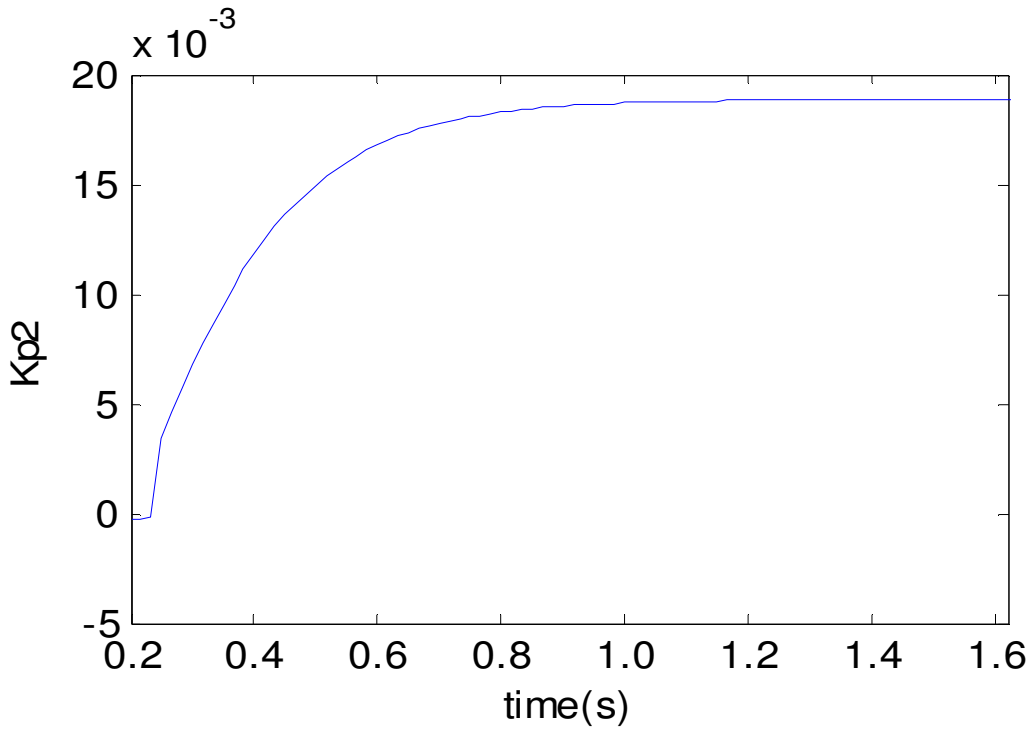


Figure 5.18. K_P of DE2 using the with-communication method when the reference voltages of DE1 and DE2 are 275.85 V and 275.70 V, respectively.

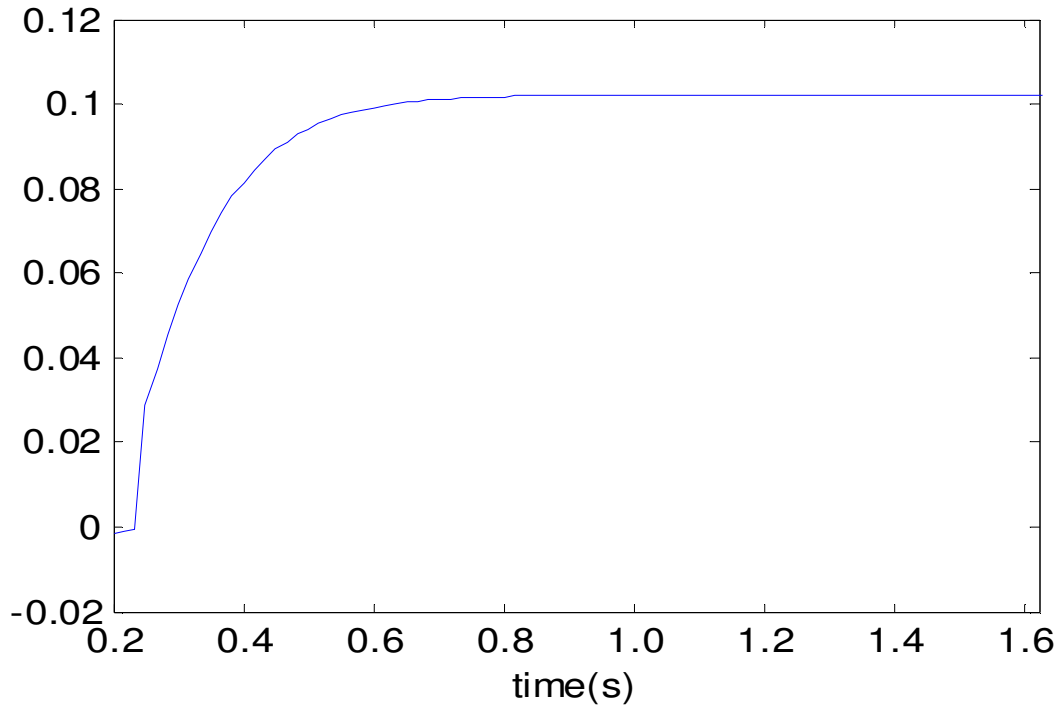


Figure 5.19. K_I of DE2 using the with-communication method when the reference voltages of DE1 and DE2 are 275.85 V and 275.70 V, respectively.

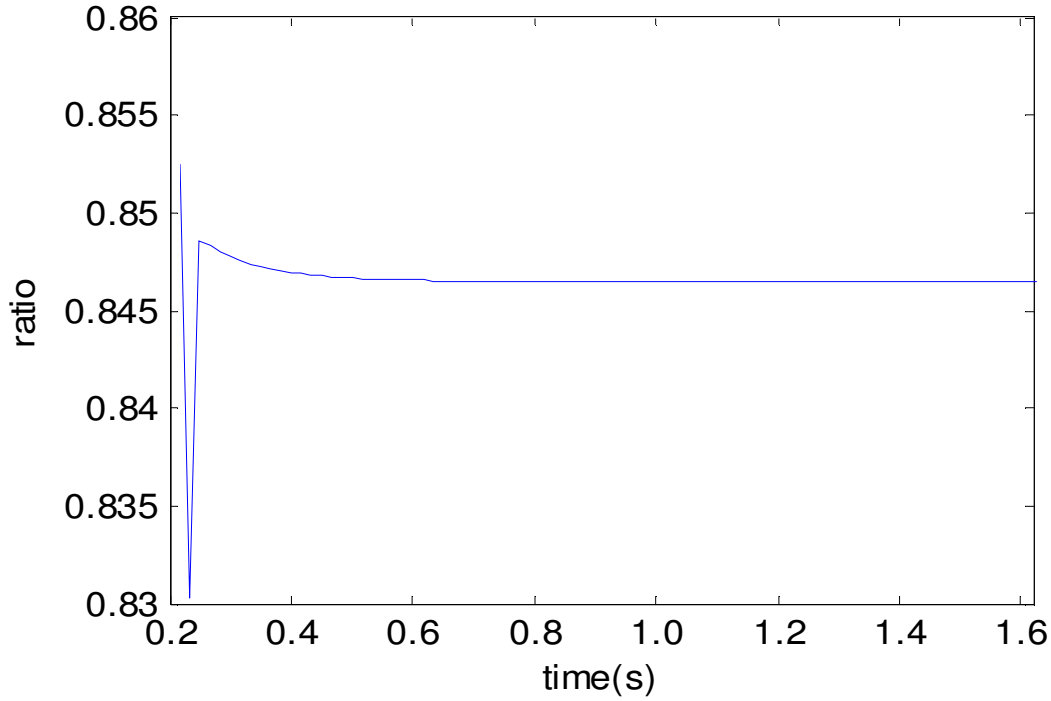


Figure 5.20. Ratio of the two consecutive voltage changes using the with-communication method when the reference voltages of DE1 and DE2 are 275.85 V and 275.70 V, respectively.

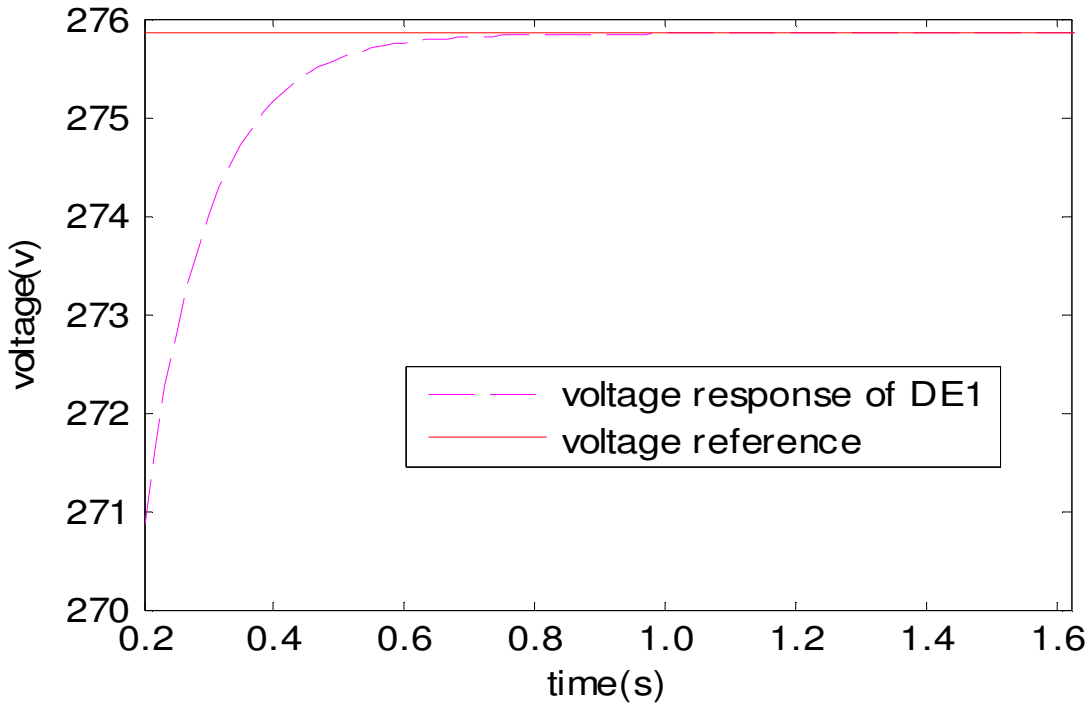


Figure 5.21. Voltage response of DE1 - only DE1 regulating voltage.

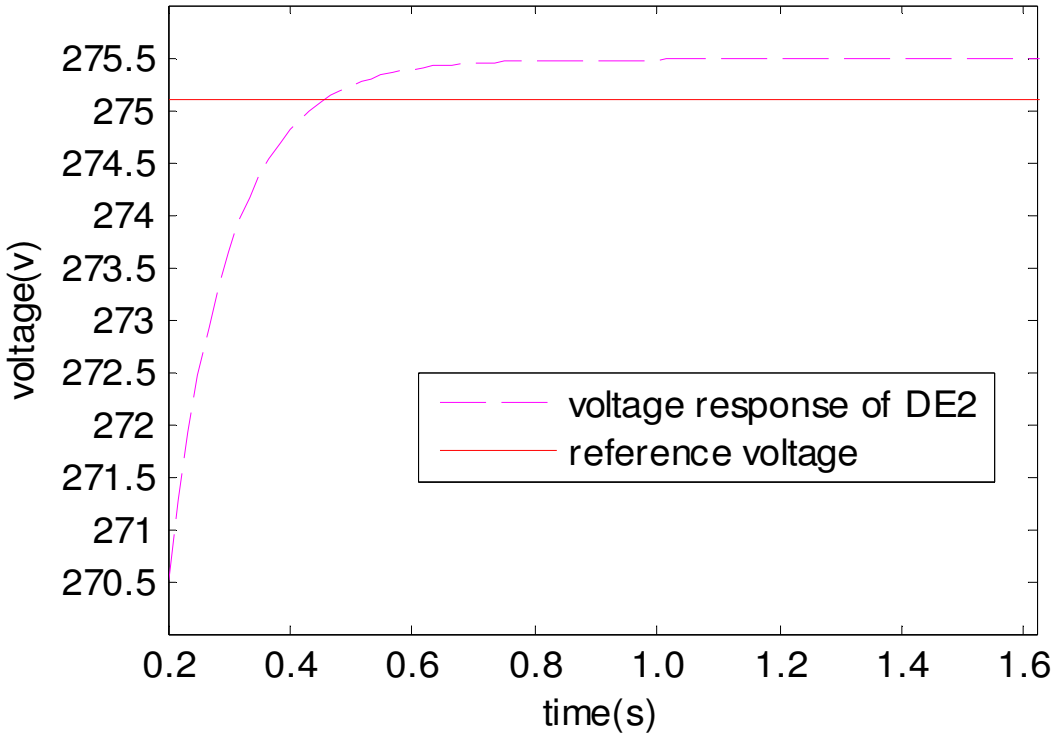


Figure 5.22. Voltage response of DE2 - only DE1 regulating voltage.

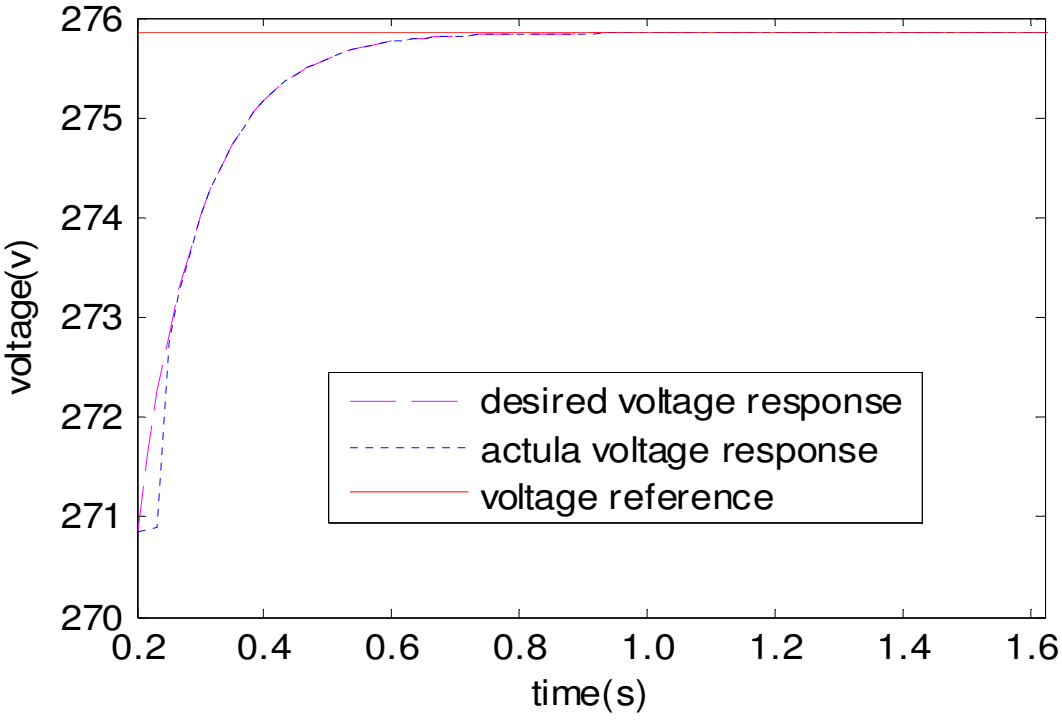


Figure 5.23. Voltage response of DE1 using the with-communication method when the reference voltages of DE1 and DE2 are 275.85 V and 275.10 V, respectively.

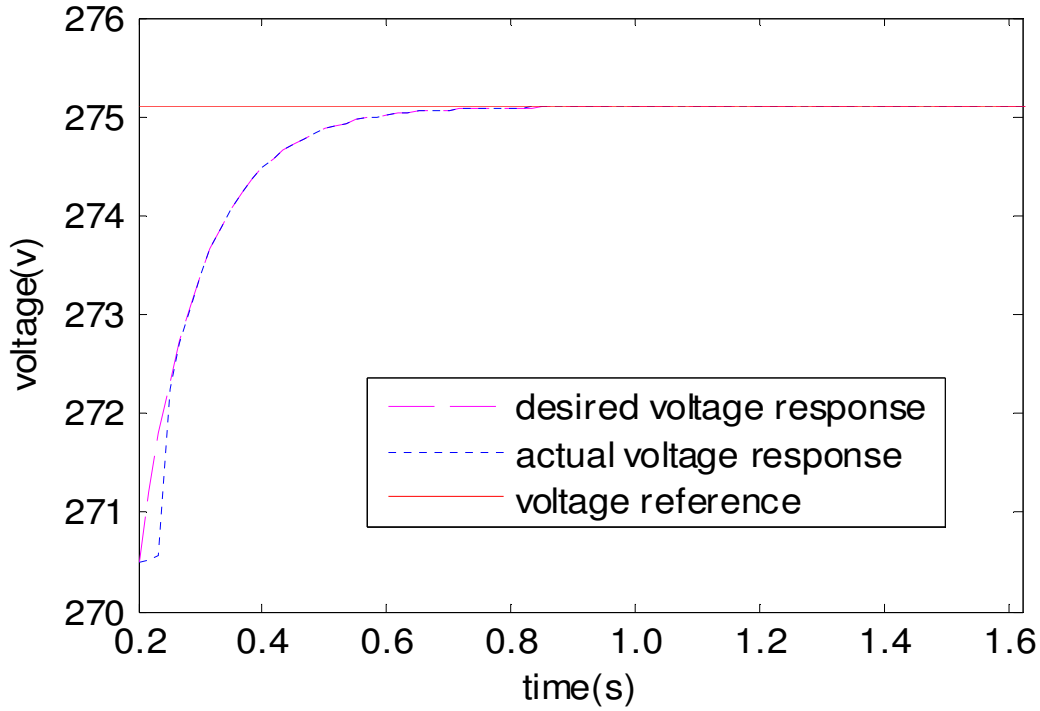


Figure 5.24. Voltage response of DE2 using the with-communication method when the reference voltages of DE1 and DE2 are 275.85 V and 275.10 V, respectively.

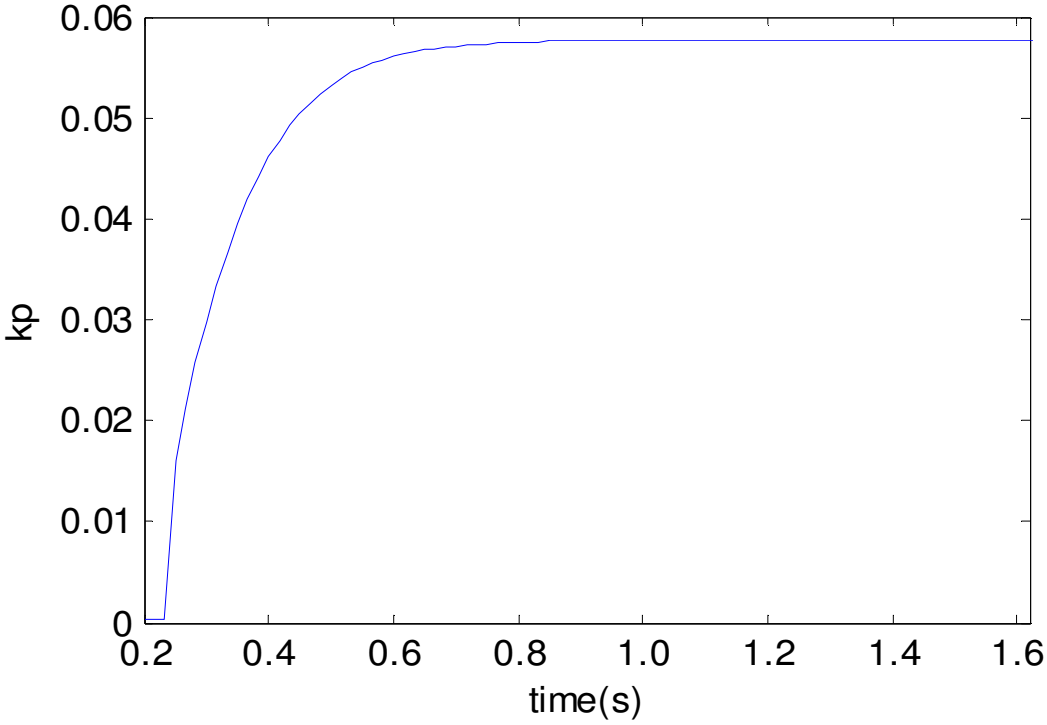


Figure 5.25. K_P of DE1 using the with-communication method when the reference voltages of DE1 and DE2 are 275.85 V and 275.10 V, respectively.

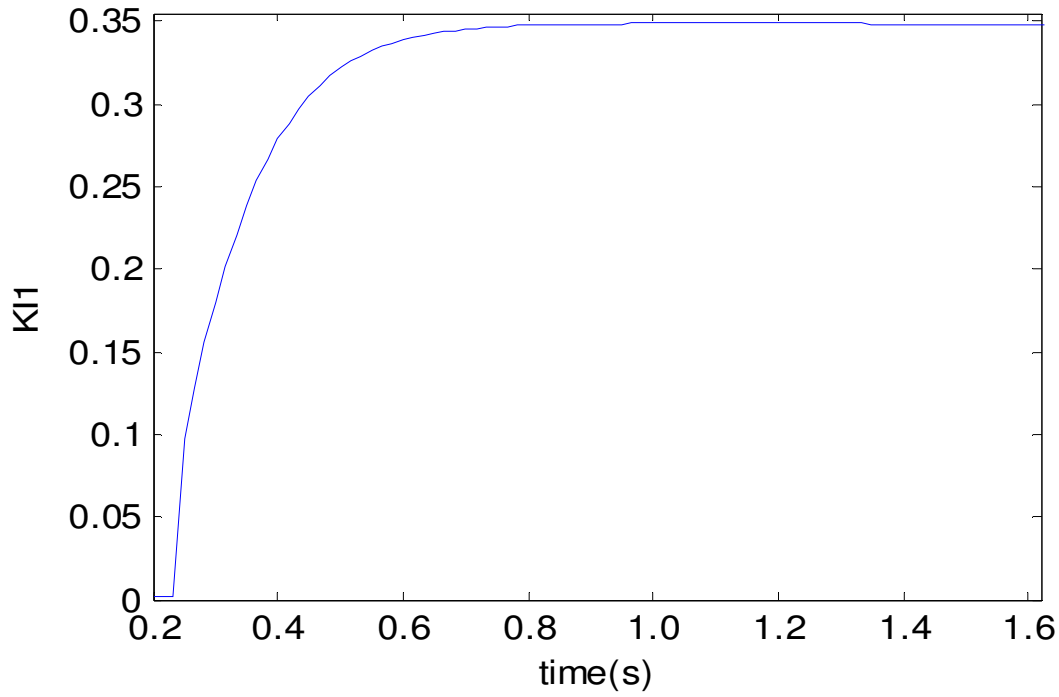


Figure 5.26. K_I of DE1 using the with-communication method when the reference voltages of DE1 and DE2 are 275.85 V and 275.10 V, respectively.

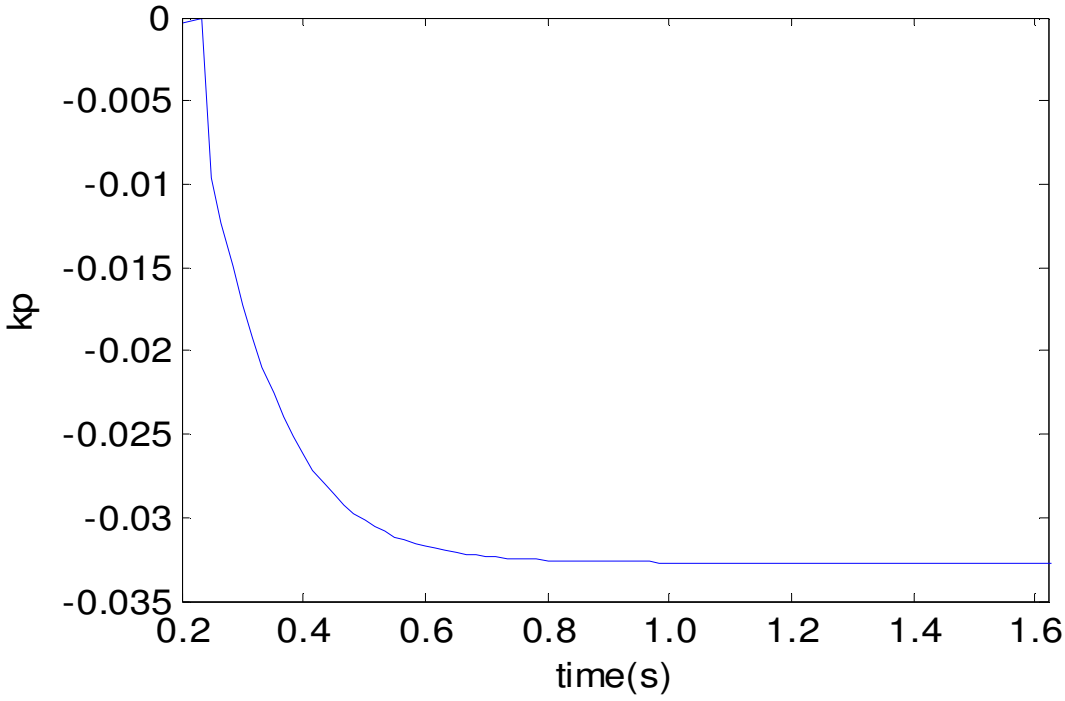


Figure 5.27. K_P of DE2 using the with-communication method when the reference voltages of DE1 and DE2 are 275.85 V and 275.10 V, respectively.

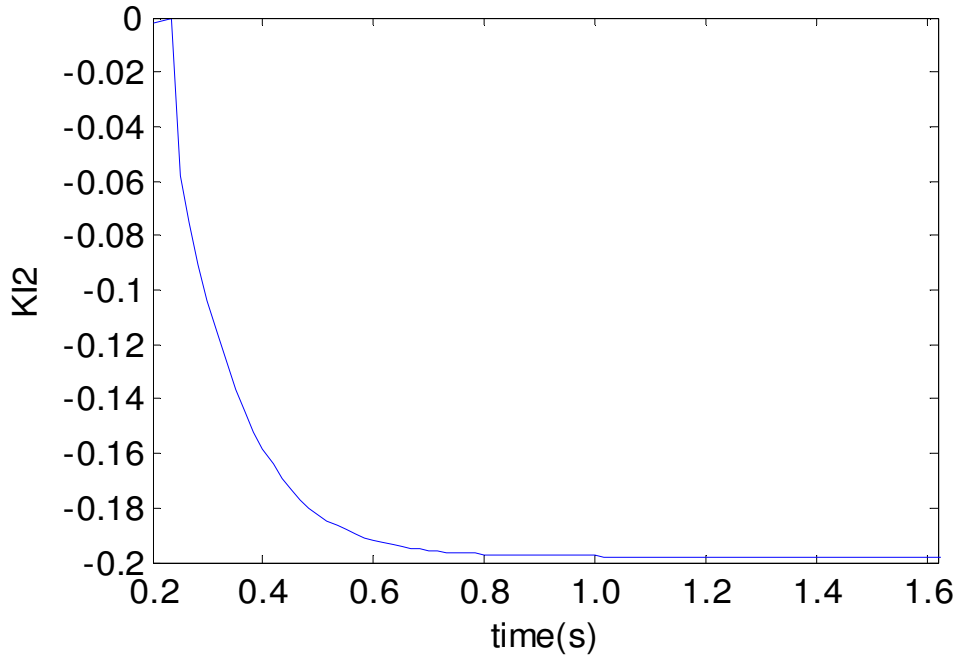


Figure 5.28. K_I of DE2 using the with-communication method when the reference voltages of DE1 and DE2 are 275.85 V and 275.10 V, respectively.

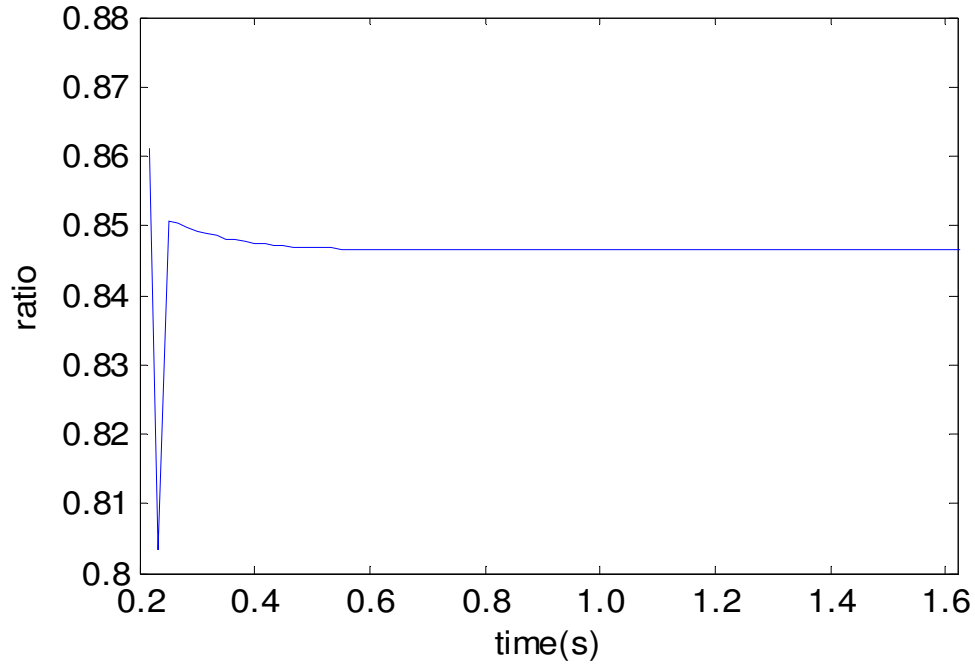


Figure 5.29. Ratio of the two consecutive voltage changes using the with-communication method when the reference voltages of DE1 and DE2 are 275.85 V and 275.10 V, respectively

5.5. Voltage Regulation without Communication

When communications among the DEs and/or with the control center are not available, each DE can only use its local information to regulate voltage. However, it is already shown by the simulation results in Subsection 5.1 that the terminal voltage of each DE also implicitly reflects the other DEs' voltage regulation behavior almost instantaneously. Moreover, the ideal response curve instead of the reference voltage, which is fixed during the regulation process, provides a timely signal of the adjusting direction. So it is possible to adaptively modify DE's output for voltage regulation to catch the ideal response and finally reach the fixed reference by using only the local information with a higher frequency adjustment.

The heuristic adaptive method is used in Chapter 4 to track the ideal response. In chapter 4, a scaling factor is defined to adaptively modify the control parameters. In the single-DE voltage-regulation case, the gain parameters are always positive since the DE output voltage changes its direction (increase or decrease) in accordance with the direction that the terminal voltage is required to change. However, in the case of multiple DEs, as shown in the previous discussion in this Chapter, the gain parameters may be negative for several DEs because the same direction rule in one DE case does not always hold true in this case. Thus, the scaling factor will not work to generate the negative gains. An alternative updating scheme which can generate either positive or negative gains is preferred. In the updating scheme, two factors need to be considered: the direction and step size of the adjustment.

A. Direction of the adjustment

The comparison of the actual voltage with the ideal voltage provides the information for the adjusting direction. The change of DE output voltage caused by the adjustment of the gain parameters can be expressed as

$$\Delta V_c = \left[1 + K_P(t_2)(V_{ref} - V(t_2)) + K_I(t_2)\int_0^{t_2}(V_{ref} - V(t))dt\right]V(t_2) - \left[1 + K_P(t_1)(V_{ref} - V(t_1)) + K_I(t_1)\int_0^{t_1}(V_{ref} - V(t))dt\right]V(t_1) \quad (5.28)$$

Since at every adjustment, the change of the terminal voltage is very small, $V(t_2)$ is approximately equal to $V(t_1)$. Also, the difference between $\int_0^{t_2}(V_{ref} - V(t))dt$ and $\int_0^{t_1}(V_{ref} - V(t))dt$ can be neglected. Therefore, we have

$$\Delta V_c \approx \left[\Delta K_P(V_{ref} - V(t_1)) + \Delta K_I\int_0^{t_1}(V_{ref} - V(t))dt\right]V(t_1) \quad (5.29)$$

When the actual local terminal voltage ($V(t_1)$) is higher than the desired terminal voltage ($V_{desired}$), a DE needs to reduce its output voltage (V_c) to reduce the actual terminal voltage and ΔV_c should be negative. Hence, according to Equation (5.29), to obtain a voltage reduction, i.e., a negative ΔV_c, ΔK_P needs to be positive if a voltage deviation beyond the reference occurs (i.e. $V_{ref} < V(t)$); or ΔK_P needs to be negative if a voltage deviation below the reference occurs (i.e. $V_{ref} > V(t)$). To the contrary, when the actual local voltage is lower than the desired voltage, the DE needs to increase its output voltage to bring the actual voltage up and ΔV_c needs to be positive.

At any given time instant, it is not clear whether the DE should really bring the voltage up or down because of the impact from other DEs, even though the DE's local voltage is lower (or higher) than the reference voltage. Therefore, based on these discussions, the updating scheme of K_P is proposed as a gradual change towards the desired direction. This

can help avoid the dramatic change of K_P that may lead to an undesired voltage response. The new updating scheme of K_P is defined as

$$K_P^{new} = K_P^{old} + \Delta K_P \tag{5.30}$$

$$\Delta K_P = \alpha \times (-1)^S \times (V_{ideal}(t) - V_{actual}(t));$$
$$and \quad S = \begin{cases} 0, \text{when voltage dip is to be corrected;} \\ 1, \text{when voltage rise is to be corrected.} \end{cases} \tag{5.31}$$

where α is a positive value, which is the adaptive scaling factor and will be discussed next.

B. Step size of the adjustment

When the deviation of the actual voltage from the ideal voltage is large, a large adjustment is expected; when the deviation is small, a small adjustment is desirable. Thus, it is reasonable to define an adaptive scaling factor as

$$\alpha = k \times \left(1 + \left|V(t)_{ideal} - V(t)_{actual}\right|\right) \tag{5.32}$$

where k is a fixed step size.

Since the ideal response is defined as an exponential decay curve, the largest step change of the terminal voltage should occur at the first adjustment, as shown in Figure 5.30. Additionally, in this adjustment, the corresponding DE output voltage change, ΔV_c, should also be the largest. The relationship between ΔV_c and ΔV can be linearized as

$$\Delta V_i = \sum_{l=1}^{m} c_l \Delta V_{cl} \tag{5.33}$$

where $c_l \Delta V_{cl} < c_i \Delta V_{ci}, l \neq i$, and $c_l < 1$, because the voltage change of the source produces less impact on the voltage of the buses with longer electrical distance from the source. And we can obtain

$$\Delta V_i = \sum_{l=1}^{m} c_l \Delta V_{cl} < m c_i \Delta V_{ci} < m \Delta V_{ci} \tag{5.34}$$

Therefore, for the largest change of terminal voltage and DE output voltage, we have

$$\frac{\Delta V_i^{(1)}}{m} < \Delta V_{ci_\max} \tag{5.35}$$

where $\Delta V_i^{(1)}$ is the voltage change of bus i in the first adjustment and it should be $(V_{i_ideal}^{(1)} - V_{i_actual}^{(0)})$. The LSV of (5.35) can be set as a limit to the step change of ΔV_c. Applying this limit in the first adjustment, we have

$$\Delta V_{ci} \approx \Delta K_P (V_{i_ref} - V_i(t)) V_i(t) \le \frac{(V_{i_ideal}^{(1)} - V_{i_actual}^{(0)})}{m} \tag{5.36}$$

Combining Equations (5.31) and (5.32) with Equation (5.36), we have:

$$k \times \left(1 + \left|V_{i_actual}^{(0)} - V_{i_ideal}^{(1)}\right|\right) \times \left(V_{i_ideal}^{(1)} - V_{i_actual}^{(0)}\right) \times (-1)^S \times \left(V_{i_ref} - V_{i_actual}^{(0)}\right) \times V_{i_actual}^{(0)} \le \frac{V_{i_ideal}^{(1)} - V_{i_actual}^{(0)}}{m} \tag{5.37}$$

Therefore, we can obtain the upper limit for the fixed step size k as

$$k \le \frac{1}{m(-1)^S (1 + abs(V_{i_actual}^{(0)} - V_{i_ideal}^{(1)}))(V_{i_ref} - V_{i_actual}^{(0)}) V_{i_actual}^{(0)}} \tag{5.38}$$

The procedure of this method is generalized in Figure 5.31.

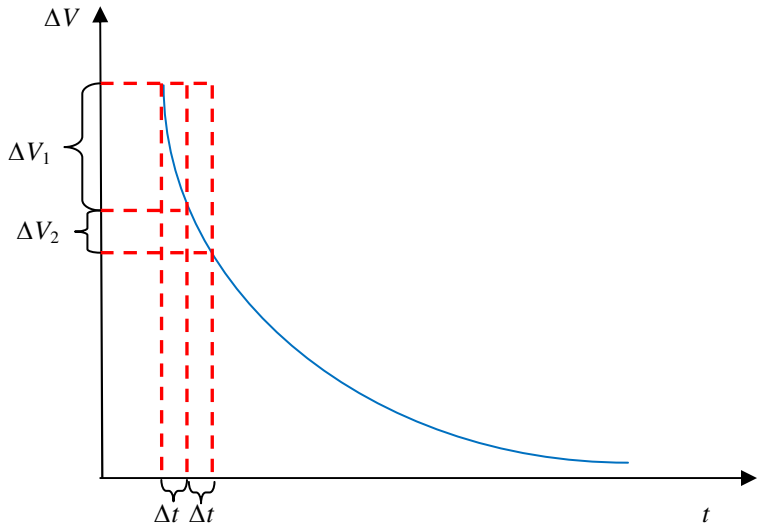


Figure 5.30. Ideal voltage deviation from the reference in the regulation process.

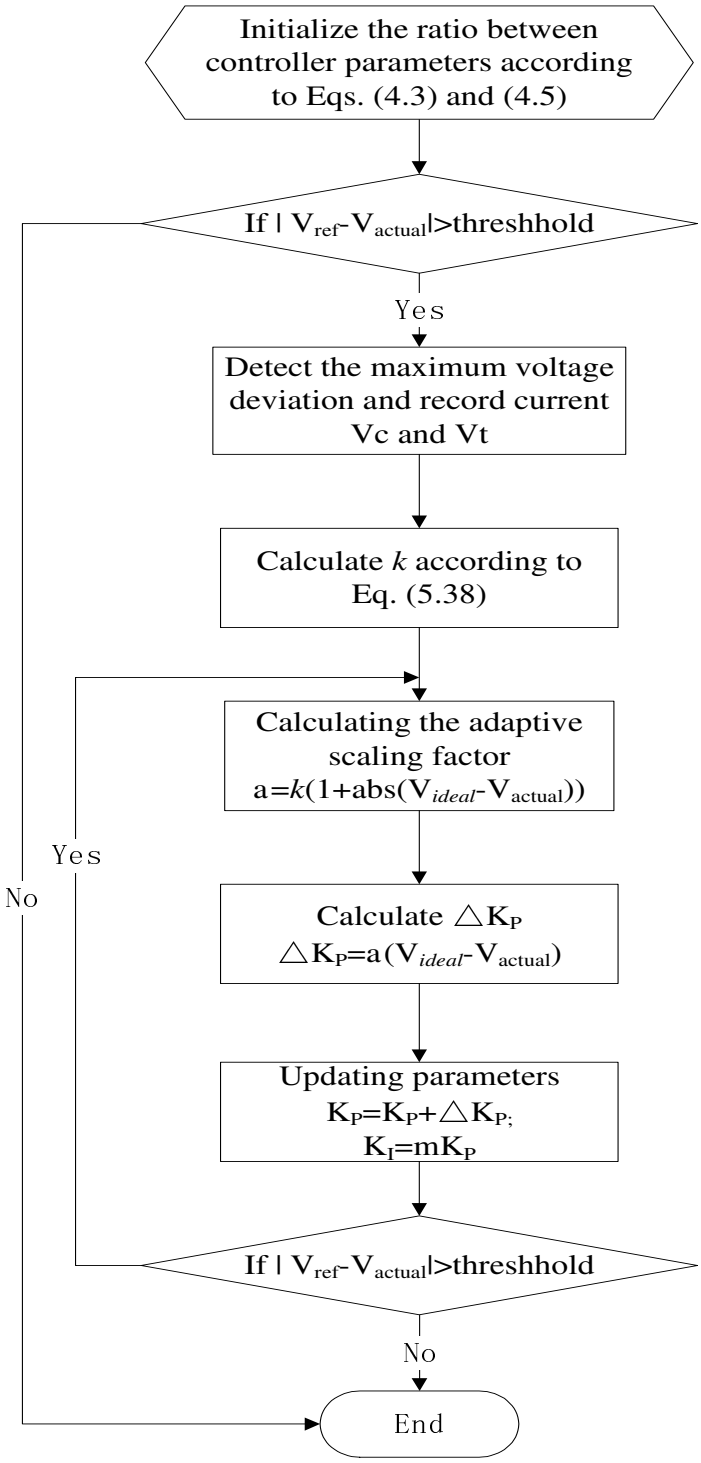


Figure 5.31. Adaptive voltage adjusting algorithm without communication.

In the following discussion, the simulation results of the adaptive voltage control method without communication on the system in Figure 5.1 will be shown. The system condition is identical to what has been described in Subsection 5.4. The frequency of the adjustment is 3000 Hz. This is reasonable since the actual sampling device can be as fast as 12.5 kHZ. The reference voltages for DE1 and DE2 are 275.85 V and 275.7 V, respectively.

1. Calculation of the upper limit of *k*.

   Since $V^{(0)}$=[270.85, 270.50]$^{\mathrm{T}}$ and the reference V^{ref}=[275.85, 275.70]$^{\mathrm{T}}$. For the first adjustment the ideal voltage is

   $$V_{ideal}^{(1)} = [275.85 - 5e^{-\frac{1/3000}{0.1}}, 275.7 - 5.2e^{-\frac{1/3000}{0.1}}]^T = [270.8666, 270.5173]^T .$$

   So, we have $\Delta V^{(1)} = V^{(1)} - V^{(0)} = [0.0166, 0.0173]^T$. According to Equation (5.38), we can obtain *k* for both DEs as

   $$k = [\frac{1}{2 \times 5 \times (1 + 0.0166)(-1)^0 270.85}, \frac{1}{2 \times 5.2 \times (1 + 0.0173)(-1)^0 270.5}]^T$$
   $$= [3.6318 \times 10^{-4}, 3.4942 \times 10^{-4}]^T$$

2. Updating the gain parameters.

   According to Equations (5.31) and (5.32), we can obtain the gain parameter changes for both DEs as

   $$\Delta K_P = \begin{bmatrix} 3.6318 \times 10^{-4} \times (1 + 0.0166)(-1)^0 (0.0166) \\ 3.4942 \times 10^{-4} \times (1 + 0.0173)(-1)^0 (0.0173) \end{bmatrix} = \begin{bmatrix} 6.1433 \times 10^{-6} \\ 6.1512 \times 10^{-6} \end{bmatrix}$$
   $$K_P^1 = \begin{bmatrix} 0 \\ 0 \end{bmatrix} + \begin{bmatrix} 6.1433 \times 10^{-6} \\ 6.1512 \times 10^{-6} \end{bmatrix} = \begin{bmatrix} 6.1433 \times 10^{-6} \\ 6.1512 \times 10^{-6} \end{bmatrix}.$$

   $$K_I^1 = mK_P^1 = (0.127/0.021) \begin{bmatrix} 6.1433 \times 10^{-6} \\ 6.1512 \times 10^{-6} \end{bmatrix} = \begin{bmatrix} 3.7152 \times 10^{-5} \\ 3.7200 \times 10^{-5} \end{bmatrix}$$

3. Generating the DE output voltage

   Recall that

$$V_c = \left[1 + K_P(V_{ref} - V(t)) + K_I \int_0^t (V_{ref} - V(t))dt\right] V(t).$$

In the first adjustment we have

$$V_c^{(1)} = \begin{bmatrix} 1+6.1433\times10^{-6}\times5+0 \\ 1+6.1512\times10^{-6}\times5.2 \end{bmatrix} = \begin{bmatrix} 270.8583 \\ 270.5087 \end{bmatrix}.$$

The according terminal voltage should be $V_{actual}^{(1)} = \begin{bmatrix} 270.8515 \\ 270.5068 \end{bmatrix}$, and the difference from the ideal voltage is $V_{difference}^{(1)} = \begin{bmatrix} 0.0152 \\ 0.0105 \end{bmatrix}$.

The above process from Step 1 to 3 will be repeated until the voltage reaches the reference. During the whole process the maximum difference between the ideal voltage and the actual one of DE1 is 0.0706 V; and for DE2 it is 0.0703 V. The comparisons of the ideal voltage and actual voltage of DE1 and DE2 in the whole regulation process are shown in Figures 5.32 and 5.33, respectively. Although the deviation from the ideal voltage is larger than what is generated by the control method with communication, the results are still satisfying. The terminal voltage can reach the reference with the expected speed without overshoot or oscillation. The values of the gain parameters for the two DEs are shown in Figures 5.34~5.37. If compared with the gain parameters generated in the method with communication shown in Figures 5.16~5.19, they are definitely close.

The method without communication is also tested in the case where one DE needs to absorb reactive power even when its reference voltage is higher than the post-disturbance terminal voltage. The simulation scenario is identical to the second simulation case based on the method with communication. The reference voltages for DE1 and DE2 are set to 275.85 V and 275.10 V, respectively. Figures 5.38 and 5.39 show the voltage responses of DE1 and

DE2, respectively. The maximum deviation of the actual voltage from the ideal one is 0.1420 V for DE1 and 0.0871 V for DE2. Although these are very small deviations, they are still larger than the maximum tracking errors in the with-communication method, which are 0.0576 V for DE1 and 0.0566 V for DE2. This is reasonable since we assume every DE knows the other DEs' actions in the with-communication approach. Nevertheless, the voltage regulation of the proposed without-communication adaptive approach can still meet the 0.5 *sec* response time requirement, and no overshoot or oscillation occurs in the regulation.

Figures 5.40~5.43 show the values of the gain parameters in the regulation. The tracking method can generate negative parameters to absorb the reactive power when the reference voltage is higher than the terminal voltage, as shown in Figures 5.42 and 5.43. Next, these values will be compared with the same parameters, but generated by the method with-communication, as shown in Figures 5.25~5.28. The values of K_P of DE1 and DE2 in the with-communication method are 0.0577 and -0.0327, respectively, after reaching the new steady state; in the method without communication those values are 0.0564 and -0.0376, respectively; and the accurate values of K_P for DE1 and DE2 calculated by the analytical formulation in (5.13) are 0.0622 and -0.0352 respectively. These values are reasonably close, as the simulation results show with the close voltage response.

From these simulation results, we can claim that this self-adaptive voltage regulation method without any communication can also effectively avoid overshoot and oscillation problems in the multiple DEs case by tracking individual ideal voltage responses. Therefore, its application in future utility practice is promising.

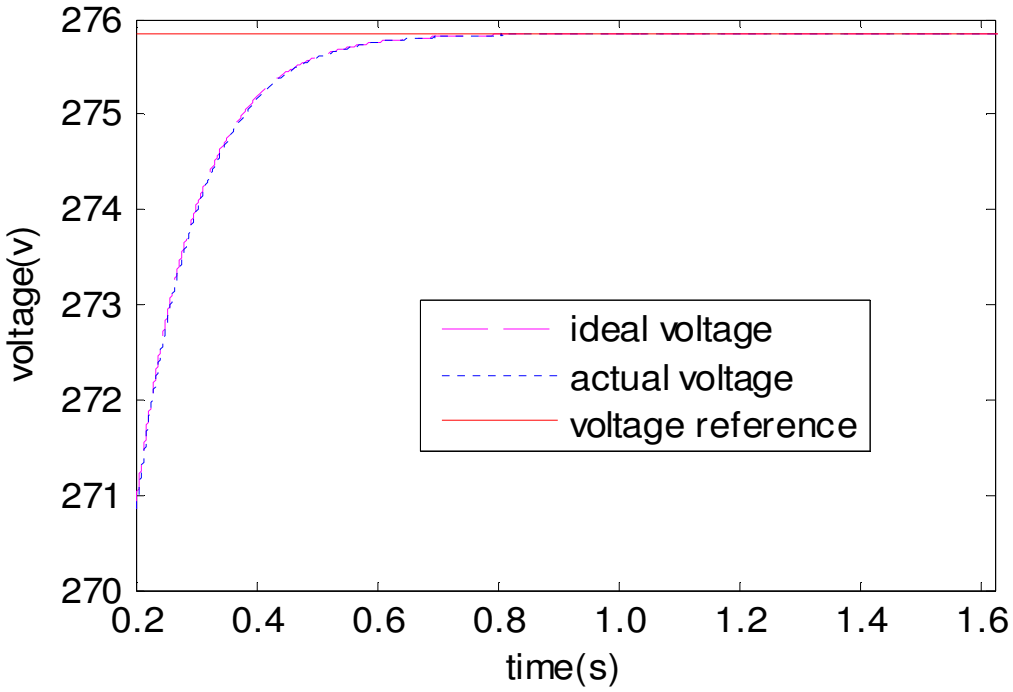


Figure 5.32. Voltage response of DE1 using the without-communication method when the reference voltages of DE1 and DE2 are 275.85 V and 275.70 V, respectively.

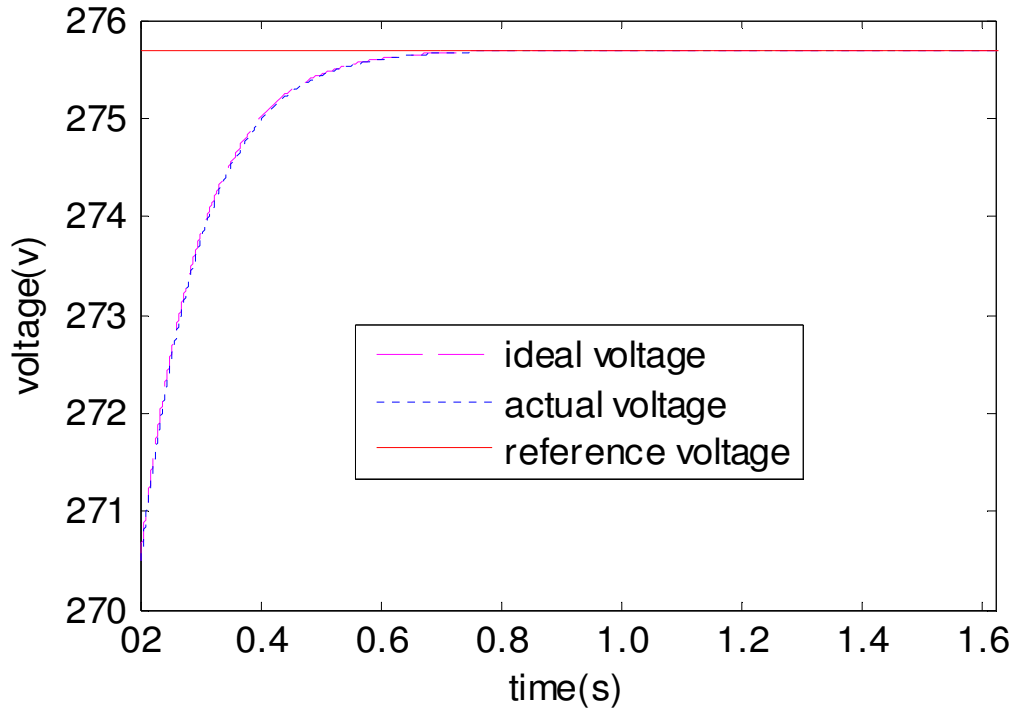


Figure 5.33. Voltage response of DE2 using the without-communication method when the reference voltages of DE1 and DE2 are 275.85 V and 275.70 V, respectively.

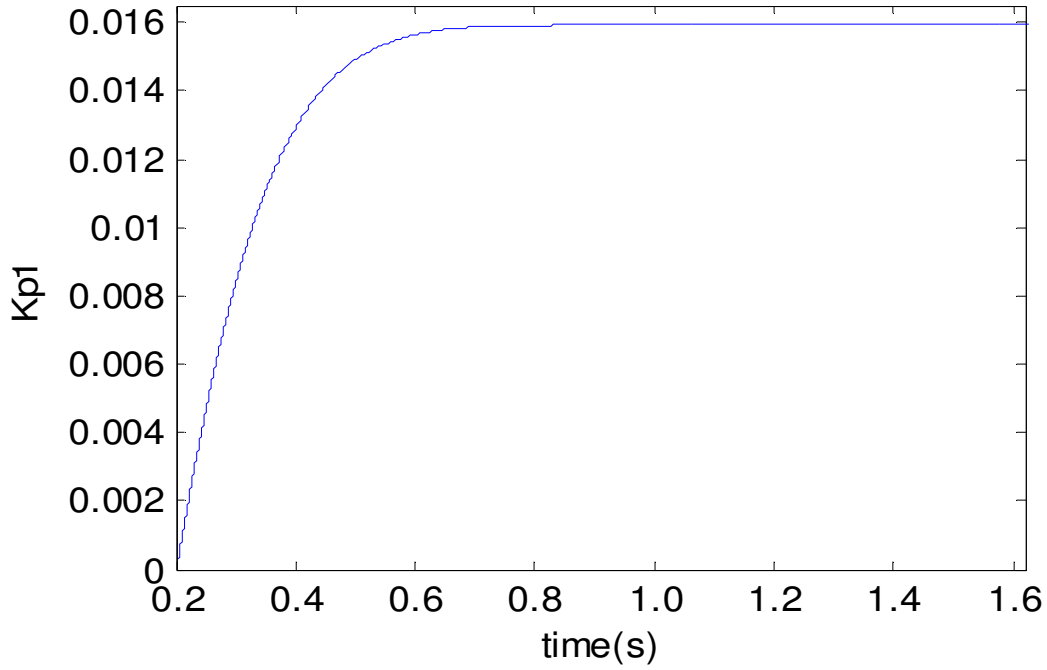


Figure 5.34. K_P of DE1 using the without-communication method when the reference voltages of DE1 and DE2 are 275.85 V and 275.70 V, respectively.

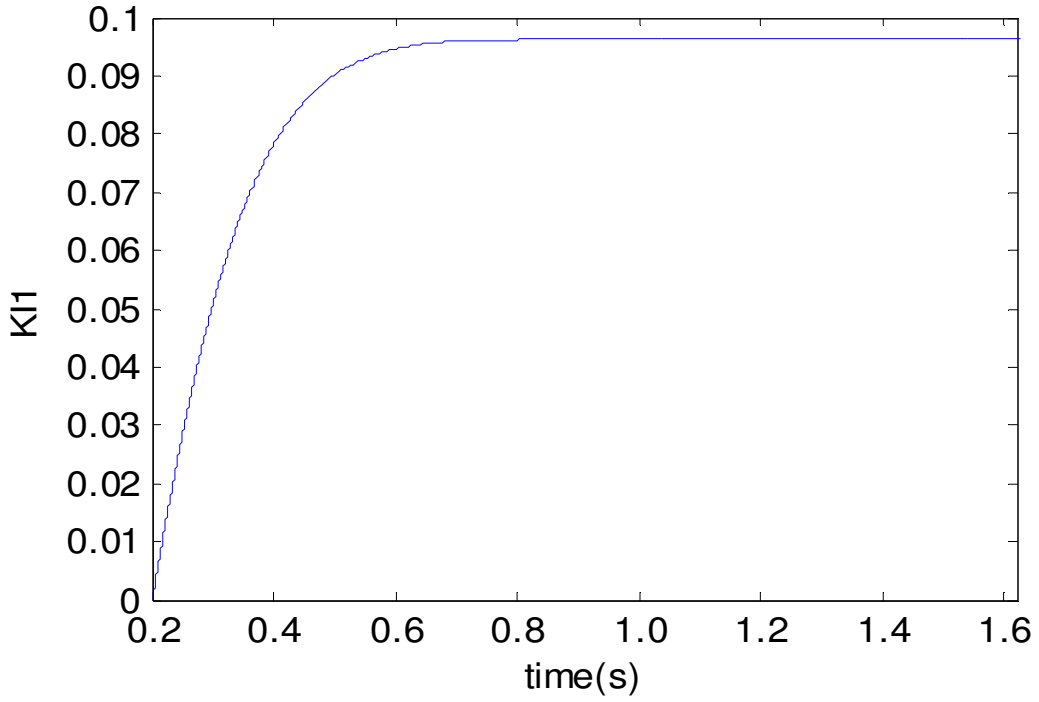


Figure 5.35. K_I of DE1 using the without-communication method when the reference voltages of DE1 and DE2 are 275.85 V and 275.70 V, respectively.

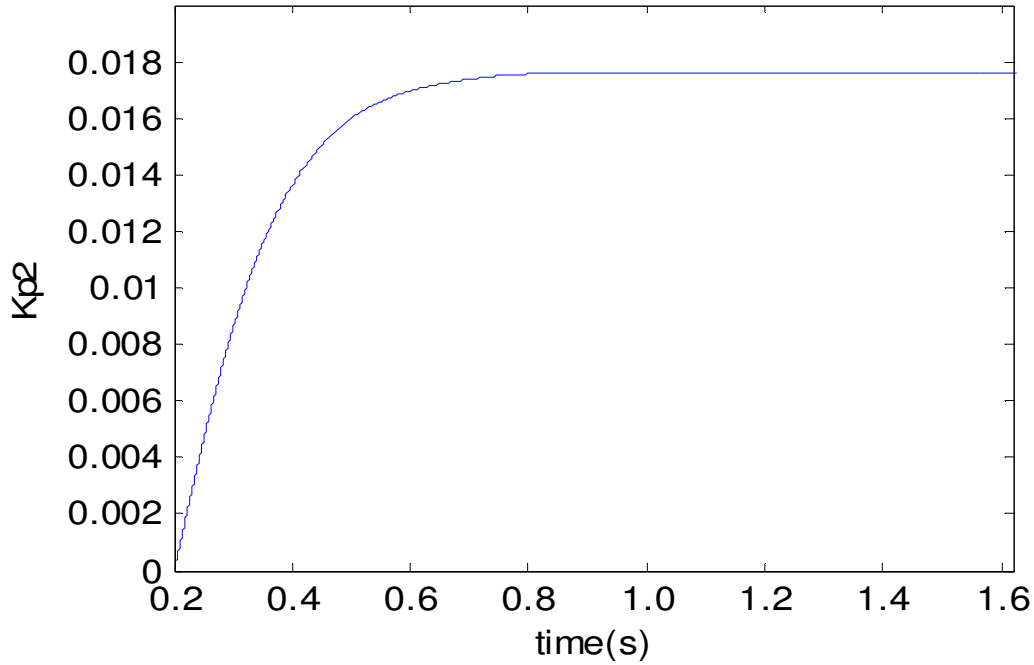
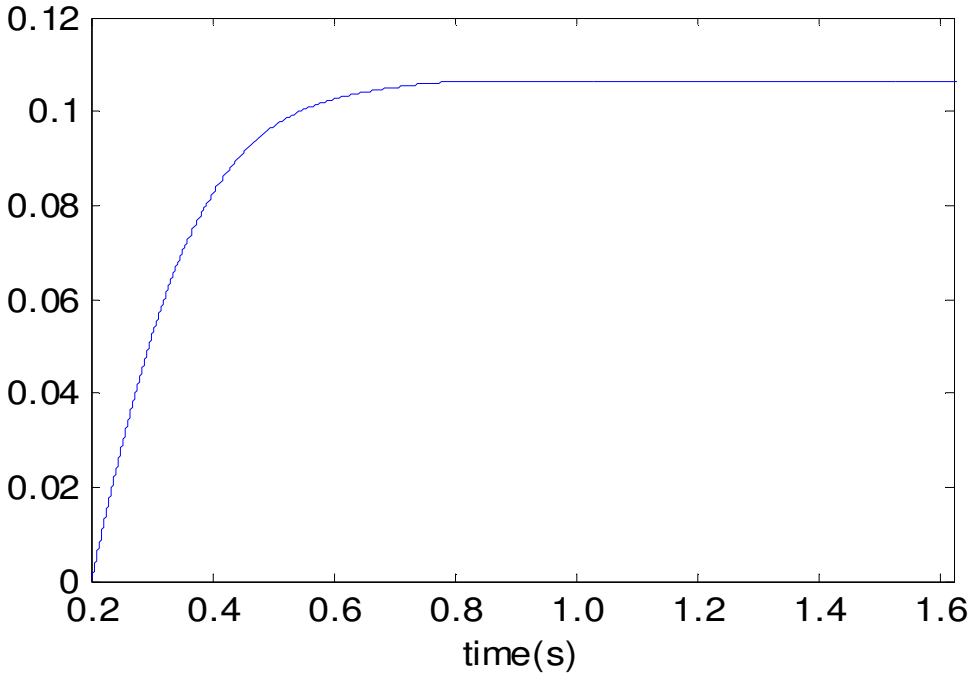


Figure 5.36. K_P of DE2 using the without-communication method when the reference voltages of DE1 and DE2 are 275.85 V and 275.70 V, respectively.



Figuure 5.37. K_I of DE2 using the without-communication method when the reference voltages of DE1 and DE2 are 275.85 V and 275.70 V, respectively.

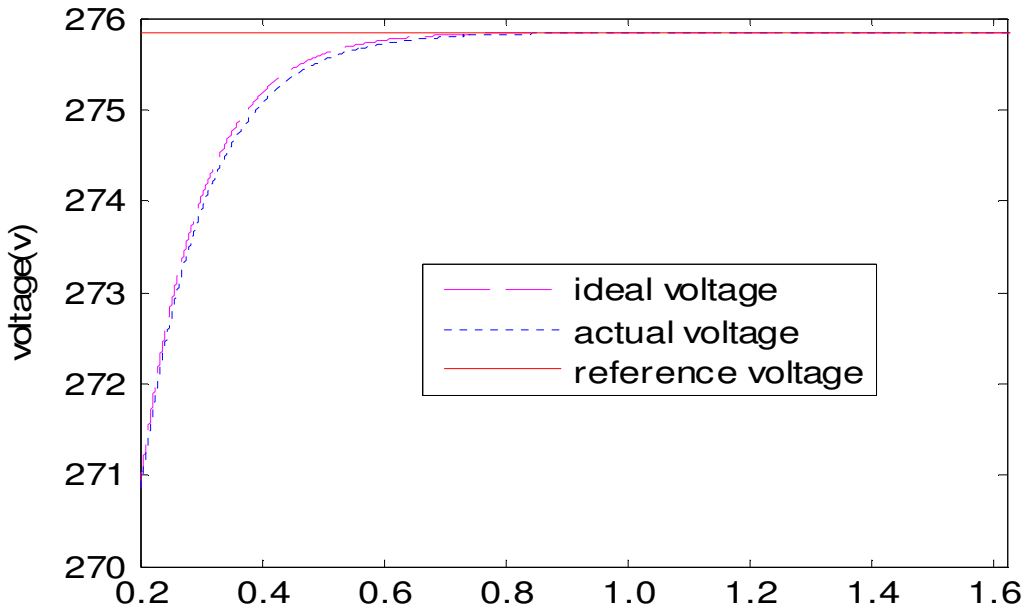


Figure 5.38. Voltage response of DE1 using the without-communication method when the reference voltages of DE1 and DE2 are 275.85 V and 275.10 V, respectively.

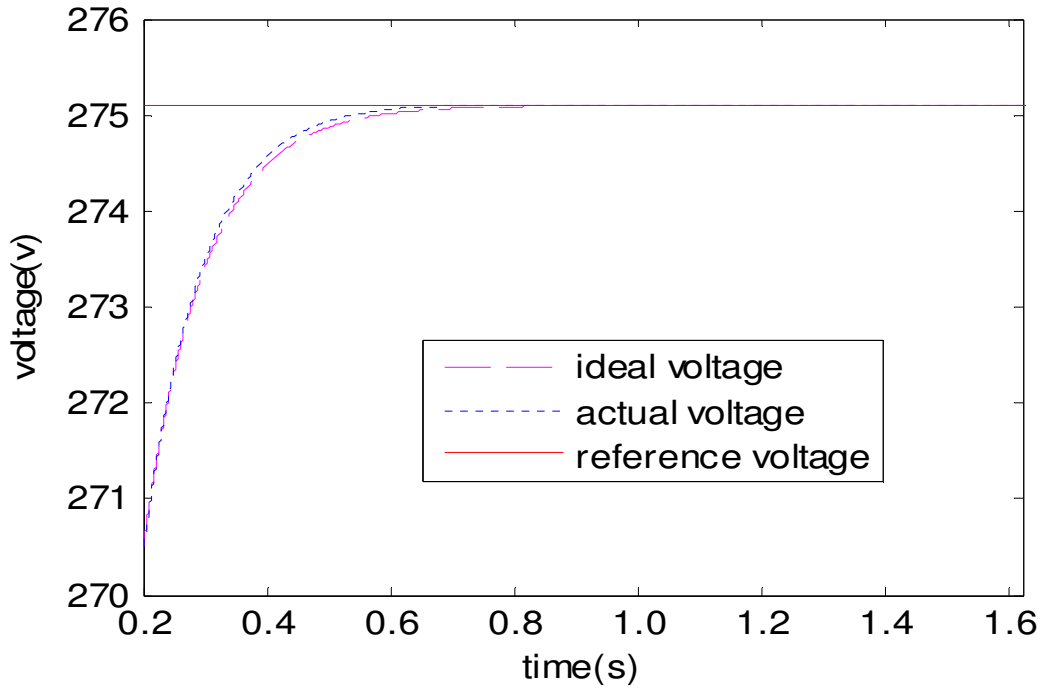


Figure 5.39. Voltage response of DE2 using the without-communication method when the reference voltages of DE1 and DE2 are 275.85 V and 275.10 V, respectively.

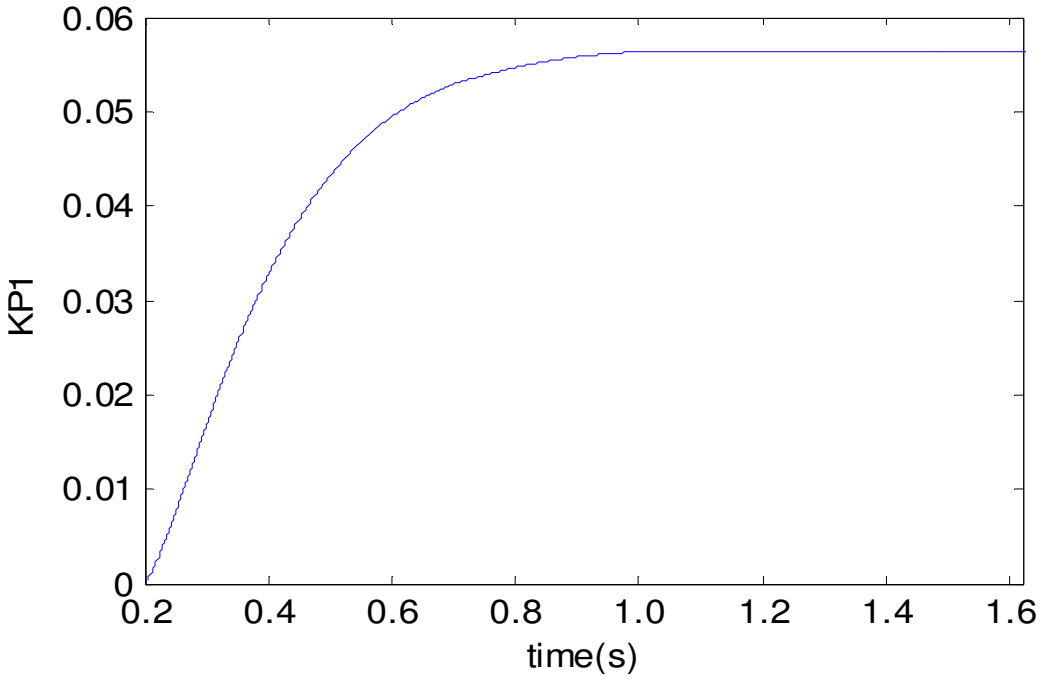


Figure 5.40. K_P of DE1 using the without-communication method when the reference voltages of DE1 and DE2 are 275.85 V and 275.10 V, respectively.

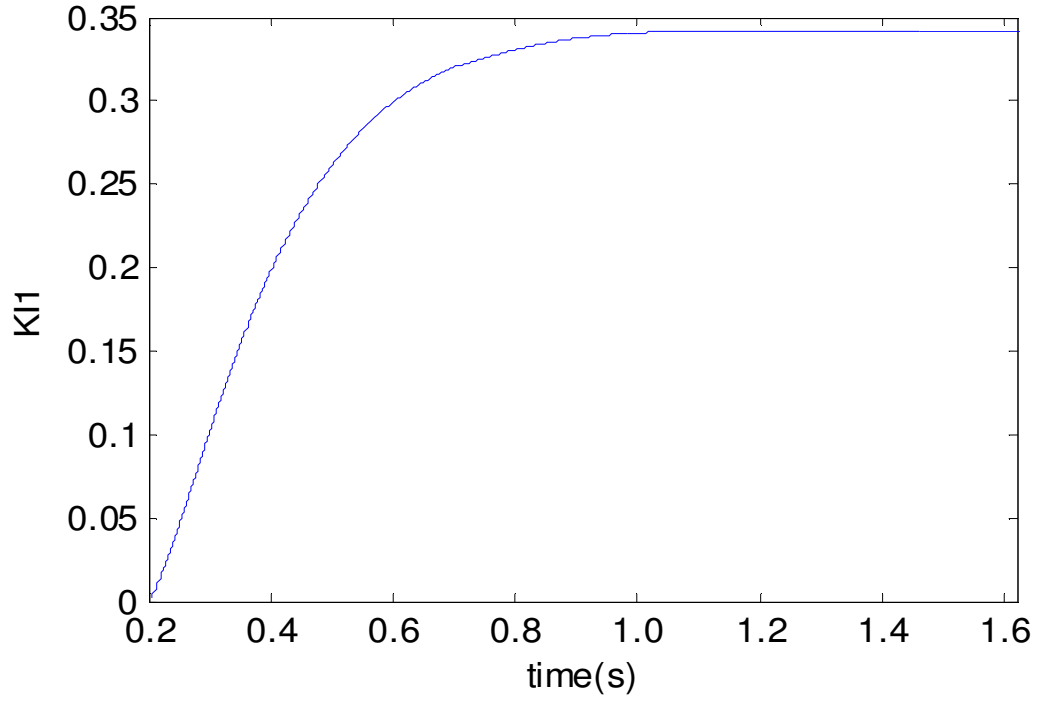


Figure 5.41. K_I of DE1 using the without-communication method when the reference voltages of DE1 and DE2 are 275.85 V and 275.10 V, respectively.

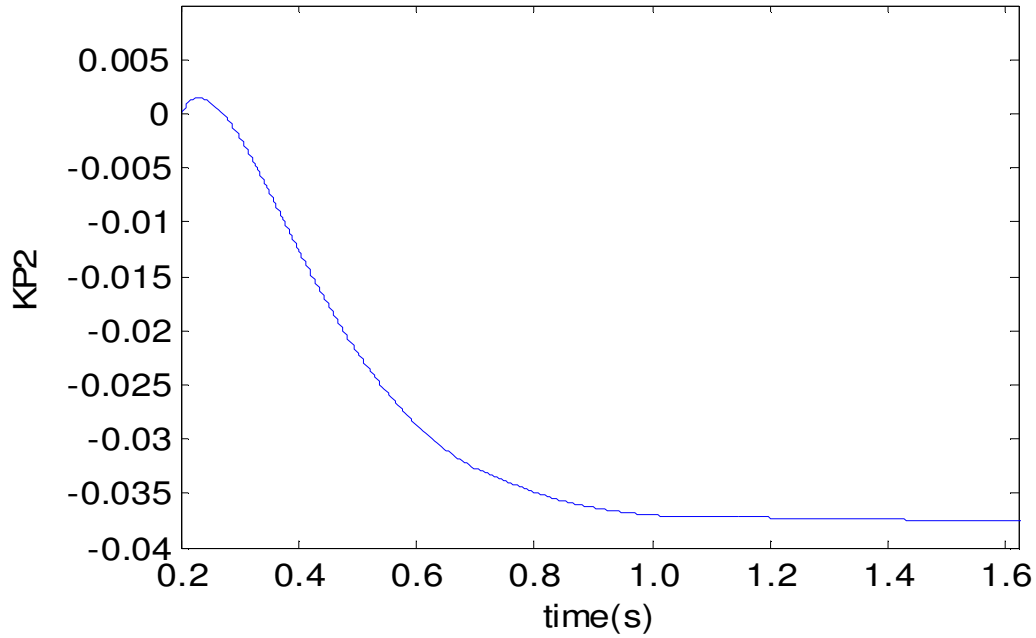


Figure 5.42. K_P of DE2 using the without-communication method when the reference voltages of DE1 and DE2 are 275.85 V and 275.10 V, respectively.

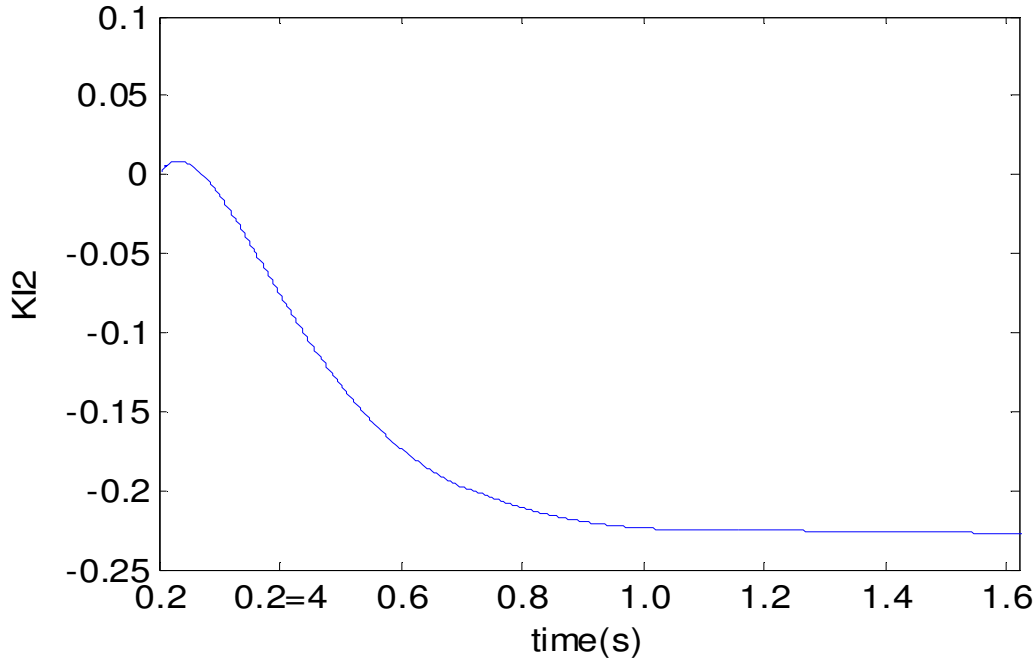


Figure 5.43. K_I of DE2 using the without-communication method when the reference voltages of DE1 and DE2 are 275.85 V and 275.10 V, respectively.

5.6. Chapter Conclusion

In this chapter, the challenges in voltage regulation with multiple DEs were analyzed. The formulations of the gain parameters were derived based on the theoretical analysis which proves the existence of a unique solution of the time-varying gain parameters to meet the desired, ideal response. Considering the availability of communications among those voltage regulating DEs, a high-end solution which requires an extensive communication system among all DEs and/or a control center and a low-end solution which does not require communication, were proposed. Simulations were performed to verify both methods. From the discussions and simulations, the following conclusions can be drawn:

- When multiple DEs participate in the voltage regulation, the terminal voltage response of each DE is the result of all the DE's regulation behavior, and the local measurement of one DE's terminal voltage can reflect the aggregated impact. Thus, it can still be used as the feedback information to adjust the controller parameters.
- The voltage correction of the other DEs may result in excessive compensation at one DE's terminal bus. In this case, the flat reference voltage as an indication of injecting or absorbing reactive power fails to provide a timely regulation direction signal and overshoot of voltage is inevitable with fixed gains. A more dynamic reference, like the ideal response curve, is preferred.
- Theoretical analysis proves that a unique, time-varying solution for the gain parameters do exist in the case of multiple voltage-regulating DEs. The parameters may be negative in the case that one DE needs to absorb reactive power even if its reference voltage is higher than its terminal voltage.

- With the presence of communication among all voltage-regulating DEs or between them and the control center, a regulation method is proposed, which can calculate how much DE output voltage is required based on the real time voltage measurements without the information of load change or some other disturbances. Simulation results show that this method can track the ideal voltage response very closely.
- Without the presence of the communication system, a method which uses only the local voltage measurement of an individual DE to track the ideal response is proposed. The simulation results show that although this method tracks the ideal response less closely if compared with the one with the availability of communication, it can still meet the requirements of no overshoot or oscillation with a fast response speed (within 0.5 seconds).

6. Conclusions and Future Work

The work of the dissertation is summarized in Subsection 6.1 and possible future works are proposed in Subsection 6.2.

6.1. Dissertation Conclusion

DEs with power electronic interfaces have the ability of dynamic reactive power support, which can benefit the system's reliability and safety. This dissertation explores how to use DEs for voltage regulation from the "system" point of view. The importance of appropriate controller parameters in voltage regulation is emphasized and challenges in setting these parameters are discussed in the case of a single voltage-regulating DE as well as in the case of multiple voltage-regulating DEs. An adaptive voltage control approach has been proposed to dynamically modify control parameters to respond to system changes. The corresponding formulation of the dynamic control parameters is derived in both the case of the single voltage-regulating DE and the case of multiple voltage-regulating DEs. In the case of multiple DEs, a high-end solution with the requirement of communication among the DEs and a low-end solution without the requirement of communication are both proposed, considering the availability of communication systems. Conclusions from the work can be summarized as:

- Proportional-integral (PI) control parameters are critical to the stability of the voltage regulation with the DEs. Incorrect parameter settings may cause inefficient (slow response), oscillatory, or worse, unstable responses that can lead to system instability.
- Many factors, including network structures, line parameters, loads, and the DE

voltage sources, affect the appropriate range of the PI control parameters. It is not feasible for utility engineers to use a trial-and-error method to identify suitable parameters in a case-by-case study. In the case of multiple DEs regulating voltages, one DE's regulation is also affected by the other DE's regulation behavior. The voltage correction of the other DEs may result in excessive compensation at one DE's terminal bus. In this case, the flat reference voltage as an indication of injecting or absorbing reactive power fails to provide a timely regulation direction signal and overshoot of voltage is inevitable if with fixed gains. Hence, an adaptive approach to dynamically set controller parameters is preferable.

- The formulation of the controller parameters proves that a unique, time-varying solution for the gain parameters do exist in both the case of the single DE regulating voltage and the case of multiple DEs regulating voltages. Since the theoretical formulation requires detailed system parameters, it is not the preferred method for practicing utility engineers. However, the analytical formulation shows that there exists a unique solution of dynamic control parameters such that the voltage response follows the desired, ideal curve. Also, this shows that the adaptive approach has a solid theoretical foundation. Since the proposed adaptive methods, based on local measurement (without communication), have a high tolerance to real-time data shortage and is widely adaptive to variable power system operational situations, it is quite suitable for broad utility applications.
- In the case of a single DE regulating voltage, both simulation and field experiment test results at the Distributed Energy Communications and Controls (DECC) Laboratory confirm that this method is capable of satisfying the fast response

requirement for operational use without causing oscillation, inefficiency, or system equipment interference.

- In the case of multiple voltage-regulating DEs, a high-end solution with extensive communication is also proposed using a direct calculation about how much DE output voltage is needed. This can be viewed as a benchmark for the low-cost approach without communication. Though both approaches meet the performance requirement very well (within 0.5 seconds to reach the reference voltage) as evidenced by the voltage response close enough to the ideal curve, this high-end solution with communication performs even faster and more accurately. Hence, it may also be useful for special cases requiring superior performance.

6.2. Future Work

The adaptive voltage control approach using DEs has been proposed and the field experiment in the case of a single DE regulate voltage has been completed. In the future, more research work in the following areas can be performed.

- The field experiment in the case of multiple (at least two) DEs regulating voltage will be conducted once another testing system is in place at the ORNL DECC lab.
- The general DE model, which is a constant DC source in the present work, may be replaced with a more detailed, actual DE model, such as the PV or distributed wind turbine models. The impacts of the variation of the DC voltage on the voltage control will be explored, and the approaches to stabilize the DC voltage can be studied.

- The adaptive control method may be extended to the constant real power injection and reactive power injection control modes. Hence, simultaneous regulation of frequency and voltage can be performed. This is particularly useful for the implementation of micro-grids. The coordination between the two control processes needs to be considered.
- The adaptive control method may be extended to other power system applications such as the wind turbine control or STATCOM control for voltage stability under small disturbance in the transmission study.

List of References

[1]. Felix A. Farret, M. Godoy Simoes, Integration of Alternative Sources of Energy , John Wiley&Sons, New Jersey, 2006

[2]. Prabha Kundur, *Power System Stability and Control*, McGraw-Hill, 1994

[3]. G. F. Franklin, J.D. Powell, and A. Emami-Naeini, *Feedback Control of Dynamic Systems*, Pearson Prentice Hall, Upper Saddle River, NJ, 2006.

[4]. G. Pepermans, J. Driesen, D. Haeseldonckx, R. Belmans and W. D haeseleer, "Distributed generation: definition, benefits and issues," *Energy Policy*, vol. 33, issue 6, pp. 787-798, April 2005

[5]. B. Kroposki, C. Pink, R. DeBlasio, H. Thomas, M. Simoes and P.K. Sen, "Benefits of Power Electronic Interfaces for Distributed Energy Systems," *IEEE PES General Meeting 2006*, June 18-22, 2006.

[6]. F. Li, J. Kueck, T. Rizy and T. King, "A preliminary analysis of the economics of using distributed energy as a source of reactive power supply," *Oak Ridge National Laboratory (ORNL) Technical Report* (ORNL/TM-2006/014), Oak Ridge, TN, April 2006.

[7]. Yan Xu, L.M. Tolbert, D.T. Rizy and J.D. Kueck, "Nonactive-Power-Related Ancillary Services Provided by Distributed Energy Resources," *IEEE PES General Meeting 2007*, June 24-28, 2007.

[8]. Xiaoyan Yu and L.M Tolbert, "Ancillary Services Provided from DER with Power Electronics Interface," *IEEE PES General Meeting 2006*, June 18-22, 2006.

[9]. Yan Xu, L. M. Tolbert, F. Z. Peng, J. N. Chiasson, and J. Chen, "Compensation-Based Non-Active Power Definition," *IEEE Power Electronics Letters*, vol. 1, no. 2, June 2003, pp. 45-50, June 2003.

[10]. Yan Xu, L. M. Tolbert, J. N. Chiasson, F. Z. Peng, J. B. Campbell, "Generalized Instantaneous Nonactive Power Theory for STATCOM," *IET Electric Power Applications*, vol. 1, no. 6, pp. 853-861, Nov. 2007

[11]. A.A. Thatte and M.D. Ilic, "An Assessment of Reactive Power/Voltage Control Devices In Distribution Networks," *IEEE PES General Meeting 2006*, June 18-22, 2006.

[12]. T. Tran-Quoc, M. Braun, J. Marti, C. Kieny, N. Hadjsaid and S. Bacha, "Using Control Capabilities of DER to Participate in Distribution System Operation," *IEEE PowerTech Conference 2007*, pp. 561 – 566, July 1-5, 2007.

[13]. J. Driesen, and R. Belmans, "Distributed generation: challenges and possible solutions," *IEEE PESGeneral Meeting 2006*, June 18-22, 2006.

[14]. N.D. Hatziargyriou and A.P. Sakis Meliopoulos, "Distributed Energy Sources: Technical Challenges," *IEEE PES Winter Meeting 2002*, vol. 2, pp. 1017 – 1022, Jan. 27-31, 2002.

[15]. H.Y. Li and H. Leite, "Increasing Distributed Generation Using Automatic Voltage Reference Setting Technique," *2008 IEEE PES General Meeting*, July 20-24, 2008.

[16]. T.G. Hazel, N. Hiscock and J. Hiscock, "Voltage Regulation at Sites with Distributed Generation," *IEEE Transactions on Inductry Application*, vol.44, issue 2, pp. 445-454, March 2008.

[17]. C.M. Hird, H. Leite, N. Jenkins, H. Li, "Network Voltage Controller for Distributed Generation," *IEE Proceedings on Generation, Transmission and Distribution*, vol. 151, no. 2, pp. 150-156, March 2004.

[18]. Miyoung Kim, R. Hara and H. Kita, "Design of the Optimal ULTC Parameters in Distribution System With Distributed Generations," *IEEE Transactions on Power Systems*, vol. 24, issue 1, pp. 297 – 305, Feb. 2009.

[19]. D. N. Gaonkar, P. C. Rao, and R. N. Patel, "Hybrid Method for Voltage Regulation of Distribution System with Maximum Utilization of Connected Distributed Generation Source," *IEEE Power India Conference*, 2006.

[20]. J. Oyarzabal, J. Marti, A. Ilo, M. Sebastian, D. Alvira and K. Johansen, " Integration of DER into power system operation through Virtual Power Plant concept applied for voltage regulation," *2009 CIGRE/IEEE PES Joint Symposium on Integration of Wide-Scale Renewable Resources Into the Power Delivery System,* July 29-31, 2009.

[21]. M. Braun, and J. Ringelstein, "Voltage Control in Electric Distribution Grids by Aggregation of Distributed Energy Units," *6th International Conference on the European Energy Market,* May 27-29, 2009.

[22]. Diana Moneta, Marco Marciandi, Carlo Tornelli and Paolo Mora, "Voltage Optimization of a LV Microgrid with DER: Field Test," *2009 20th International Conference and Exhibition on Electricity Distribution*, June 8-11, 2009.

[23]. A. Borghetti,; M. Bosetti, C. A. Nucci,; M. Paolone, S. Massucco, F. Silvestro and S. Scalari, "A procedure for the Automatic Scheduling of Distributed Energy Resources in Medium Voltage Networks ," *2009 20th International Conference and Exhibition on Electricity Distribution*, June 8-11, 2009.

[24]. M. E. Baran and I. M. El-Markabi, "A Multiagent-based dispatching scheme for distributed generators for voltage support on distribution feeders," IEEE Transactions on Power Systems, vol. 22, no. 1, pp. 52 – 59, February 2007.

[25]. T.E. Kim and J.E. Kim, “Voltage Regulation Coordination of Distributed Generation System in Distribution System,” *IEEE PES Summerl Meeting 2001*, vol.1, pp. 480 – 484, July 15-19, 2001.

[26]. T. Tran-Quoc, et al, “Intelligent voltage control in distribution network with distributed generation,” *19th International Conference on Electricity Distribution (CIRED 2007)*, 2007.

[27]. M. Braun, "Provision of Ancillary Services by Distributed Generators- Technological and Economic Perspective", *Renewable Energies and Energy Efficiency, Vol. 10, 2009, ISBN 978-3-89958-638-1 (print)*, ISBN 978-3-89958-639-8 (online).

[28]. P. N. Vovos, A. E. Kiprakis, A. R. Wallace and G. P. Harrison, “Centralized and distributed voltage control: impact on distributed generation penetration,” *IEEE Transactions on Power Systems*, vol. 22, no. 1, pp. 476 – 483, February 2007.

[29]. K. De Brabandere, B. Bolsens, J. Van den Keybus, A. Woyte, J. Driesen, and R. Belmans, “A Voltage and Frequency Droop Control Method for Parallel Inverters,” *IEEE Transactions on Power Electronics*, vol. 22, issue 4, pp. 1107-1115, July 2007.

[30]. J.C. Vasquez, J.M. Guerrero, E. Gregorio, P. Rodriguez, R. Teodorescu and F. Blaabjerg, “Adaptive Droop Control Applied to Distributed Generation Inverters Connected to the Grid,” *ISIE 2008*, pp. 2420-2425, June 30-July 2, 2008.

[31]. D. Feng, Z. Chen, “System Control of Power Electronics Interfaced Distribution Generation Units,” *IEEE 5th International Power Electronics and Motion Control Conference 2006*, vol. 1, pp. 1-6, Aug. 14-16 2006.

[32]. Chia-Tse Lee, Cheng-Chieh Chuang, Chia-Chi Chu and Po-Tai Cheng, “Control Strategies for Distributed Energy Resources Interface Converters in the Low Voltage Microgrid,” *IEEE ECCE 2009*, pp. 2022-2029, Sept. 20-24, 2009.

[33]. P. Karlsson, J. Bjornstedt and M. Strom, "Stability of Voltage and Frequency Control in Distributed Generation Based on Parallel-connected Converters Feeding Constant Power Loads," *European Conference on Power Electronics and Applications 2005*.

[34]. M. H. J. Bollen and A. Sannino, "Voltage Control with Inverter-based Distributed Generation," *IEEE Transactions on Power Delivery*, vol. 20, no. 1, pp. 519-520, January 2005.

[35]. J. Morren, S.W.H. de Haan, J.A. Ferreira, "Distributed Generation Units Contribution to Voltage Control in Distribution Networks," *39th International Universities Power Engineering Conference (UPEC) 2004*, vol. 2, pp. 789- 793, Sept. 6-8, 2004.

[36]. R. Mienski, R. Pawelek, I. Wasiak, P. Gburczyk, C. Foote, G. Burt and P. Espie, "Voltage Dip Compensation in LV Networks Using Distributed Energy Resources," *11th International Conference on Harmonics and Quality of Power*, pp. 774 – 778, Sept. 12-15, 2004.

[37]. D. Yazdani, A. Bakhshai, G. Joos and M. Mojiri, "A Nonlinear Adaptive Synchronization Technique for Grid-Connected Distributed Energy Sources," *IEEE Transactions on Power Electronics*, vol. 23, issue 4, pp. 2181-2186, July 2008.

[38]. S. Chakraborty, B. Kroposki and W. Kramer, "Evaluation of VAR Control and Voltage Regulation Functionalities in a Single-Phase Utility-Connected Inverter for Distributed Energy Applications," *IEEE ECCE 2009*, pp. 1753 – 1759, Sept. 20-24, 2009.

[39]. S. Ko, S.R. Lee, H. Dehbonei, C.V. Nayar, "Application of Voltage- and Current-Controlled Voltage Source Inverters for Distributed Generation Systems," *IEEE Transactions on Energy Conversion*, vol. 21, no. 3, pp. 782-792, September 2006.

[40]. M. Prodanovic, K. De Brabandere, J. Van Den Keybus, T. Green and J. Driesen, "Harmonic and Reactive Power Compensation as Ancillary Services in Inverter-based

Distributed Generation," *Generation, Transmission & Distribution, IET*, vol. 1, issue 3, pp. 432 – 438, May 2007.

[41]. Simon R. Wall, "Performance of Inverter Interfaced Distributed Generation," *IEEE Transmission and Distribution Conference and Exposition 2001*, pp. 945-950, vol.2, Oct. 28 -Nov. 2, 2001.

[42]. Y. Xu, F. Li, J. Kueck, T. Rizy, "Experiment and Simulation of Dynamic Voltage Regulation with Multiple Distributed Energy Resources," *Bulk Power System Dynamics and Control - VII. Revitalizing Operational Reliability, 2007 iREP Symposium*, August 2007.

[43]. M.N. Marwali and A. Keyhani, "Control of Distributed Generation Systems—Part I: Voltages and Currents Control," *IEEE Transactions on Power Electronics, vol. 19, issue 6,* pp. 1541 - 1550, Nov. 2004.

[44]. H. Ko, G. Yoon and W. Hong, "Active Use of DFIG-based Variable-speed Wind-turbine for Voltage Regulation at a Remote Location," *IEEE Transactions on Power Systems*, vol. 22, no. 4, pp. 1916 – 1925, Nov. 2007.

[45]. M.N. Marwali, Min Dai and A. Keyhani, "Robust Stability Analysis of Voltage and Current Control for Distributed Generation Systems," *IEEE Transaction on Energy Conversion*, vol. 21, issue 2, pp. 516-526, June 2006.

[46]. F. Wu, X. Zhang, K. Godfrey and P. Ju, " Small Signal Stability Analysis and Optimal Control of a Wind Turbine with Doubly Fed Induction Generator," *IET Generation, Transmission & Distribution*, vol. 1, issue 5, pp. 751-760, Sep. 2007.

[47]. Karl Johan Astrom and Bjorn Wittenmark, *Adaptive Control*, Addison-Wesley Publishing Company, 1989

[48]. Masanao Aoki, George A. Bekey etc., *Modern Control Systems Theory*, Mcgrw-Hill Book Company, 1965

Publications during Ph.D. Study

Submitted:

1. **Huijuan Li,** Fangxing Li, Yan Xu, D. Tom Rizy, John D. Kueck, "Dynamic Voltage Regulation using Multiple Distributed Energy Resources: with and without communication" (to be submitted to) *IEEE Transactions on Power Systems*.

Journal papers:

2. **Huijuan Li,** Fangxing Li, Yan Xu, D. Tom Rizy, John D. Kueck, "Adaptive Voltage Control with Distributed Energy Resources: Algorithm, Theoretical Analysis, Simulation and Field Test Verification," *IEEE Transactions on Power Systems,* vol. 25, no. 3, pp. 1638-1647, August 2010.
3. Yan Xu, Fangxing Li, **Huijuan Li**, D. Tom Rizy, and John. D. Kueck, "Using Distributed Energy Resources to Supply Reactive Power for Dynamic Voltage Regulation," *International Review of Electrical Engineering (IREE)*, vol. 3, no. 5, pp. 795-802, October 2008.

Conference papers:

4. Yan Xu, **Huijuan Li**, D. Tom Rizy, Fangxing Li, John D. Kueck, and Chester L. Coomer, "Instantaneous Active Power and Nonactive Power Control of Distributed Energy Resources with a Current Limiter," *2nd IEEE Energy Conversion Congress and Exposition (ECCE)*, Atlanta, GA, Sept. 12-16, 2010.
5. D. Tom Rizy, Fangxing Li, **Huijuan Li**, Sarina Adhikari, John D. Kueck, "Properly Understanding the Impacts of Distributed Resources on Distribution Systems," (invited) *IEEE PES General Meeting 2010*, Minneapolis, MN, July 25-29, 2010.

6. **Huijuan Li**, Fangxing Li, Sarina Adhikari, Yan Xu, D. Tom Rizy, and John D. Kueck, "An Adaptive Voltage Control Algorithm with Multiple Distributed Energy Resources," *North American Power Symposium (NAPS) 2009*, Starkville, MS, October 04-06, 2009.
7. Sarina Adhikari, Fangxing Li, **Huijuan Li**, Yan Xu, John D. Kueck, and D. Tom Rizy, "Modeling Stalled Induction Motors with Voltage-Regulating Distributed Energy Resources," *PowerTech Conference 2009*, Bucharest, Romania, June 28-July 02, 2009.
8. **Huijuan Li**, Fangxing Li, Pei Zhang and Xiayang Zhao, "Optimal Utilization of Transmission Capacity to Reduce Congestion with Distributed FACTS," *PowerTech Conference 2009*, Bucharest, Romania, June 28-July 02, 2009.
9. **Huijuan Li**, Fangxing Li, Yan Xu, Tom Rizy and John Kueck, "Voltage regulation with multiple distributed energy resources," (invited) *IEEE PES General Meeting 2008*, Pittsburgh, PA, July 20-24, 2008.

Technical report:

10. John D. Kueck, D. Tom Rizy, Fangxing Li, Yan Xu, **Huijuan Li**, Sarina Adhikari and Philip Irminger, "Local Dynamic Reactive Power for Correction of System Voltage Problems," Oak ridge National Laboratory (ORNL) Technical Report (ORNL/TM-2008/158), Oak Ridge, TN, Sept. 2008.

Award

Significant award received during Ph.D. study:

[1]. First Place Prize Award at the Student Poster Contest (1st out of 97) at 2009 IEEE PES General Meeting (GM09), July 2009, Calgary, Canada.

[2]. UT Citation Award in Extraordinary Professional Promise, April 2010.

Vita

Huijuan Li received her B.S. and M.S. degrees both in electric power engineering from North China Electrical Power University in 1999 and 2002, respectively. From 2002 to 2006, she worked at Shanghai Sieyuan Electrical Company. She started her Ph.D. study at The University of Tennessee, Knoxville, in August 2006. Her current interests include integration of distributed energy resources and voltage control. She has been a student member of IEEE since 2007.

Huijuan won the first place prize award at the Student Poster Contest at 2009 IEEE Power and Energy Society (PES) General Meeting 2009 (PES GM09) in July 2009, Calgary, Canada. She also received the UT Citation Award in Extraordinary Professional Promise in April 2010.